STUDY OF PRE-SHEARING PROTOCOL AND RHEOLOGICAL PARAMETERS OF SHEAR THICKENING FLUIDS CONTAINING NANO PARTICLES

Thesis submitted in partial fulfilment for the requirement for the award of degree of

Master of Technology

in

Chemical Engineering

By

Pavni Passey

M. Tech. 2nd year

(Roll No. 601411001)

UNDER THE GUIDANCE OF

Dr. Rajeev Mehta
Professor
Department of Chemical Engineering
Thapar University, Patiala

Department of Chemical Engineering
Thapar University
Patiala-147004, Punjab

July 2016

Dedicated to my family

DECLARATION

This is to certify that the thesis entitled **'Study of pre-shearing protocol and rheological studies of shear thickening fluids containing nano particles'**, is an authentic record of my own work carried out as requirements for theaward of degree of Master of Technology in Chemical Engineering from Thapar University, Patiala, under the supervision of Dr. Rajeev Mehta, Professor, Department of Chemical Engineering, Thapar University, Patiala, from a period of March 2015 to July 2016.

Date: 11/06/2016

Pavni Passey
(Roll No: 601411001)

CERTIFICATE

This is certified that the thesis entitled **'Study of pre-shearing protocol and rheological parameters of shear thickening fluids containing nano particles'** which is being submitted by Ms. Pavni Passey in partial fulfilment of the requirements for the award of the degree of **M.Tech (Chemical Engineering)** in the Department of Chemical Engineering, Thapar University, Patiala, is a bonafide work carried out by her under my guidance and supervision and that no part of this thesis has been submitted for the award of any other degree.

Rajeev Mehta

Dr. Rajeev Mehta
Professor
Department of Chemical Engineering
Thapar University, Patiala

Countersigned by:

Dr. R.K. Gupta
Head
Department of Chemical Engineering
Thapar University, Patiala

Dr. S.S. Bhatia
Dean
Academic Affairs
Thapar University, Patiala

ACKNOWLEDGEMENT

The past fifteen months have been a period of intense learning for me, not only in the field of scientific arena, but also on a personal level. Reading research papers, experimenting and then writing this thesis has had a great impact on me. I owe my gratitude to all those people who have supported and helped me so much throughout this period and made this dissertation possible and because of whom my master's experience has been the one that I will cherish forever.

Firstly, my deepest gratitude is to my mentor, **Dr. Rajeev Mehta** (Professor, Department of Chemical Engineering). I have been amazingly fortunate to have an advisor who gave me the freedom to explore on my own, and at the same time the guidance to recover when my steps faltered. Dr. Mehta taught me how to question thoughts and express ideas. His professionalism and diligent work has helped me overcome many crisis situations and finish this dissertation. He has continuously steered me to the right direction whenever he thought I needed it. I express my sincere gratitude for his patience, enthusiasm and immense knowledge. I could not have imagined a better and a friendlier guide for my M.Tech thesis.

I am also thankful to **Dr. R.K. Gupta** (Head of the Department of Chemical Engineering and Associate Professor) and **Dr. J.P. Kushwaha** (P.G. Coordinator, Department of Chemical Engineering and Assistant Professor) for being a continuous source of motivation and inspiration that prompted me for the thesis work.

I would also like to thank the other faculty members for their encouragement, insightful comments and hard questions. Their constructive criticisms at different stages of my research were thought-provoking and they helped me focus on my ideas.

I would like to thank my fellow lab mates for working together and for all the fun we had during this duration. **Ms. Mansi Singh** has always supported me and was always willing to help me. I thank her for the excellent cooperation and valuable guidance.

I am also indebted to the other seniors of my department with whom I have interacted during the course of my research work. Particularly, I would like to acknowledge **Mrs. Harkirat Kaur Sandhu, Ms. Arshdeep Kaur, Ms. Harjot Kaur, Mr. Nitin Goyal,** and **Ms. Shivani Kalotra**, for the many valuable discussions that helped me understand my research area better.

I am also thankful to the departmental staff who helped in maintaining all the equipment in my lab very efficiently. Many of my friends have helped me stay sane through these difficult months. Their support and care helped me overcome any setbacks and stay

focused. I greatly value their friendship and I deeply appreciate their belief in me. All my colleagues at Thapar University have always been motivating, friendly and supportive.

Most importantly, none of this would have been possible without the blessings of the almighty and the love and patience of my family. My family to whom this dissertation is dedicated to, has been a constant source of love, concern, support and strength all these years. I express my heart-felt gratitude to them. They have always aided and encouraged me throughout this endeavour. I give a special mention to my brother **Dr. Sumiran Passey** who has always provided me unfailing support and continuous encouragement throughout my study, the process of researching and writing this thesis. This accomplishment would not have been possible without him.

Finally, I appreciate the financial support from TBRL, Chandigarh, a unit under the Defence Research and Development Organization that funded for the raw materials used in my research.

Thank you very much, everyone!

Pavni Passey.

(PAVNI PASSEY)

ABSTRACT

Suspensions having viscoelastic property are ubiquitous and find applications in variety of fields. One such suspension is that of the shear thickening fluid, which is non-Newtonian in nature and shows an increase in viscosity when subjected to shear. Thus, these fluids have the ability to change from liquid to solid phase when they undergo shear and then return back to their original state when the shear is released. This reversible nature is highly useful in defence applications. Previous studies show that the shear thickening fluids have the potential of impact and stab resistance and can be used as a coating material on Kevlar fabric to be used as a soft body armour. With modifications in the fluids, these armours can be made more durable and light weight, which will help in increasing the flexibility of the soldier.

Like most of the viscoelastic materials, shear thickening fluids are also made up of polymers, and have a tendency to store its previous shear history, thereby making it a memory fluid. In the present work, a protocol has been developed in order to remove this shear history from the fluids and thus enhance its properties. The shear thickening fluid for which such protocol has been developed is a bi-dispersed mixture of fumed silica (11 nm) and simple silica (400 nm). The past history was removed using the pre-shearing technique. Such technique has been used for the first time for any such bi-dispersed suspension composed of different sized particles. The rheological protocol developed for such a shear thickening fluid is quite different from that reported in the past. Using this method it can be observed how much initial shear and rest period is required by the sample so as to become stable and provide reproducible rheological results. The outcomes have been found to indicate a significant increase in critical viscosity of the material.

Another important feature which affects the thickening behaviour of these fluids is the particle shape. Elongated particles provide high viscosity to the fluid whereas spherical particles show thickening behaviour at higher shear rates. Thus, composite shear thickening fluid was prepared using halloysite nanotubes (rods) and fumed silica (spheres) and its rheological properties were studied. A better non-flocculated structure was obtained at 1% halloysite and 20% fumed silica composition compared to that of only spherical particle STF. The oscillatory tests showed that this composition was also suitable as a high impact resistant material as no gel formation takes place rather the fluid behaves like a dispersed sol. Furthermore, composites having higher percentages of halloysite nanotubes were also prepared and a comparison of the rheological properties of the three halloysite nanotubes-fumed silica composites was done.

LIST OF FIGURES

LIST OF TABLES

NOMENCLATURE

S. No.	Abbreviation	Full name
1.	CNT	Carbon nano tubes
2.	CS	Corn starch
3.	CST	Continuous shear thickening
4.	DST	Discontinuous shear thickening
5.	EG	Ethylene glycol
6.	FS	Fumed silica
7.	GNT	Graphite nano tubes
8.	HNT	Halloysite nano tubes
9.	PEG	Poly ethylene glycol
10.	PEO	Poly ethylene oxide
11.	POE	Poly oxy ethylene
12.	PPG	Poly propylene glycol
13.	STF	Shear thickening fluid

LIST OF SYMBOLS

S. No	Symbols	Description
1.	φ	Solid volume fraction (Packing fraction)
2.	μ	Viscosity
3.	η	Apparent viscosity
4.	η_{eq}	Equilibrium viscosity
5.	η_c	Continuous phase viscosity
6.	η^*	Complex viscosity
7.	τ	Shear stress
8.	τ_c	Criticalshear stress
9.	τ_{max}	Maximum shear stress
10.	$\dot{\gamma}$	Shear rate
11.	$\dot{\gamma}_c$	Critical shear rate
12.	$\dot{\gamma}_{max}$	Maximum shear rate
13.	G'	Storage modulus
14.	G''	Loss modulus
15.	G^*	Dynamic modulus
16.	ρ_x	Nano filler density
17.	$\emptyset_x$	Percolation concentration

CONTENTS

Chapter 1

INTRODUCTION

Viscosity and elasticity are two distinct properties of materials. Viscosity gives an account of the flowing tendency of the material, whereas elasticity tells us about its stretching behaviour. Elastic substances have an ability to return to their original shape and size when an applied deformative force is removed from them. On the other hand, in case of viscous materials, when the force is removed they do not return to their original shape, because the force of deformation is utilized by the material thus giving rise to it's fluidly nature.
Another class of materials, which possess both viscous as well as elastic characteristics, are called viscoelastic materials. Such substances follow the simple deformation behaviour models for an ideal material, which are:

1. **Hooke's Linear Elasticity Model** in the solid state, and
2. **Newton's Linear Viscosity Model** in the liquid state.

The behaviour of many 'real materials' do not follow these idealised models, especially polymers, which show a marked deviation. In particular, their solid state deformation is time-dependent and nonlinear and thus resembles some different combination of elastic and viscous responses. Time-dependency and nonlinearity are the important features of certain non-Newtonian fluids also. Such fluids are known as:

1. **Rheopectic Fluids**, and
2. **Thixotropic Fluids**

The fluids in which the viscosity decreases with respect to time on application of shear are known as thixotropic fluids, whereas, rheopectic fluids are the ones in which the apparent viscosity of the fluid increases with time as the fluid continues to undergo shear, i.e. longer the shearing force on the material, higher is its viscosity. The viscosity of such fluids depend on shear rate as well as deformation history. These are also termed as memory materials. Such nonlinear rheological behaviour of particle suspensions arises from a microstructural rearrangement of the particles within the system. Among all nonlinear rheological behaviours, **Shear Thickening** (increasing viscosity with applied shear rate), is the most unique property of fluids. This makes them ideal for several potential applications; one of the most important being its capability to enhance the performance of body armour against ballistic impact and for stab resistance.

1.1 SHEAR THICKENING FLUID BEHAVIOUR

Shear thickening is defined in the 'British Standard Rheological Nomenclature' as "the increase of viscosity [of a fluid] with increase in shear rate" (Barnes, 1989). Shear thickening fluids (STFs) can be both dilute as well as concentrated colloidal suspensions composed of non-aggregating solid particles suspended in fluids. Such suspensions have the property of increasing the fluid viscosity with increasing shear rate and thus fall under the category of non-Newtonian fluids (figure 1.1). Under high speed shear rate the viscosity of STF increases radically and it behaves like a solid. However, after the removal of impact stress, STF reverses its status to liquid like as soon as the shear is removed. Thus, shear thickening is completely reversible i.e. after the removal of impact stress, the suspension return back to an easy flowing state and flow like any other liquid. STF is a combination of hard metal oxide colloidal particles such as silica or silicon dioxide suspended in a fluid base, which can be Newtonian in nature, such as water or polyethylene glycol (PEG) or other polymeric fluids (Hasanzadeh and Mottaghitalab, 2014).

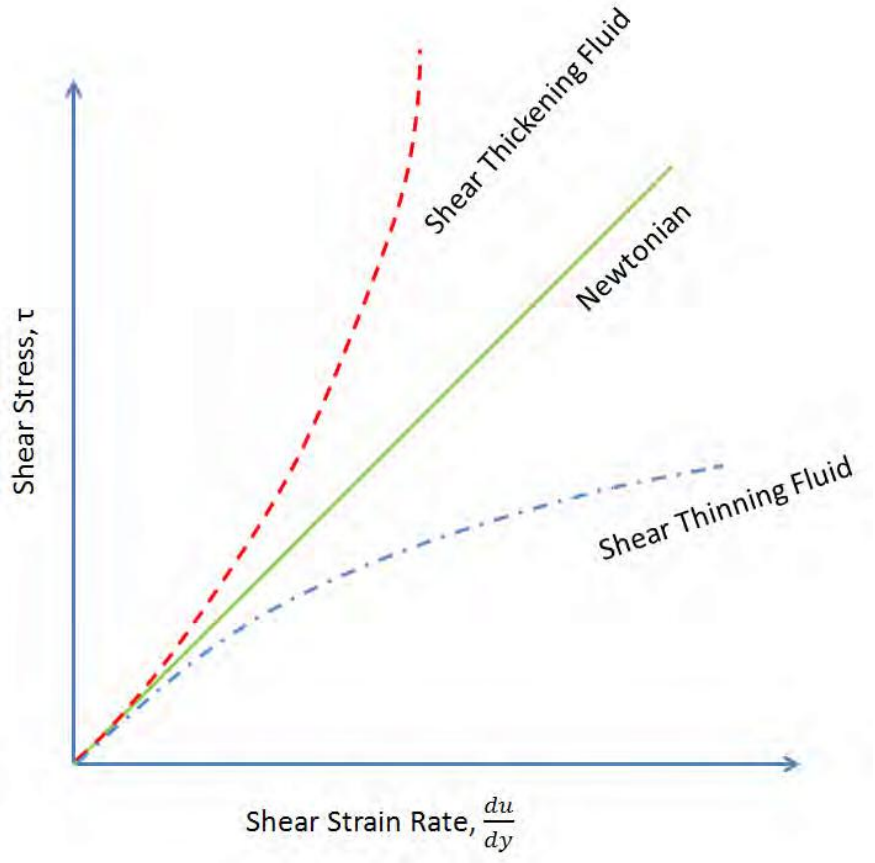

Figure 1.1: Shear stress and shear strain rate relationship (Zhu, 2011).

1.2 TYPES OF SHEAR THICKENING SYSTEMS

Shear thickening systems can be of two types: (Ding *et al*., 2013)

1. Particle based shear thickening systems, and
2. Non-particle based shear thickening systems.

Particle Based Shear Thickening Systems

A shear thickening fluid is composed of a carrier liquid as the dispersion medium and rigid, colloidal particles, as the dispersed phase. The particles are generally selected from a number of the groups which include nano silica, fumed silica, titanium oxide, calcium carbonate, corn-starch, synthetically and naturally occurring minerals, polymers or a mixture of these. Many carrier fluids have been investigated, including water, ethylene glycol (EG), polyethylene glycol (PEG), polypropylene glycol (PPG) etc. PEG and PPG are the most widely used due to their combination of stability, high boiling point, polarity and non-flammable properties (Chen *et al*., 2005). Such STF dispersions formed fall into the colloidal particle size range of 1 nm to 1000 nm.

Non-particle based Shear Thickening Systems

There are several important non-particle based shear thickening systems including segmental mobility of amorphous polymers about their glass transition and physically cross-linked polymer networks. When any amorphous polymer is at glass transition, it will shear thicken when the shear rate is increased (Montgomery and MacKnight, 2005). The cross linked polymer networks will shear thicken when the energy of the physical bond is same as that of the thermal energy. The particles show an intermittent physical bonding with the liquid at low shear rates, whereas they are considered to be fixed showing a solid like behaviour at higher shear rates. Polyvinyl alcohol containing boric acid and polydimethylsiloxane containing boric acid are two well-known examples.

1.3 CLASSIFICATION OF SHEAR THICKENING PHENOMENON

The Shear thickening phenomenon can be classified in the following forms:

1. Continuous shear thickening (gradual increase in viscosity)
2. Discontinuous shear thickening (very rapid increase in viscosity)

Continuous shear thickening (CST)

The degree to which the viscosity increases with shear rate depends on the volume fraction or packing fraction $'\varphi'$ of the solid particles. Shear thickening phenomenon is very rare in dilute suspensions, but gradually appear at intermediate packing fractions, typically around $0.3 \leq \varphi \leq 0.4$ for suspensions of solid spheres (Brown and Jaeger, 2013).

At these particle concentrations, the viscosity increase is relatively mild. This type of shear thickening is referred to as 'continuous'. The rate of rise in viscosity with shear rate gradually intensifies with the increasing packing fraction, and it is usually found that the shear thickening regime starts at a critical stress $'\tau_c'$ which is roughly independent of packing fraction. Below this stress, shear thinning or a Newtonian behaviour is observed, depending on the type of suspension.

Discontinuous shear thickening (DST)

In many shear thickening fluids, a steep rise in viscosity is detected with increasing packing fraction, and shows a sudden jump at a certain shear rate (Warren *et al.*, 2015). In such cases it is often said that the shear thickening advances from a continuous to discontinuous shear thickening with growing packing fraction. Discontinuous shear thickening (DST) shows the most vivid viscosity behaviour among any type of shear thickening. The common fluid mixtures where such behaviour is observed are corn-starch in water, solutions of micelles etc. The DST regime has its onset at the critical shear stress and tends to occur in a well-defined range of shear stress (Hoffman, 1982). Once started, the viscosity or the shear stress reaches a maximum value and the thickening regime ends at a maximum point of τ_{max} or η_{max}. Beyond this stressor viscosity, shear thinning, distortion or rupture of the suspension is observed.

The apparently discontinuous jump in the viscosity or the shear stress tends to be observed only over a range of packing fractions of a few percent in compactly packed suspensions, around $\varphi \approx 0.6$ for nearly spherical particles (Brown and Jaeger, 2009; Maranzano and Wagner, 2001).

1.4 FACTORS AFFECTING SHEAR THICKENING BEHAVIOUR

The main shear thickening behaviour used in liquid armour designing is the reversible increase in viscosity with the increase in shear rate. The parameters or the factors, on which the rheological properties of STF are based on, are categorised as:

Dispersed phase parameters

- Solid volume fraction
- Particle size
- Particle shape
- Particle size distribution
- Particle-particle interactions

Dispersion medium parameters

- Viscosity of continuous phase

Flow Field

- Type of deformation taking place
- Rate of deformation
- Time of deformation

The effects of these factors are briefly discussed as follows:

1. **Solid Volume Fraction:** Represented as φ, this is the fraction of the total volume of the system occupied by the particles. It is the most important factor affecting shear thickening. In the initial researches the value of φ kept for the onset of shear thickening was 0.5 (or 50%). Later it was observed that the critical shear rate can also be achieved at greater volume fractions. But in such cases the critical shear rate decreases rapidly (Barnes, 1989). Increase in the solid volume fraction improves the shear thickening behaviour, due to gradual decrease in the critical shear rate. This can be clarified with the help of the "jamming model", which suggests that the reversible shear thickening is attributed to shear induced orderly transition of particles into clusters. Increased viscosity is caused by aggregated clusters jamming the flow while relatively low volume fraction region may be hard to achieve the jamming tightly and thereby resulting in a similar viscosity. Thus, the effect of volume fraction on viscosity of suspension exists as an "accelerating effect" (Chen *et al.*, 2015).

2. **Particle Size:** The effects of particle size on reversible shear thickening of hard spheres which are dispersed have been studied by Maranzano and Wagner (Maranzano and Wagner, 2001). It is shown that as particle size increases, the critical shear rate systematically shifts to lower shear stresses (figure.1.2). In general, an average particle size is considered and critical shear rate is determined.

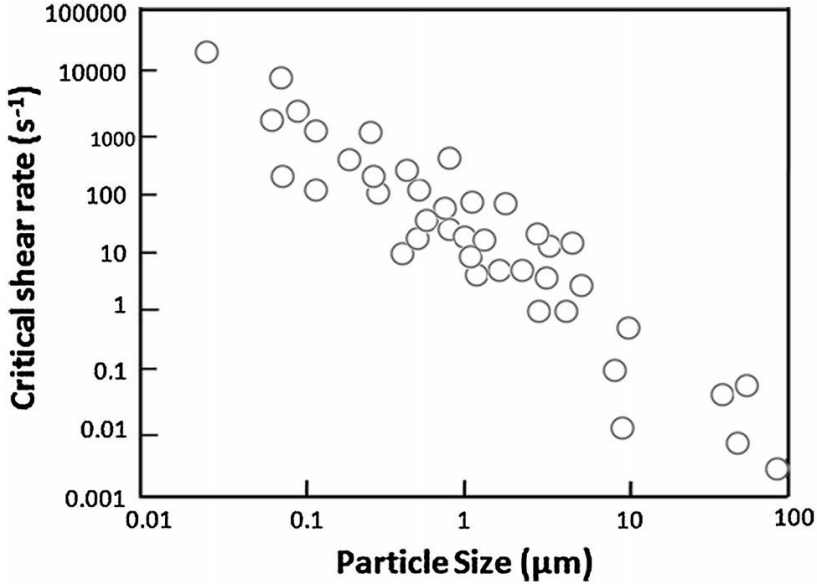

Figure 1.2: Effect of average particle size on critical shear rate for dispersions with volume fraction of $\varphi = 0.5$ (Hasanzadeh and Mattaghitalab, 2014).

3. **Particle Shape:** The rheology of shear thickening suspensions changes according to the shape of the constituent particles. The increase in viscosity of rod shaped or elongated particles, is much more than in case of disc shaped spherical or granular particles. It is observed that higher the aspect ratio of particles, shear thickening is achieved at a lower solid volume fraction (Hasanzadeh and Mattaghitalab, 2014). It is also shown that de-laminating the clay particles to increase anisotropy gives much more shear thickening (Barnes, 1989).

4. **Particle Size Distribution:** A wider particle distribution leads to an increase in critical shear rate. Removing very small particles from suspension causes the shear thickening to occur at lower shear rates. It is also referred by Barnes that distribution of another particle of a greater size can lead to complete elimination of shear thickening property of the suspension (Barnes, 1989). This has been demonstrated using calcium carbonate blends (figure 1.3).

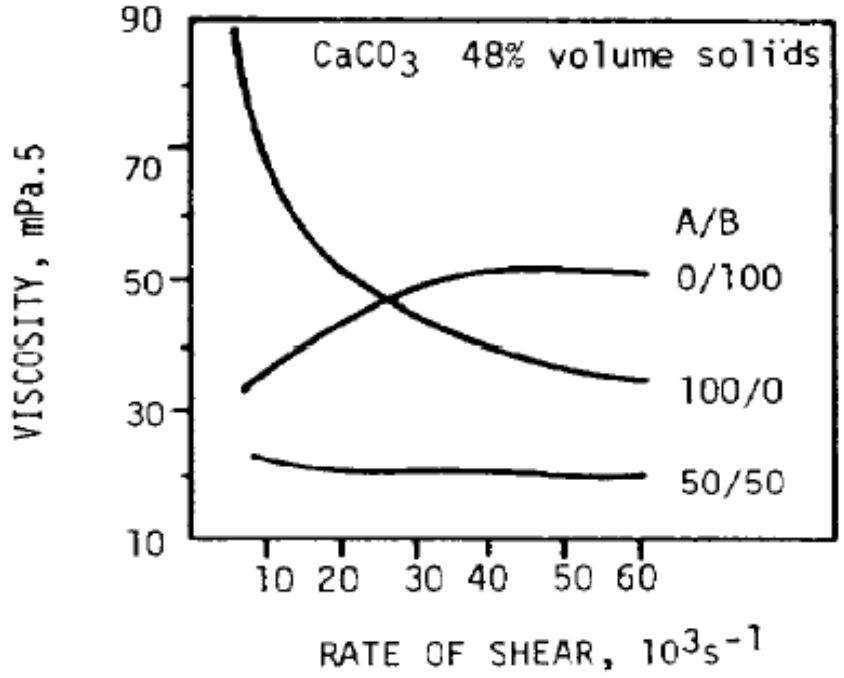

Figure 1.3: Viscosity of calcium carbonate blends at 48% solid content by volume (71.4% by weight) as a function of shear rate. Clay A=12μm; Clay B=0.65μm (Barnes,1989).

5. **Particle-Particle Interactions:** For a suspension to show shear thickening behavior, its particles must not readily flocculate and there must be no net attraction between the particles, i.e. the particles should either be neutral or repel each other. Thus, particle-particle interaction plays a very vital role in deciding the behaviour of shear thickening suspensions. Net repulsion between particles can be produced by surface modification by providing an electrostatic charge or by steric repulsion (Ding *et al.*, 2013). It was found that deflocculated suspensions have lower viscosity at low shear rates, but are shear thickening at high shear rates and can show rheopexy. On the other hand, flocculated suspensions have high viscosity at low shear rate, but are shear thinning at high shear rates, thus showing thixotropy (Barnes, 1989; Hasanzadeh and Mottaghitalab, 2014).

6. **Viscosity of Continuous Phase:** In suspensions the overall viscosity (η) is almost always a direct function of the continuous phase viscosity (η_c). This relationship takes the form:

$$\eta = \eta_c \text{ Function of (phase volume, size, shape, particle size distribution)}$$

All things being equal, doubling the continuous phase viscosity doubles the suspension viscosity. This effect must be borne in mind when considering the effect of temperature on suspension viscosity, because often its effect is due only to a change in the continuous phase viscosity. Apart from the effect of viscosity, it should be noted that exchanging one continuous phase liquid for another can often change the extent of particle interaction. There can then be an increase in the average particle size due to flocculation, or because better solvent properties can cause the suspended particles to swell by ingress of the continuous phase. This gives larger particles and an increased phase volume, thus greatly increasing the possibility or extent of shear thickening (Barnes, 1989).

7. **Type, Rate and Time of Deformation:** It has been shown that, for a high phase volume system, the acceleration rate in a loop test governs the behaviour such that a large change could give either thixotropy or rheopexy.

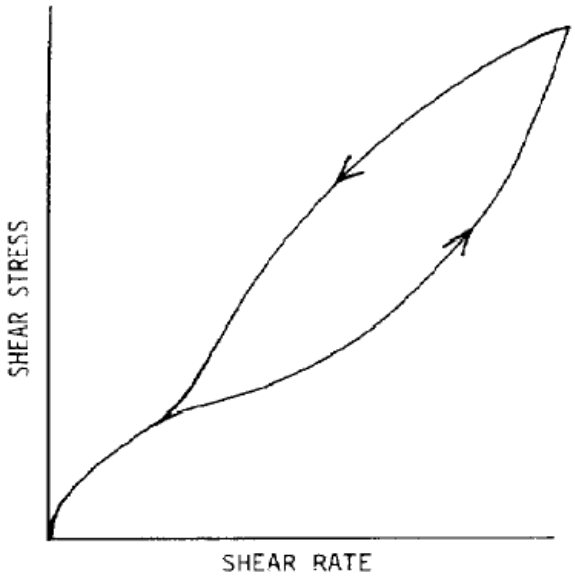

Figure 1.4: A schematic representation of hysteresis, displayed by a shear thickening clay (Barnes, 1989).

In these loop tests (figure 1.4), the shear rate increases from zero to some maximum value and then decreases again, with various degrees of acceleration possible. Given enough time, the structure induced in the shear thickening region during the high shear rate part of the loop can relax, but fast acceleration means that the structure formed at high shear rate persists into the low shear rate parts of the loop and exhibits behaviour quite different to that of the relaxed structure.

1.5 THEORIES EXPLAINING THE MECHANISM OF SHEAR THICKENING

Due to technical importance of shear thickening phenomenon, mechanisms underlying the shear thickening behaviour have been studied extensively. There are two main theories explaining the mechanism of STFs:

i. **Order-disorder Theory**, and
ii. **Hydrocluster Theory**.

The revolutionary work relating to the micromechanical properties of shear thickening fluid was made by Hoffman. This study was the foundation of the order-disorder theory. He proposed that below the critical shear rate, particles are hexagonally packed in the suspension. Beyond the critical shear rate, the packed particles disorder and form aggregates. This alteration from order to disorder causes a drastic increase in the viscosity (Hoffman, 1972; Hoffman 1975; Hoffman 1998).

Hydrocluster theory was first introduced by Brady with Stokesian dynamics simulations (Bossis and Brady, 1989). Hydrocluster mechanism arises from particle interactions in the liquid suspension. Under the high level stress, particles have contact with each other. This effect yields an increase in the hydrodynamic forces. With the increase in viscosity and the jammed behaviour of the fluid, particles set to form aggregates thereby leading to hydroclusters. The detailed explanation of the above theories is presented as follows:

1.5.1 Order-disorder transition

The order-disorder transition mechanism was first recognized and established by Hoffmann (Hoffman, 1974). He found that in some cases, when the microstructure changes from the ordered layers at low shear rates to disordered layers at high shear rates a transition to DST may also occur. Similar to the hydrocluster model, this scenario has been successful at predicting the critical shear rate$\dot{\gamma}_c$. But, it is also shown that DST can occur without an order-disorder transition (Brown and Jaeger, 2013). Thus, while the order-disorder transition is a possible way of microstructural reorganization corresponding to shear thickening behaviour, it is not a required mechanism.

1.5.2 Hydroclustering

The hydrocluster mechanism was first introduced by Brady and Bossis (Brady and Bossis, 1985). According to this mechanism particles collide into each other when acted upon

by shear, and then to divert from each other they must overcome the viscous drag forces from the small lubrication gaps between neighbouring particles (figure. 1.5). This suggests a critical shear rate above which particles stick together transiently by the lubrication forces and later propagate into larger clusters. At lower shear rates, the particles motions are more independent. The particle clusters result in a higher effective viscosity, so this critical shear rate $\dot{\gamma}_c$ and a corresponding shear stress τ_c signal the onset of shear thickening. It is often assumed that this model for shear thickeningwill lead to DST at higherpacking fractions, as particle clusters get larger and potentiallyspan the system (Brown and Jaeger, 2013).

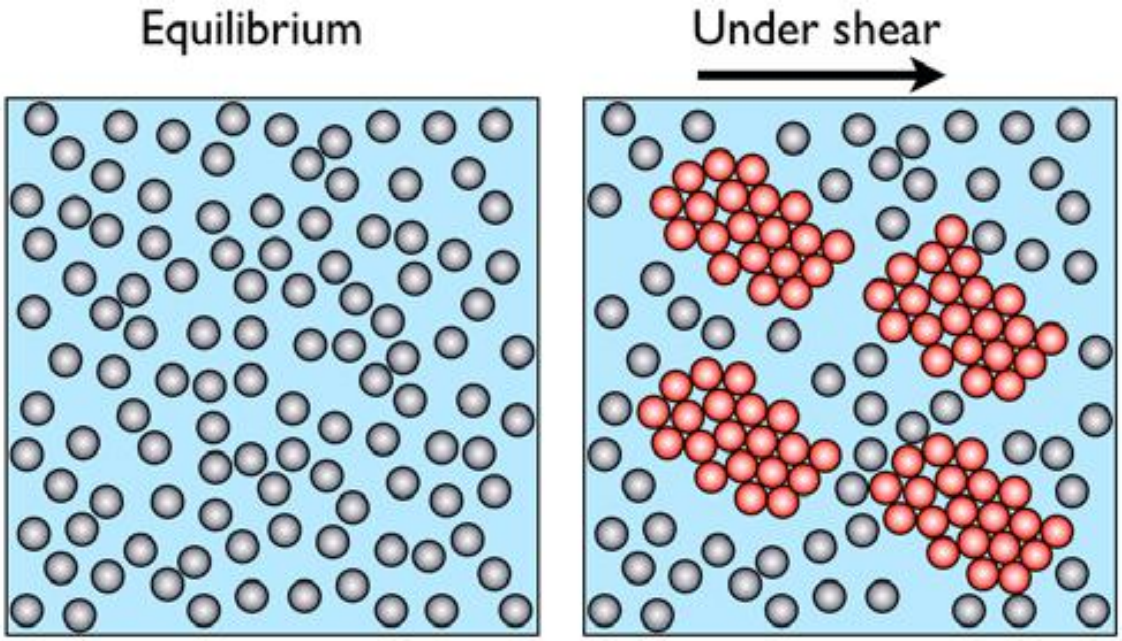

Figure 1.5: Schematic of particles forming hydroclusters under shear (Ding *et al*., 2013).

For silica polymer suspensions the theory of hydro-cluster formation is applicable for the reversible shear thickening behaviour as it depends upon the hydrodynamic forces. Thus for reversible region when the same hydrodynamic energy is applied, the same hydroclusters are formed. Because there is no volume filling network structure, the same structural level is developed and similar transient responses are observed, independent of the previous state. This reversible region exhibits a shear stress response at a certain value of shear rate that does not appreciably depend on the previous state of aggregation in contrast to the behaviour of flocculated samples. This is important for those suspensions related with any application as energy absorber (e.g. shear thickening fluids) (Galindo-Rosales *et al.*, 2009).

1.6 APPLICATIONS OF SHEAR THICKENING FLUIDS

Shear thickening fluids provide extensive energy dissipation in response to external stimuli. Hence, they display significant advantage for use in sports shoe cushioning, damping devices, ballistic protection etc. STFs in armour systems are a very new technology and open to developments. This technology provides two main improvements: reduced weight and flexible motion. The materials currently used in body armoursare unable to provide the whole body protection due to their stiffness and bulk. Novel liquid body armour based on STFs have shown promising prospects towards improved protection and flexibility (Ding *et al.*, 2013). Besides personal protection, STFs can also be applied to aerial vehicles such as helicopters and used in expandable spacecraft (Cohen, 2008). Shear thickening property of a material can be applicable for a wide range of industrial processes and is of great interest due to its energy absorbing capacity (Brown and Jaeger 2009; Lootens *et al.*, 2004; Hebraud and Lootens, 2005). One of the remarkable features of shear thickening fluids is its impact resistance property which helps it to be used in protective coverings for defence services.

Shear thickening fluids composed of colloidal particles are highly complex in nature. One of the earliest classical examples of a fluid showing shear thickening behaviour is ‘oobleck’, a mixture of corn-starch and water (Wagner and Brady, 2009). Initially, just used as a playful material for children, this mixture has since then evolved greatly, and the thickening property has been utilized worldwide by various researchers to find applications in day to day use. Now, fluids containing such thickening property are synthesizes using a variety of raw materials for numerous uses and the work still goes on, on improving its properties and basic constituents making it more economical, affordable and efficiently useful as an industrial fluid replacing many other costly and less effective fluids.

Views on the use of STF as an industrial fluid are not widely accepted and its practical implementation in the industry is minimum. This is because of its negative consequences on the industrial equipment such as breakage and fouling of pipelines, spray equipment and pumps. Engineers and scientists have been continuously finding more and more of its applications as pure or as a composite fluid. A rare industrial use of the shear thickening fluids is in the chemical mechanical polishing process used in microprocessors and semiconductor industries to reduce the size of micro electric devices (Crawford *et al.*, 2013). Some of its other innovative applications include: bullet proof soft body armour, machine mounts, dampers, driving fluids for enhanced oil recovery (Dawson, 1983), shock absorptive skies etc.

1.7 PRE-SHEARING

From the thixotropic and rheopectic properties displayed by fluids, it is known that the viscosity may depend on the structural changes taking place in the fluids with time. The stress and deformation of the body are thus time dependent. It is expected that longer the time interval smaller is the contribution to the current stress resulting from a given strain (principle of fading memory). Viscoelastic materials also exhibit memory since they experience both viscosity and elasticity; hence the deformation associated with them is time dependent.

Pre-shearing, of any dispersion or filled polymer system, as the name suggests, is carried out before the main rheological test is conducted on the fluid material. This effectively eliminates any processing history prior to loading, thereby clearing its past memory. This also helps to determine a pseudo-viscosity profile for the material, in the form of viscosity vs torque/stress or viscosity vs shear rate plots. The material properties change over the time of testing (i.e. the amount of time necessary to form a stable structure), hence it is also very important to set and control the duration in which the pre-shear is given.

Pre-shear can be done in various ways such as:

1. At a constant shear rate
2. At varying shear rate, which can either have

If pre-shearing is not done before the main rheological test, then over the shear rate range considered, a different rheological behaviour is displayed, depending on the shear history previously experienced by the fluid. The temperature conditions as well as the pH range also influence the fluid behaviour. Thus, all the experiments should be performed at a constant temperature (preferably room temperature i.e. 25℃) and an acidic pH (around 3 to 5) (Chen *et al.*, 2014).

Pre-shearing technique is also applicable for re-liquefaction. If the shear thickening mixture solidifies or thickens with time, pre-shearing should be performed, so that the solidified mixture can again be converted to a liquid state. Sometimes stress history or part history of rotation of the principal stress also play a role in such phenomenon. The re-liquefaction resistance may or may not increase, even if the mixture becomes dense. But generally, larger the pre-shearing history applied during previous liquefaction, the weaker the material response against re-liquefaction. The primary reason could be the increase in the anisotropy induced by the pre-shearing history from the previous experiments (Wahyudi *et al.*, 2013).

The pre-shearing conditions may not always be fixed for all the fluids, but instead may vary according to the raw material constituents. Thus, the physical and chemical properties of all the raw materials have to be known before setting the conditions of the pre-shear tests.

Beside the rheology, pre-shear can also be used before the manufacturing of STF and its application i.e. impregnation in the Kevlar fabric.

1.7.1 LIMIT OF REVERSIBILITY

Stable and controllable shear rheological behaviour is beneficial for the application of STF. Such behaviour contributes to the two aspects of reversibility and reproducibility, which can be achieved by removing the loading effects (Lee and Wagner, 2003). Thus pre-shear is necessarily followed by some equilibrium time. The pre-shear conditions are determined by observing the evolution of viscosity at different shear rates (Chu *et al*., 2014; Khandavalli and Rothstein, 2014). A pre-shear stage should always be applied before the main rheological test, in order to erase this pre-shear history dependent behaviour. It can be observed from fig. 1, that a steady pre-shear is applied till an equilibrium state is reached, and this value of applied shear rate is the limit of reversibility (Galindo-Rosales *et al.*, 2009; Galindo Rosales and Rubio-Hernandez, 2010). Some researchers suggest that the shear rate should be chosen below the limit of reversibility to avoid any sample denaturation (Khandavalli and Rothstein, 2014). For reversibility and reproducibility of shear rheological behaviour, viscosity can be measured through both ascending and descending shear rate sweeps (Chen *et al.*, 2015). Thus the limit of reversibility is the maximum shear rate value that a sample can endure without losing its unique properties. It can be determined by comparing the apparent viscosity equilibrium values at each time interval. It is the maximum shear rate $\dot{\gamma}_{max}$ after which the sample is to be able to recover 90% of the equilibrium viscosity η_{eq} value, at that fixed shear rate (Galindo-Rosales and Rubio-Hernandez, 2010).

Pre-shear should be stopped after the constant shear stress is attained and before the shear stress eventually starts to decrease or at least before it decreases too much (i.e. the localization effect is limited). It is observed that higher the shear rate value, lower is the time of pre-shear, but at the same time if the shear rate is too high, a disruption in the micromolecular structure of the sample may occur.

1.7.2 EQULIBRIUM TIME (RESTING TIME)

Microstructure of STF suspension, is due to the agglomerate formation between primary particle aggregates, which link to each other by hydrogen bonds. Resting time influences the final size of the agglomerates. It is the time needed to achieve the equilibrium structure at rest. It is observed that lower molecular weight dispersion medium suspension takes less time to develop its equilibrium microstructure and form small aggregates. While larger molecular weight dispersion medium form bigger agglomerates and hence need more time to form its equilibrium structures (Galindo-Rosales *et al.*, 2009; Galindo Rosales and Rubio-Hernandez, 2010). The resting time should be long enough to let the primary particle aggregates contact each other to develop a volume filling network structure (Galindo-Rosales and Rubio-Hernandez, 2010). This means that the polymeric aggregates are evenly dispersed in the entire volume of the fluid sample.

Thus we can say that the resting time intervals are those in which $\dot{\gamma} = 0$, i.e. no shear is applied on the sample. The resting intervals are given at the start of the test to enable the relaxation of the sample after the gap setting of the measuring system (this may cause high internal stresses especially when testing highly viscous and viscoelastic samples), or after a pre-shear interval. This period is suited to enable temperature equilibrium.

Usually a low shear rate is taken and an intermediate equilibrium time is kept for resting, but some suggest that the suspension should be pre-sheared at a higher rate with very less equilibrium time (e.g. 100 s^{-1} for 30 s followed by 5 s rest time (Chu *et al.*, 2014). With longer equilibration and averaging times, irregular curves or termination of measurement by the machine itself (probably due to stress overloading) are frequently observed, especially for suspensions of higher concentrations. These anomalies are due to stress fluctuation often observed in measurements taken by a controlled shear rate rheometer. These may be caused by temporary jamming of suspensions. For shear thickening fluids fast measurement is better to avoid data fluctuations. Lower the equilibrium time, the starting shear rate or stress is reproducible (Chu *et al.*, 2014).

The various aspects of shear thickening fluids and their properties have remained a constant topic of research from the last 2-3 decades. A brief review of the work done on different kinds of shear thickening fluids is discussed in the next chapter.

LITERATURE REVIEW

In the recent years a pronounced effort has been put into understanding the rheological properties and microstructure of shear thickening fluids. In order to amplify these properties further, it is highly important to study various significant researches done in the past on STFs. The following chapter devotes to the brief review of numerous investigations done on shear thickening fluids.

2.1 SHEAR THICKENING FLUID PARAMETERS AND PROPERTIES

Nano technology has revolutionised the development of novel materials, by providing basic design, new properties and structures, resulting in increased performance and enhanced functionality of the material.One of the most advanced use of nano materials have been in the synthesis of shear thickening fluids. As stated above, there has been numerous studies related to shear thickening fluids in various fields. For example, the earliest use of STF was in the oil drilling sector as a well control fluid (Mintz *et al.,* 1983; Drake *et al.,* 1984).The studies of design, testing and modelling of smart viscous STF dampers were conducted by Zhang, Chang and Yeh (Zhang *et al.,* 2008, Chang *et al.,* 2011and Yeh *et al.,* 2012). Shear thickening fluids have also found immense use in other fields as, foam filling system in energy absorption devices (Ramirez J.G., 2004), medical fluid to minimize head and neck injury (Harrera *et al.,* 2013), as an adhesive fluid (Tabassum *et al.,* 2013) and as ballistic protection and stab resistant fluid (Joanna *et al.,* 2007; Decker *et al.,* 2007). Another major sector of polymer based nanocomposite materials composing of nano material fillers have also found potential use in various defence applications (Kurahatti *et al.,* 2010).

A lot of factors influence the behaviour of the shear thickening fluid, which may vary according to its specified use. Size of the dispersed phase has a great impact on all stages of the development of the fluid. The small size (<100 nm) of polymer nanocomposites, leads to a large interfacial area, which controls the degree of interaction between the filler and the polymer thereby controlling the properties. For nanoclay reinforced composite, the aspect ratio is of 1000, for well dispersed clay platelets without breaking. At high shear and high shear stress, the platelets break to cause the aspect ratio to be 30 to 300. The promising applications of nano composites for the production of shear thickening fluids have led to the production of body armour with more flexibility and reduced weight (Schadler, 2003; Lee *et al.,* 2002; Lee and Wagner, 2003; Lee *et al.,* 2003; Kushan *et al.,* 2014).

Particle size variation has been studied by many researchers, by varying the concentration of any one of the components in the STF (Zhang *et al.,* 2008). These studies are related to bi-dispersed suspensions constituting silica of two different sizes. The rheograms of colloidal suspensions with 'small' sized particles leads to an abrupt or sharp increase in the viscosity at critical shear rates. The 'large' particles contribute to the shear thickening effect above a shear rate of 1000 s^{-1}. The validity of Cox-Merz Rule, strain thickening at higher amplitudes and the decreasing trend of critical strain amplitudes with the rise in frequency can also be observed.

Colloidal dispersions have been a topic of deep research form many decades. (Cosgrove, 2005). Various models have been generated to study their fluid behaviour. Rheometries of various Non-Newtonian fluids and the theories related to the calculation of their yield stress have been explained by Barnes (Barnes, 1993). Empirical equations have been generated and simulations are performed, depicting the shear thickening behaviour using the Stokesian Dynamics technique (Brady and Bossis, 1988; Durlofsky *et al.,* 1987). This can be applied for both Brownian as well as non-Brownian motion particles (Banchio and Brady, 2003). These are important to study the hydrodynamic interactions and the lubrication force effects on the particles of the suspensions (Brady *et al.,* 1988). Both continuous and discontinuous thickening are observed using finite element numerical models and continuum mechanical models (De los Reyes and Stadler, 2010).

Especially for its use as a body armour and other defence applications, temperature plays a vital role in changing the behaviour of the shear thickening fluids. The effect of temperature on fumed silica suspensions have been studied in detail by Tian, Wu and Warren (Tian et al., 2013; Wu et al., 2012 and Warren et al., 2015). An inverse relation of temperature was observed with the critical shear rate and a direct relation with the fluid viscosity. The variation of molecular weight of both the media as well as the particles was also seen on the shear rate and the temperature dependent behaviour of the sample. The breaking of hydrogen bonds between the suspending silica particles and the dispersion medium is more when the molecular sizes of both the components are large and thus this gives rise to a continuous shear thickening. Hydrogen bonds existing between the individual molecules of PEG and silica, reduces the rate of exchange of the suspended molecules at the surface with the bulk fluid.

Table 2.1: Different STFs reported in literature:

S.No	Nanoparticles	Size (nm)	Dispersion Medium	Weight Fraction (%)	Volume Fraction (%)	Reference
1.	Precipitated Calcium Carbonate	30-200	Glycerine	-	37,41,43, 45,51,54	Chen, *et al.*, 2015
2.	Silica (SiO_2)	550	Anhydrous Ethylene Glycol (EG)	10, 67.5	-	Chu, *et al.*, 2014
3.	Corn-starch	0.014	Isopycnic CsCl brine	53.5 (% CsCl aq. Brine)	40	Chu, *et al.*, 2014
4.	Fumed Silica (Aerosil 200)	12	Poly Ethylene Oxide (PEO)	0.1 – 2	-	Khandavalli and Rothstein, 2014
5.	Fumed Silica	200 ± 25	KCl + Water	25, 27,29	-	Crawford, *et al.*, 2013
6.	Fumed Silica	7 &200	Poly Propylene Glycol (PPG 425)	5-50	20, 25, 30, 35	Idzkowska and Szafran, 2013
7.	Fumed Silica (Aerosil 200)	12	Poly Propylene Glycol (PPG 400 & PPG 2000)	10.378 & 10.286 % w/w for PPG resp.	5	Galindo-Rosales and Rubio-Hernandez, 2010
8.	Colloidal Silica	-	PEG 400 +additives (PEG 4000, 6000, 10000)	50 (Silica), 0,1,3,5 (additives)	-	Xu, *et al.*, 2010
9.	Corn-Starch &	0.014(CS),	Water &	-	-	Brown and

	Glass Spheres	0.088-0.125(GS)	Mineral Oil			Jaeger, 2009
10.	Fumed Silica (Aerosil R816)	12	Poly Propylene Glycol (PPG 400 & PPG 2000)	10.378 & 10.286 %w/w for PPG resp.	5	Galindo-Rosales, *et al.* 2009
11.	Spherical Colloidal Silica (MP 1040) & Ellipsoidal Precipitated $CaCO_3$ (MD 1074)	120+-5 (Silica) 328±103, 233±71, 201±77 (PCC)	Poly Ethylene Glycol PEG 200, 300, 400, 600	5-50	-	Wetzel, *et al.* 2004
12.	Colloidal Silica (MP 4540)	446± 8.4	Ethylene Glycol	40	55 & 60	Lee and Wagner, 2003
13.	Fumed Silica (Aerosil 200)	10-12	PEG 300 & PPG 425	10	-	Raghavan, *et al.*, 2000
14.	Sphere Silica coated with TPM	160, 330, 400	Tetrahydrofurfural Alcohol	-	64	Bender and Wagner, 1996
15.	Fumed Silica (Aerosil D150)	14	PPG 725	5	-	Raghavan and Khan, 1997
16.	Fumed Silica (Aerosil D150 & R805)	7-40	Mineral Oil and PPG	5 (in MO), 10 (in PPG)	-	Raghavan and Khan, 1995
17.	Polystyrene Latex	197±5				Chow and Zukoski, 1995
18.	Polystyrene	0.00161-	Water &	-	58.4	Boersma, *et*

	(PS)	0.00260	Water/Glycol Mix.			*al.,* 1991

2.2 PRE-SHEARING STUDIES

Fumed silica suspensions have a distinct time dependent behaviour. At the same time the presence of PEG as the polymeric dispersion medium make the shear thickening fluids as a 'memory fluid'. Thus the application of pre-shear in order to erase the stored shear history in the sample becomes mandatory. Applying the pre-shear ensured that the sample microstructure is not denatured and an equilibrium structure is established (Galindo Rosales *et al.,* 2009; Raghavan *et al.,* 2000 a, b; Khan *et al.,* 1994)

The pre-shearing concept covered the two aspects of limit of reversibility (Dullaert, 2005) and the resting time. The resting time affects the size of the agglomerates which thereby influences the strength of the microstructure. It was also deduced that using a higher molecular weight dispersion medium, but at the same time the hydrodynamic energy needed to increase the viscosity by dominating the hydrodynamic lubrication forces. The dynamic shear behaviour was also studied to differentiate the effect of flocculation with the properties of the non-flocculated suspension.

The diamagnetic property of SiO_2 finds its application in the production of magnetorheological fluids (Desai and Upadhyay, 2014). The chain like models and the micromechanical models were applied for such fluids. The mathematical modelling involving velocity function was used to perform numerical simulations for steady flows involving STFs (Galindo-Rosales *et al.*, 2011; Cherizol *et al.*, 2015).

Table 2.2: Pre-shear and equilibrium time studies reported in literature:

S.No	STF Constituents	Pre-Shear Condition	Resting Time	Test Conducted	Fixture Used	Test Temperature (℃)	Reference
1.	Precipitated calcium carbonate (PCC), Glycerine	0.1 s^{-1} for 90 s	90 s	Both Steady Shear and Oscillatory Shear Tests	Cone-and-Plate with cone angle of $20^{o}$and diameter of 25	25.0	Chen *et al.*, 2015

					mm		
2.	Nano silica-550 nm, Ethylene glycol (EG)	100 s^{-1} for 30 s	5 s	Steady Shear Tests	Plate-and-Plate with diameter of 25 mm	30.0	Chu *et al.*, 2014
3.	Fumed silica: Aerosil@200, Poly ethylene oxide (PEO)	50 s^{-1} for 240 s	240 s	Steady Shear and Amplitude Oscillatory Shear Tests	Parallel Plate with diameter of 40 mm	23.0	Khandavalli and Rothstein, 2014
4.	Fumed silica: Aerosil®200, PPG 400 and PPG 2000	1 s^{-1} for 300 s	60 s for PPG 400 1800 s for PPG 2000	Both Steady and Dynamic Oscillatory Shear Tests	Cone-and-Plate with cone angle of 2^o and diameter of 35 mm	25.0 ± 0.1	Galindo-Rosales and Rubio-Hernandez, 2010
5.	Fumed Silica: Aerosil®R816, PPG 400 and PPG 2000	1 s^{-1} until equilibrium apparent viscosity is achieved	60 s for PPG 400 1800 s for PPG 2000	Both Steady and Dynamic Oscillatory Shear Tests	Cone-and-Plate one with cone angle of 2^o and diameter of 35 mm and other with cone angle of 1^o and diameter of 60 mm	25.0 ± 0.1	Galindo-Rosales and Rubio-Hernandez, 2009
6.	Colloidal silica: MP4540, Ethylene glycol (EG)	1 s^{-1} for 60 s	Not given	Dynamic Shear Tests	Cone-and-Plate with cone angle of 0.1 rad and diameter of 25 mm and Parallel Plate with diameter	25.0	Lee and Wagner, 2003

					of 25 mm		
7.	Polystyrene latex, 10^{-3} M KCl	100 s^{-1} for 10 s	3600 s to 10800 s	Creep and Recovery Experiments	Couette Geometry with bob diameter of 25 mm	Not given	Chow and Zukoski, 1995
8.	Fumed silica: Aerosil D150 and R805, Mineral oil and PPG 725	2% strain for 60 s	12 s	Oscillatory Shear Tests	Cone-and-Plate One with cone angle of 0.1 rad and diameter of 25 mm and other with cone angle of 0.04 rad and diameter of 50 mm	Room Temperature	Raghavan and Khan, 1995
9.	Polystyrene, water, water-glycerol mixture	No pre-shear	1800 s - for thermal equilibrium	Steady Shear Tests	Concentric cylinder geometries with similar ratios of cup and bob diameters	20.0 ± 0.1 or 50.0 ± 0.1	Boersma, *et al.*, 1991

2.3 STF-FILLER COMPOSITES

Clays have been used since ancient time to provide strength as well as high viscosity to suspensions (Christie *et al.,* 2011; Larson; Harvey and Murray). Clays also provide high polymer thermal stability by reducing the thermal expansion coefficient of polymers thereby making it suitable of use as a protective armour in different temperature zones (Uddin 2008). Few investigations of the STF loaded with clay (e.g. Kaolin clay) for the use in protective fabric, have been done in the past decade (Rosen *et al.,* 2007). These studies also show the effect of different geometries or shapes of suspended solid on the shear thickening behaviour. Various quasi-static resistance tests have been performed in the sample to deduce its ballistic performance. The morphological studies and the stab-resistant tests on STF-glass fabric composites were conducted by Yu (Yu *et al.,* 2012). The damage mechanism of fabric experiencing low viscosity impact ware discussed by Kirkwood (Kirkwood*et al.,* 2004). Among various nano fillers, the CNTs or carbon nano tubes have also shown properties of enhance shear thickening despite of giving a greater aggregation effect (Sha *et al.,* 2013). Even on comparison of graphite nano platelets and the carbon nano tubes, it is seen that the CNTs gives a higher maximum viscosity in STFs having similar composition of the filler.According to the model mechanism it was shown that the volume fraction of the filler was proportional to the percolation concentration, whereas the filler density $\rho_x$was inversely proportional to the percolation concentration $\emptyset_x$ (Sun *et al.,* 2009).

$$\rho_x \propto \frac{1}{\emptyset_x}$$

The adsorption of dispersion medium PEG on the clay minerals as well as the effect of their molecular weights are discussed using adsorption isotherms. The thermodynamic parameters of enthalpy and entropy of adsorption were determined and their effects on the clay mixture was studied (Parafitt and Greenland, 1969)

A comparison of various properties of clays such as Kaolinite, Montmorillonite, Illite etc. is discussed by Ayadi (Ayadi *et al.,* 2013). One of the disadvantages of using clay minerals is its high settling tendency in its suspensions. The use of rod shaped hollow nano tubular structured halloysite clay resulted in a significant decrease in the sedimentation rate, thereby giving a consistent behaviour for a longer time duration (Hong *et al.,* 2013).

RESEARCH PROBLEM

The present study is mainly focused upon the effect of the addition of a second dispersed phase in the form of a nano-filler in the fumed silica based shear thickening fluid forming a composite mixture. This fluid can be used in protective body armours, such that the addition of nano-filler can increase its mechanical strength thereby making it more durable and high impact resistance and at the same time reducing its cost making it economically feasible for mass production.

3.1 RESEARCH OBJECTIVES

From the literature it is well known that most of the shear thickening fluids formed and studied till now are composed of a single solid and liquid phase. With the advent of the nano-materials, composite STFs can be created using:

1. Different size of silica particles (the main constituent which results in the shear thickening behaviour)
2. Nano fillers such as HNT, CNT, GNT etc. along with simple or fumed silica.

The present study dealing with the work on shear thickening fluids accomplishes the following objectives:

1. Synthesis of the bi-dispersed STF composing of fumed silica (11 nm) and simple silica (400 nm) using PEG 200 as the dispersion medium.
2. Forming a rheological protocol for the above fluid so as to remove its previous shear history providing more significant and reproducible results.
3. Production of composite STF using halloysite nano-tubes (HNTs) and fumed silica and study of its rheological properties.
4. Comparison of steady state as well as dynamic test results of higher percentage HNT-fumed silica composites.

MATERIALS AND METHOD

4.1 MATERIALS

The materials used for sample preparation of shear thickening fluids are:

4.1.1 Dispersed phase (solid)

A. Simple Silica

Silicon dioxide, also called silica, is an oxide of silicon with the chemical formula SiO_2. Silica is most commonly found in nature as quartz, as well as in various living organisms. It is the major constituent of sand. Silica is also present in a highly complex form in various minerals and can also be produced synthetically. Silica can also naturally occur in the form of flint and in some plants in crystalline phase. All its parameters such as particle size, surface area, pore size, pore volume etc. vary according to its different forms. The crystalline silica can be classified as:

- Quartz,
- Tridymite, and
- Cristobalite

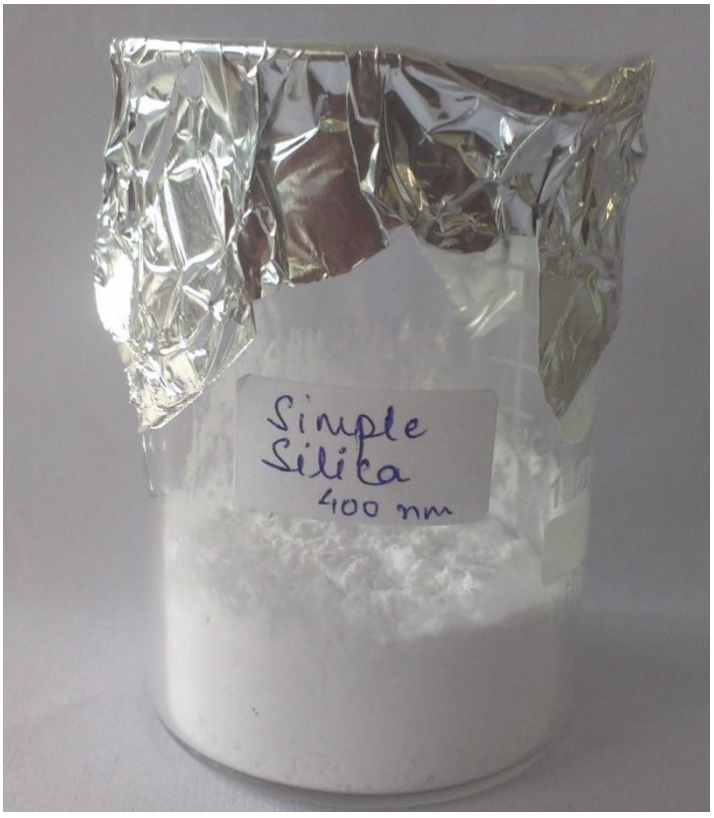

Figure 4.1: Silica

Some of the important applications of silica are:

1. Synthesis of silicates
2. Used for catalytic growth of oxide and nitride nanowires
3. As structural material in microelectronics
4. An important constituent in food industry

It is the major component of STF because of its enormous surface area and its tendency to show thickening and thixotropic properties. Particle sizes are for primary particles, which form branched, chain-like aggregates a few tenths of a micron long. They may contain adsorbed H_2O and CO_2 which is removable by calcining at temperature greater than 900°C.

Silica to be used for experimentation is obtained from Om laboratories, India.

Table 4.1: Specifications of simple silica

Formula	SiO_2
Molecular weight	60.08
Particle Size	400 nm
Assay	99.8%
Surface Area	175-225 m^2gm^{-1}
Aggregation Form	Branched aggregates, a few tenth micron long

B. Fumed Silica

Fumed silica (also known as silicic anhydride and silicon dioxide amorphous) is the most favoured material as a rheological modifier, due to its thixotropic behaviour and thickening property. It has high specific surface area and branching structure, which displays its remarkable rheological properties. Some of the technological applications of fumed silica are:

1. Preparation of shear thickening fluids,
2. As solid electrolytes in fuel cell technology,
3. Stabilizing agent in foams and emulsions,
4. Viscosity modifier for enhanced oil recovery,

5. Fillers in polymer composites due to improved thermomechanical properties,
6. Preparation of photo catalytic materials,
7. Preparation of reinforced nano-composites,
8. Preparation of epoxied natural rubber composites.

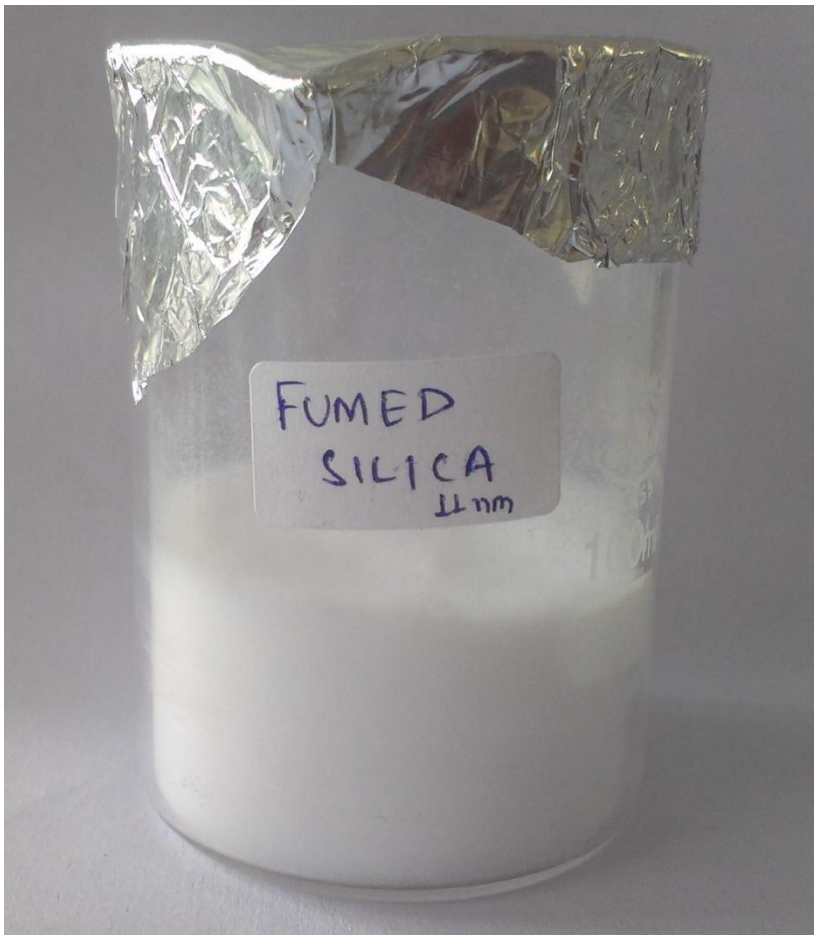

Figure 4.2: Fumed Silica

Fumed silica is amorphous non porous silica, synthesized by high temperature (flame) hydrolysis of $SiCl_4$, in O_2 (N_2)/H_2 flame. It is hydrophilic in nature due to the presence of hydroxyl or silanol group (-OH) on the surface. These groups let particles link each other in liquids by means of hydrogen bonding and are responsible of its ability to form network structures. This is the main reason why fumed silica systems are widely used in the emerging technologies.Fumed silica used in the present study is supplied by Sigma Aldrich.

Table 4.2: Specifications of fumed silica

Manufacturer	Sigma Aldrich
Model	S5130
Appearance	White powder
Refractive Index	n20/D 1.46
Particle Size	0.007 µm (7 nm)
Surface Area	395 ± 25 m^2gm^{-1}
Density	0.0368gcm^{-3} at 25^oC (Bulk density)

C. Halloysite nanotube (clay)

Halloysite is a 1:1 alumino silicate clay mineral with the major constituents as aluminium (20.9%), silica (21.76%) and hydrogen (1.56%). Halloysite is one of the most important member of the kaolin sub group of minerals. It has a similar composition as that of kaolinite, except that it contains additional water molecules in between its layers, which can be lost easily. It has a bi-layer tubular morphological structure. Halloysite formed due to hydro thermal alteration of the clay minerals, occurs naturally in a cylindrical shape. Due to its structure it can be used as a filler in natural or modified form in nano composites. Halloysite is environmental friendly and biocompatible.

Advantages of halloysite:

- Nanotubular fillers eliminate the need for exfoliation
- Tubular geometry provides a mechanism for increasing the binding for the tubes to the polymer matrix, with minimum required surface modification of clay nanotubes.
- Additional functionality of tubular geometry, is enabled by the inner open space or cavity of the tube.
- HNTs have low density of hydroxyl functional groups, when compared to clays, which makes HNTs disperse better in the polymer matrix better than the other clays or the CNTs (Carbon nano tubes).
- Tetrahedral structure results in a less constrained structure.

- Silica and Alumina differ in their respective reactivity.
- Shows thermal stability and flame retardant effects.

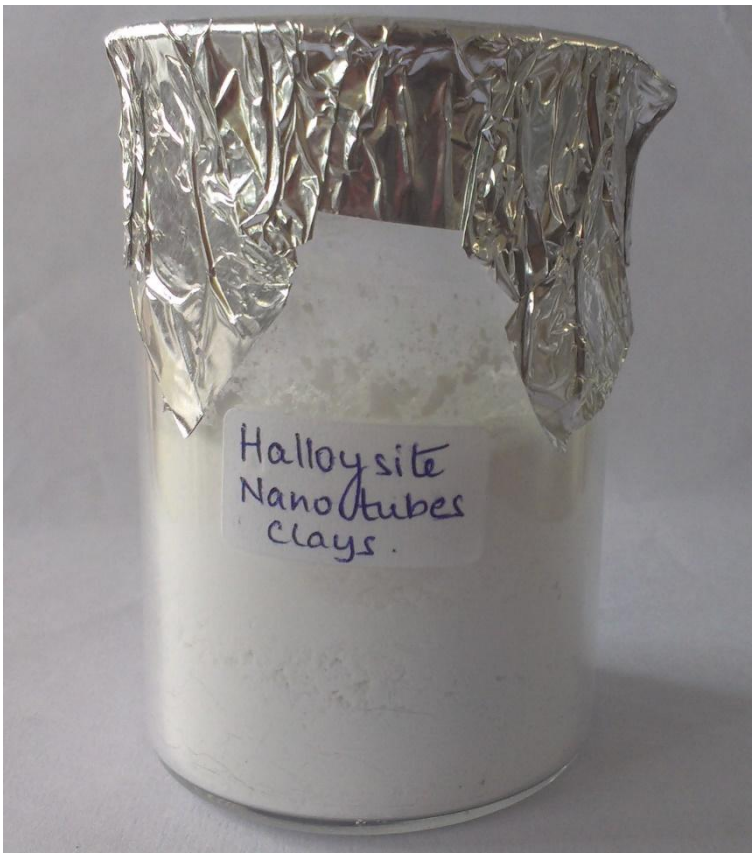

Figure 4.3: Halloysite nanotube clay

Table 4.3: Specifications of halloysite nanotube clay

Manufacturer	Sigma Aldrich
Formula	$Al_2Si_2O_5(OH)_4.2H_2O$
Molecular weight	294.19 $gmol^{-1}$
Appearance (colour)	White to Tan
Appearance (form)	Powder
Geometry	Monoclinic
Pore Volume	1.26 – 1.34 $mlgm^{-1}$
Specific gravity	2 – 2.65

pH	6.5 – 6.9
Diameter	30 – 70 nm
Length	1 – 3 μm
Average aspect ratio	40

4.1.2 Dispersion Medium (Liquid)

A. Polyethylene glycol (PEG 200)

Polyethylene glycols are available in a range of low to medium molecular weight poly-ethers having primary hydroxyl groups at each end. PEG is also known as Polyethylene oxide (PEO) or Polyoxyethylene (POE), depending on its molecular weight. All polyethylene glycols are completely soluble in water. Some major features of poly ethylene glycol are:

1. Good solvent action,
2. Good stability,
3. Good lubricating property,
4. Very low toxicity,
5. Non-irritating, and
6. Highly compatible with other compounds.

Due to its use as a solvent, lubricant as well as a binder, PEG is found as a major constituent in various commercial as well as non-commercial applications in field of pharmaceuticals, cosmetics, paper, textile, rubber, ceramics, wood processing, packaging and manufacturing of surfactants, dispersant resins, plastics etc. Its use an organic media in STF production is widely known.

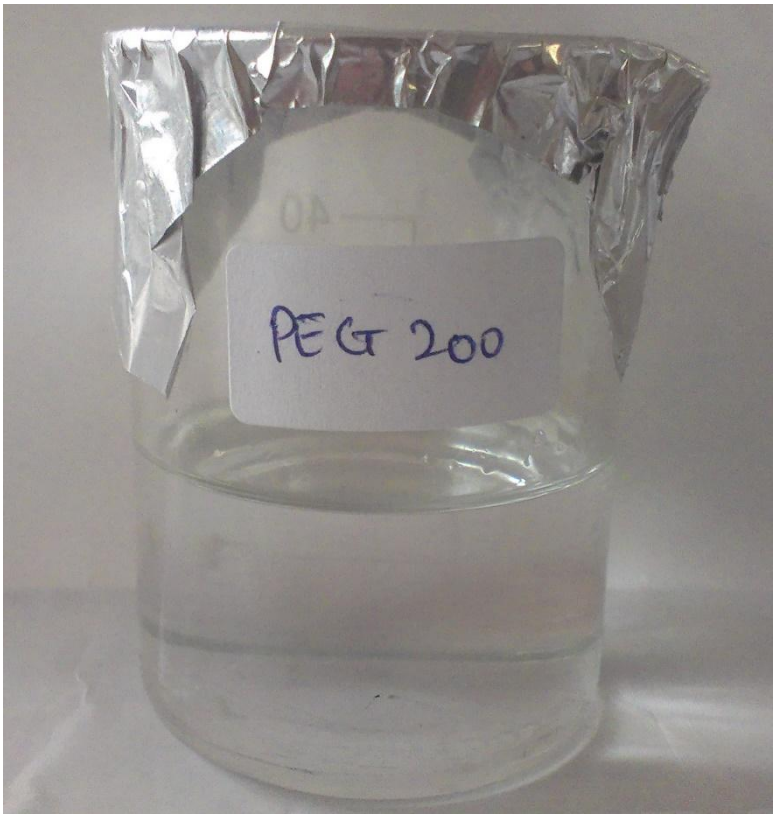

Figure 4.4: Polyethylene glycol (PEG 200)

Table 4.4: Specifications of polyethylene glycol

Average Molecular weight	200 (for PEG 200)
Linear Formula	$H(OCH_2CH_2)_nOH$
Vapour density	>1(vs. air)
Vapour Pressure	<0.01 mmHg (20^oC)
Form	Liquid
Auto ignition Temperature	305^oC
Viscosity	4.3 cSt (98.88^oC)

4.2 SILICA BI-DISPERSED NANO COMPOSITE

4.2.1 METHODOLOGY FLOW-CHART

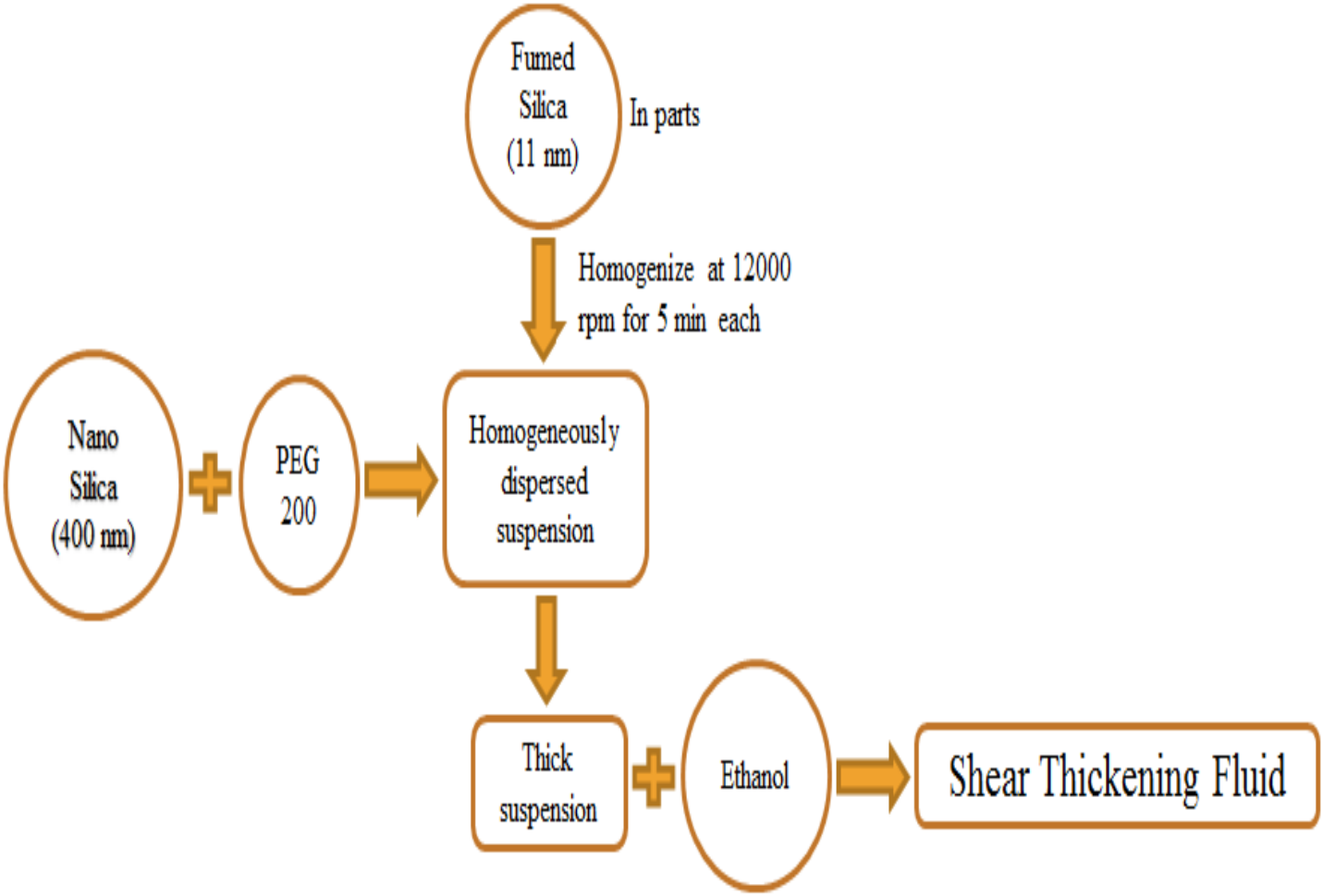

Figure 4.5: Methodology flowchart

4.2.2 SAMPLE PREPARATION

Initially 10.8 gm of nano silica was added to 25 gm of PEG 200 and hand-stirred until a homogeneously dispersed suspension was formed. Then a total of 8.36 gm of fumed silica was added to this. Because of nano sized particles, homogeneous dispersion of fumed silica is difficult, thus a high speed homogenizer had to be used. Small quantity (1-2 gm) of fumed silica was added in batches and the mixture was homogenized at 12000 rpm for 5 min. If the viscosity of the mixture was too high, small quantity of ethanol was added to dilute the suspension.

On adding all the constituents a thick paste was formed into which again some ethanol was added and this completely fluidic mixture was homogenized for 10 min at the end. Then it was allowed to stay at rest for 18 h. Later it was sonicated using a sonication probe for 20 min in intervals of 10 min, with a resting time of 10-15 min between each so as to cool down the heated probe.

Figure 4.6: Simple silica – Fumed silica composite STF

4.2.3 PRE-SHEARING PROCEDURE

Pre-shearing, which is necessary to remove the loading effects and the previous shear history of the fluid sample has two main elements:

i. A constant shear rate or a shear rate range at which the sample is pre-sheared, and
ii. The time for sample pre-shearing.

A step by step procedure is followed to determine these properties. All measurements are taken considering an error of ± 5 s while taking the readings i.e. a time laps of ± 5 s is present between the tests which occurred while setting the conditions etc.

Guidelines for pre-shearing time:

The pre-shearing time can be determined using the following empirical relation:

$$\frac{d\tau(t)}{dt} \leq 0.01$$

(Galindo-Rosales and Rubio-Hernandez, 2009)

where, τ is the shear stress, t is the time, μ is the viscosity, and $\dot{\gamma}$ is the shear rate.

Solution:

$$d\tau(t) \leq 0.01\ dt$$

$$d\left[\mu\left(\frac{du}{dy}\right)\right] \leq 0.01\ dt$$

$$\frac{du}{dy} = \dot{\gamma}$$

The optimum value of $\dot{\gamma}$ is taken as 1 s^{-1}(obtained experimentally).

$$\dot{\gamma}\ d\mu \leq 0.01\ dt$$

$$1.\ d\mu \leq 0.01\ dt$$

$$\int_{132}^{138} d\mu \leq \int_{0}^{t} 0.01\ dt$$

(132 Pa.s and 138 Pa.s are the lower and upper limits of the viscosity range between times 156 s and 600 s, obtained experimentally. Theses limits were chosen from the tabulated data generated during the experiment. Within this range the viscosity of the sample was nearly constant.)

$$6 \leq 0.01\ t$$

$$t \geq 600$$

Hence, the time for pre-shear would be greater than or equal to 600 s.

A. ROTATIONAL TESTS PRE-SHEARING PROCEDURE:

1. Determination of the limit of reversibility:
   i. After the sample was loaded, a gap of about 5 min (or until the set temperature wasachieved) was maintained to let the sample equilibrate.

ii. A constant shear rate of 0.1 s^{-1} was applied for 600 s, with readings taken at aninterval of 6 s.
iii. Then viscosity vs time graph was obtained by increasing the shear rate to $\dot{\gamma}$ s^{-1}, where $\dot{\gamma}$ s^{-1} values are 1, 2, 3, and 5 s^{-1}.
iv. The test was again repeated at 0.1 s^{-1}, for 600 s.
v. The values obtained from point (iv) were compared with those obtained in (ii). Thesevalues must lie within 80 to 90 % range of the previous values.

2. Determination of the resting time or the equilibrium time:
   i. After loading the sample, an initial shear rate of 0.1 s^{-1} was applied for 600 s. Thistime was sufficient to attain a steady state.
   ii. Then the pre-shear of 0.1 $s^{-1}$was applied for 600 s.
   iii. A resting time of 't' s was given to the sample.
   iv. Immediately after that, again the loaded sample was sheared at 0.1 s^{-1} for 600 s, to check its stability.
   v. The values of time 't' varied as 300, 600, 900, 1200 and 1500 s. Lower as well asupper values of the time are taken compared to the pre-shearing time.

After the pre-shearing and the equilibrium resting time, the main rheological tests were performed.

B. OSCILLATORY TESTS PRE-SHEARING PROCEDURE:

1. To show the variation at higher strain percentages:
   i. Assume a lower strain rate for the sample (here, 10%).
   ii. Obtain the storage modulus variation for the specified strain rate for a set time duration (here 600 s).
   iii. Notice the nature of the G' values. If it lies in a straight or nearly straight line, select this as the lower limit for the rheological tests.
   iv. If not, again repeat the step using a higher value of strain percent.
   v. Following this, the next time sweep performed was again on the previously assumed value.
   vi. For both similar strain percentages the graphs were compared for the structural recovery.

The values of higher strain percentages were selected as 50 %, 100%, and 150%.

2. To obtain the lower strain percentage:
   i. Repeat the experiment for the previously assumed lower strain rate (10%).
   ii. Again, check the nature of the G'curve.
   iii. Perform the same experiment for same time duration (600 s) using different lower values of strain %.
   iv. The value of strain percent at which minimum distorted curve is obtained is selected as the lower limit of strain %.

The values of lower strain percentages were selected as 7%, 5%, 3%, 2%, and 1%.

4.2.4 MAIN RHEOLOGICAL TESTING PROCEDURE

The rheological tests were performed immediately after that. These tests were performed on Rheometer MCR 52 of Anton Paar, Germany. A cone and plate geometry, with a diameter of 40 mm and a cone angle of 1^o (smaller cone angle is advantageous for viscometric flows), was used for all the measurements. While performing the rotation tests using a plate and plate (or parallel plate) geometry, the outer fluid moves faster, whereas near the centre it hardly moves at all. Thus, a cone and plate geometry becomes significant for this, with the cone surface leading to a homogeneous distribution of shear rate. A constant temperature of 25^oC was maintained during all the tests. Two type of rheological tests are performed on this sample:

i. Rotation Tests (Steady shear measurements)
ii. Oscillatory Tests (Dynamic shear measurements)

The entire process of rheological testing consists of a set protocol, which includes 3 main steps, as follows:

i. Pre-shearing of the sample to remove the loading effects.
ii. Resting time of the sample so as to achieve equilibrium.
iii. Main rheological test, to check the shear thickening property.

A. STEADY SHEAR (ROTATION TESTS PROCEDURE)

The main rotational test was performed in the shear rate range of 1 s^{-1} to 1000 s^{-1}. Total 100 measuring points were plotted in the time duration of 200 s with each measuring

point plotted after 2 s. Here, the viscosity vs. shear rate and the shear stress vs shear rate graphs were generated. Once the test was performed directly after loading the sample, and the second time it was performed when the pre-shear and the equilibrium time conditions were given prior to it. Both these tests were performed twice, each with a new sample loading.

B. DYNAMIC SHEAR (OSCILLATORY TESTS PROCEDURE)

The main oscillatory test was performed in the shear strain range of 1% to 100%. A total of 100 measuring points were plotted in the time duration of 600 s with each measuring point plotted after 6 s. Here, the elastic modulus (storage modulus, G') and the viscous modulus (loss modulus, G'') vs. the shear strain graph was generated. Ones the test was performed directly after loading the sample, and the second time it was performed when the pre-shear and the equilibrium time conditions were given prior to it. Both these tests were performed twice, each with a new sample loading.

In the dynamic oscillatory shear measurements, a sinusoidal deformation $\gamma = \gamma_\circ \sin \omega t$ was imposed on the sample at a fixed frequency, ω, and the maximum strain amplitude, $\gamma_\circ$. The resulting stress, τ_{xy}, has components given by:

$$\tau_{xy} = G'\gamma_\circ \sin \omega t + G''\gamma_\circ \cos \omega t$$

In this equation, the stress component which is in-phase with the deformation defines the storage or elastic modulus, G', whereas, the stress component which is out-of-phase with the strain defines the loss or viscous modulus, G''. The shape and magnitude of the elastic modulus is sensitive to the microstructure of the system (Khan *et al.*, 1994).

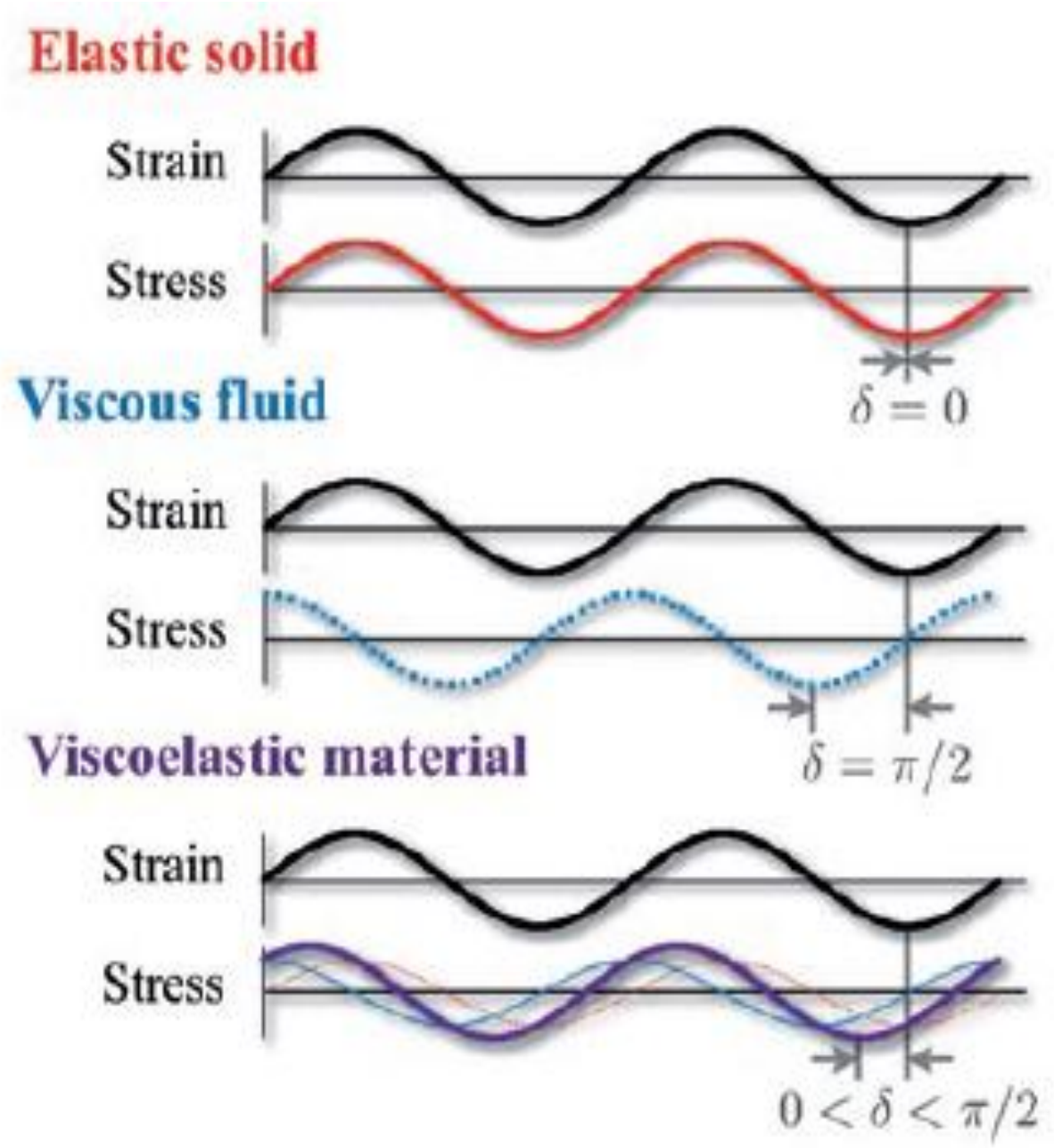

Figure 4.7: Schematic stress response to oscillatory strain deformation for an elastic solid, a viscous fluid and a viscoelastic material (Wyss *et al.*, 2007).

As shown in figure. 4.7, viscoelastic materials show a response that contains both in-phase and out-of-phase contributions. Such response reveal the extent of solid-like (red line) and liquid-like (blue dotted line) behaviour. As a consequence, the total stress response (purple line) shows a phase shift δ with respect to the applied strain deformation that lies between that of solids and liquids, $0 < \delta < \frac{\pi}{2}$.

4.3 HNT-FUMED SILICA NANO COMPOSITE

4.3.1 METHODOLOGY FLOW-CHART

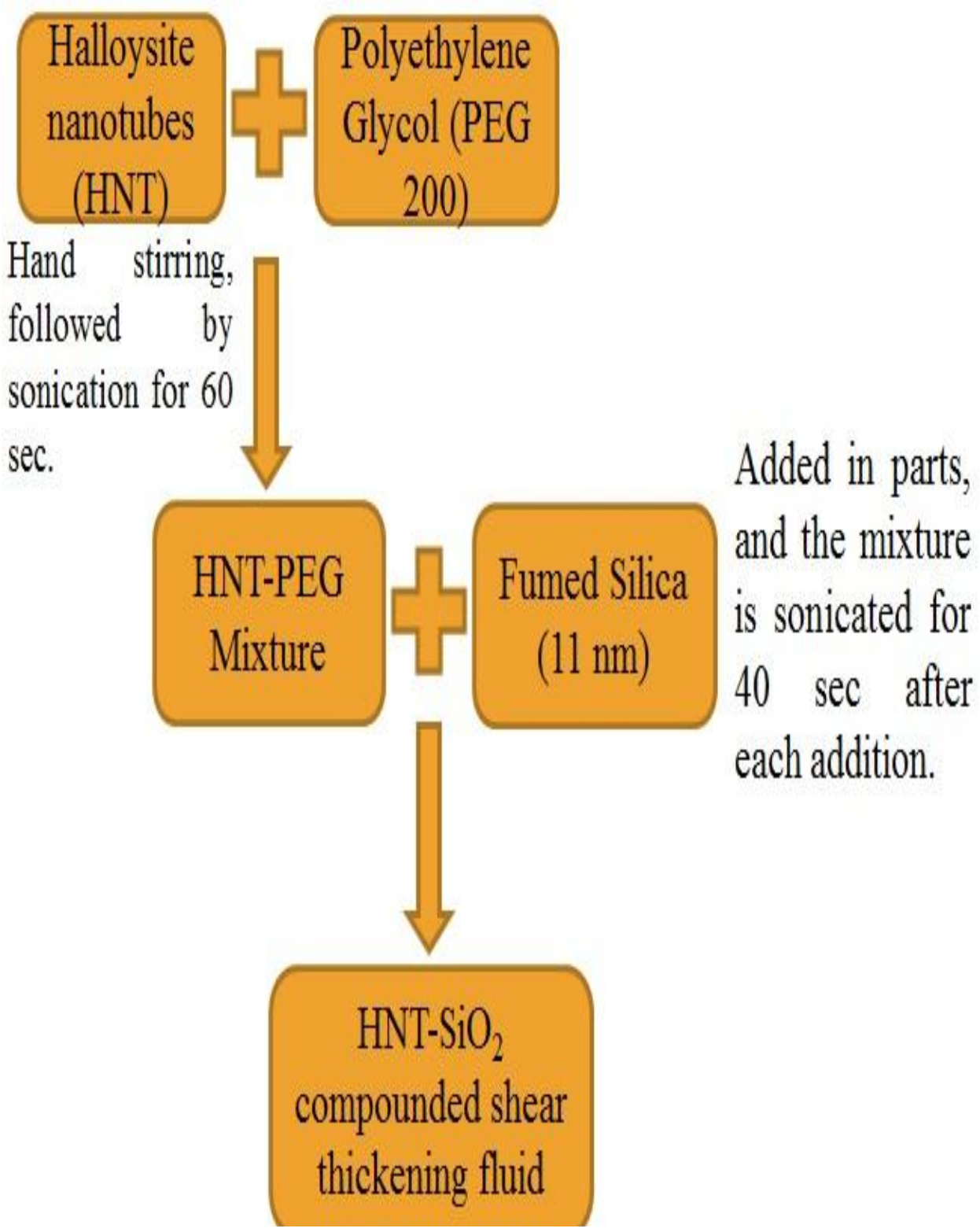

Figure 4.8: Methodology flowchart

4.3.2 SAMPLE PREPARATION

Fumed silica has the ability to form network structures in a polymeric liquid and the clay helps in building strong hydrogen bonds, linking itself to fumed silica. Initially, halloysite was dispersed in PEG 200 by simple hand stirring followed by sonication, until all lumps were broken. Then fumed silica was added in parts in the above mixture and sonicated after each addition to obtain proper consistency of the mixture. The final shear thickening fluid generated constituted 20% fumed silica (by weight) and 1% halloysite clay (by weight) in PEG.

This mixture was allowed to rest for 24 hours to remove ant air bubbles trapped inside and then the rheological tests were performed on it. These tests were performed on Rheometer MCR 52 of Anton Paar, Germany. A cone and plate geometry, with a diameter of 40 mm and a cone angle of 1^{o} was used for all the measurements. Both rotational (steady shear measurements) as well as oscillatory (dynamic) tests were performed on this sample.

Similarly, 3% and 5% HNT-fumed silica composites were prepared by increasing the weight percentages of HNT in PEG 200.

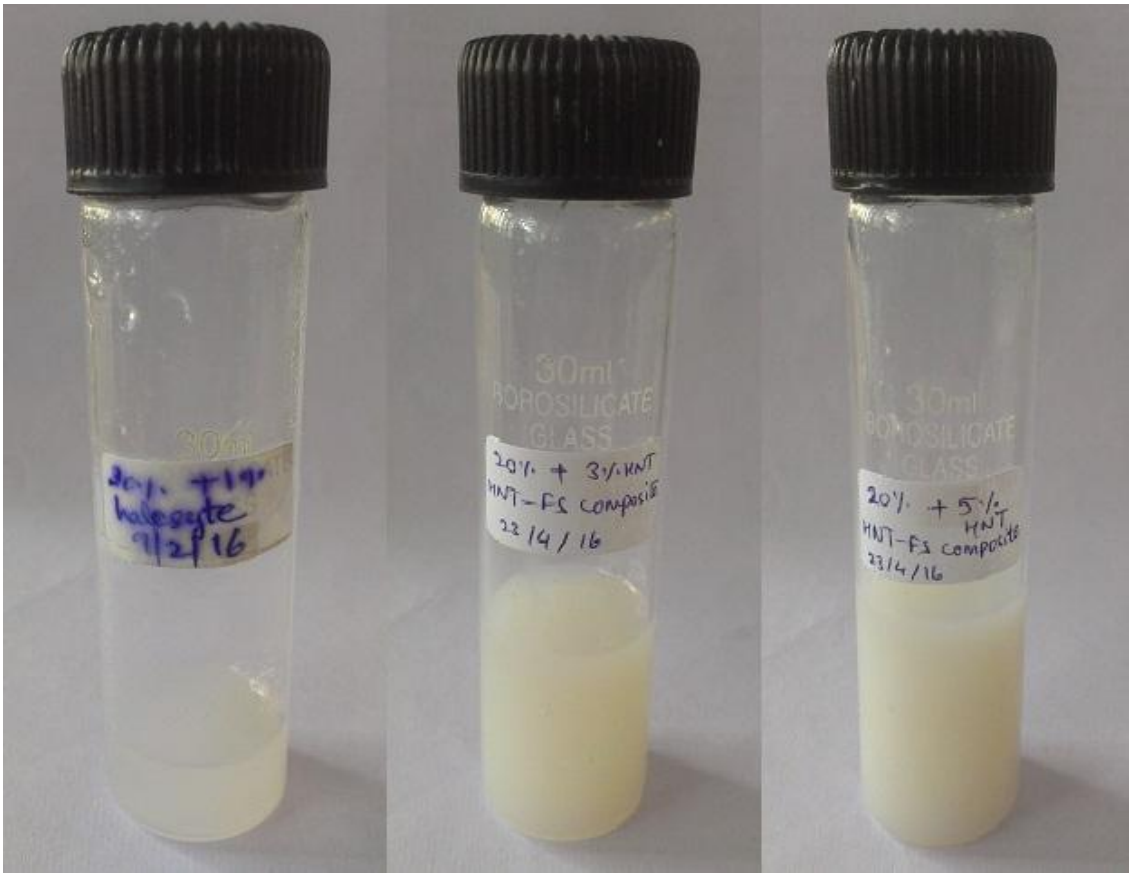

Figure 4.9: 1%, 3% and 5% HNT-fumed silica composite shear thickening fluids

RESULTS AND DISCUSSION

5.1 PRE-SHEARING TEST RESULTS

A. ROTATION TESTS

The pre-shear conditions were determined by observing the evolution of viscosity at different shear rates. The time required to reach a steady state value at a given shear rate was set as the duration of pre-shear, and the shear rate was chosen below the limit of reversibility to avoid any sample denaturation. The following results were obtained from the different tests conducted for the determination of pre-shear conditions.

1. A comparison between the behaviour of the sample at two different loadings:

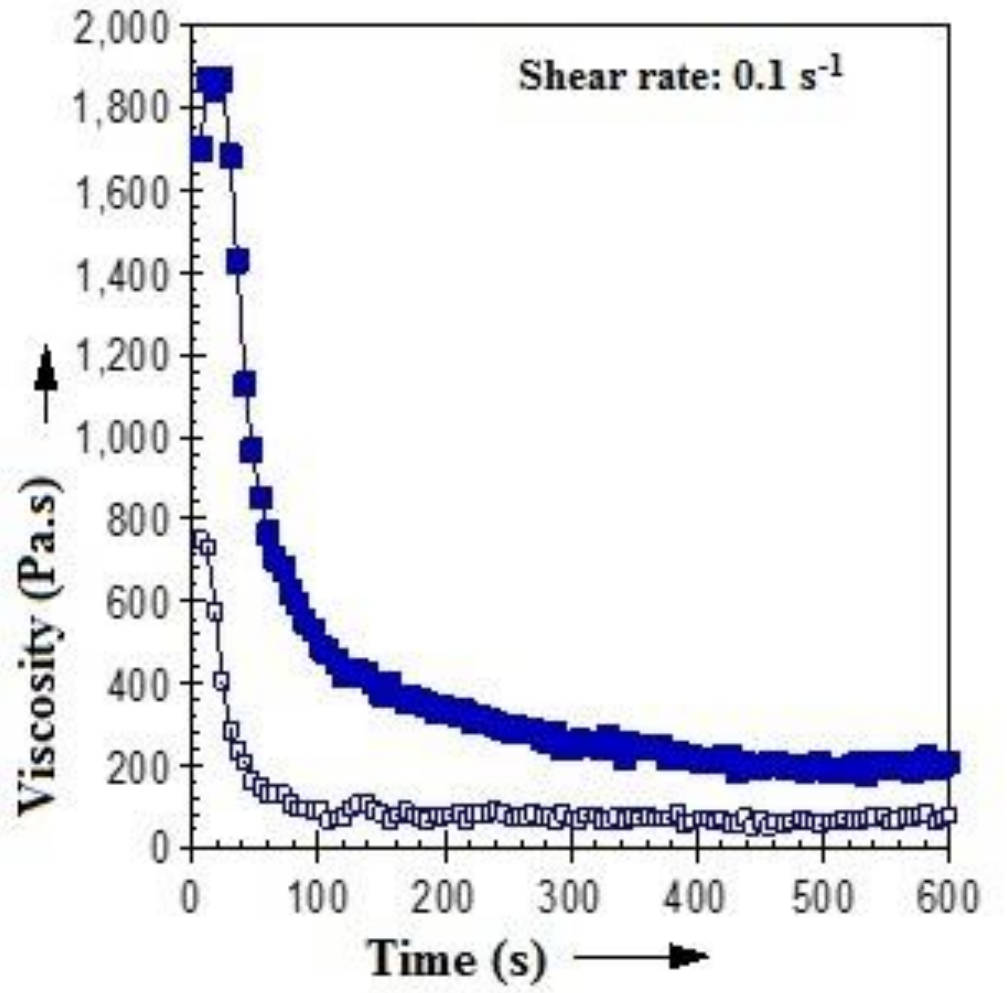

Figure 5.1: Variation of apparent viscosity withtime at a shear rate of 0.1 s^{-1}

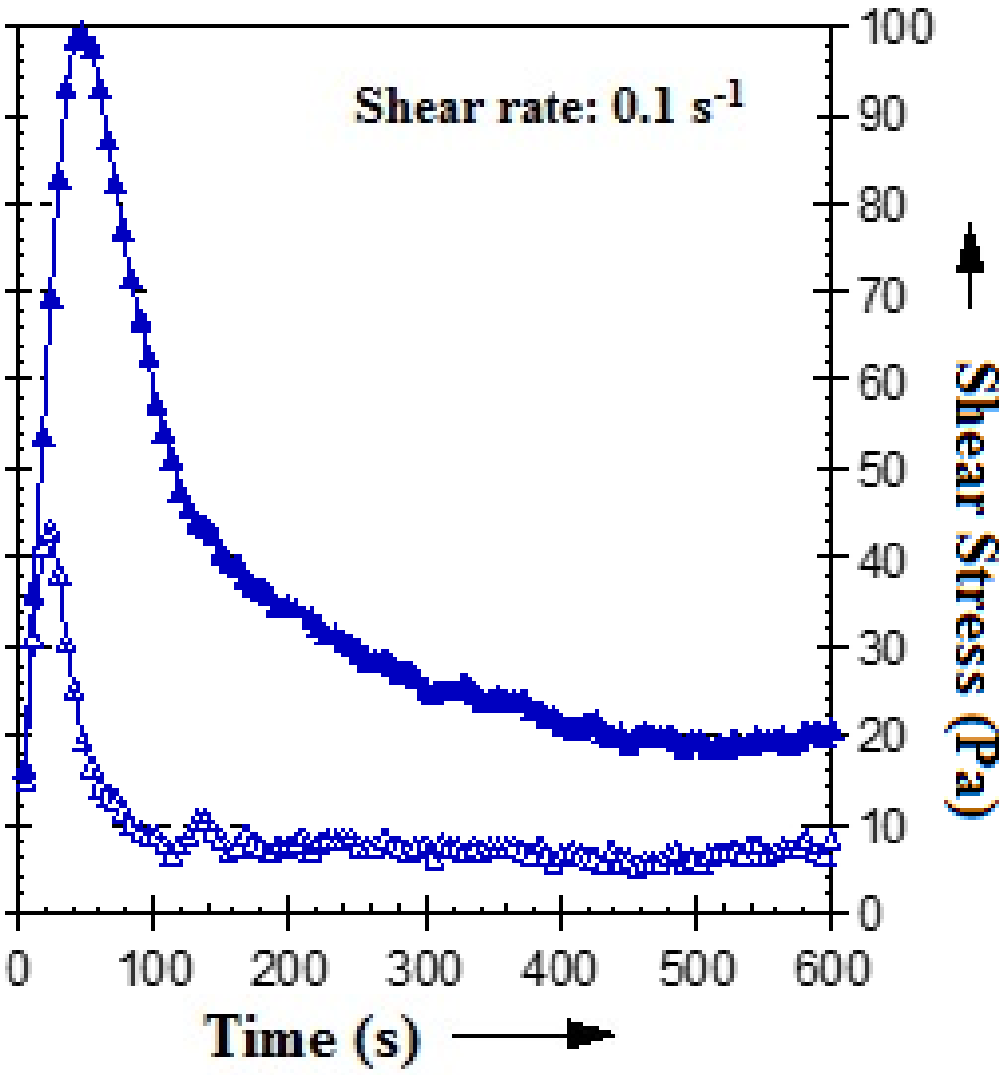

Figure 5.2: Variation of shear stress with time at a shear rate of 0.1 s^{-1}

Figures. 5.1 and 5.2 show the variation of apparent viscosity and shear stress with time at a specified shear rate (0.1 s^{-1}). These graphs demonstrate that the sample behaves in a different manner every time a new loading is done on the geometry, for fresh readings under identical conditions. The nature of the curves are same, and after a particular time nearly stable values of the parameters are achieved. Such behaviour of the sample may be attributed to two reasons:

a. The sample tested was prepared about 60 days ago. During the long time span between the preparation and the testing of the sample many microstructural change could have occurred in it, leading to variability in the parameter readings.

b. The mixture sample was directly loaded on the geometry without providing sonication.

Though, the long interval of 60 days leads to inconsistency of the readings, it also helps in understanding how the shear thickening fluid will behave practically once it has been coated on the fabric for the ballistic performance. Even, sonication which helps in proper dispersion of the solids in the polymer liquid and breaking of any flocs formed in the sample, also leads to air bubble formation in the fluid. These air bubbles alter the initial viscosity of the sample and also cause hindrance in shearing, thereby giving rise to highly modulating readings. These reasons will be applicable for all the readings taken with this shear thickening fluid sample.

2. Comparison of the reproducibility of the readings after denaturation of the sample:

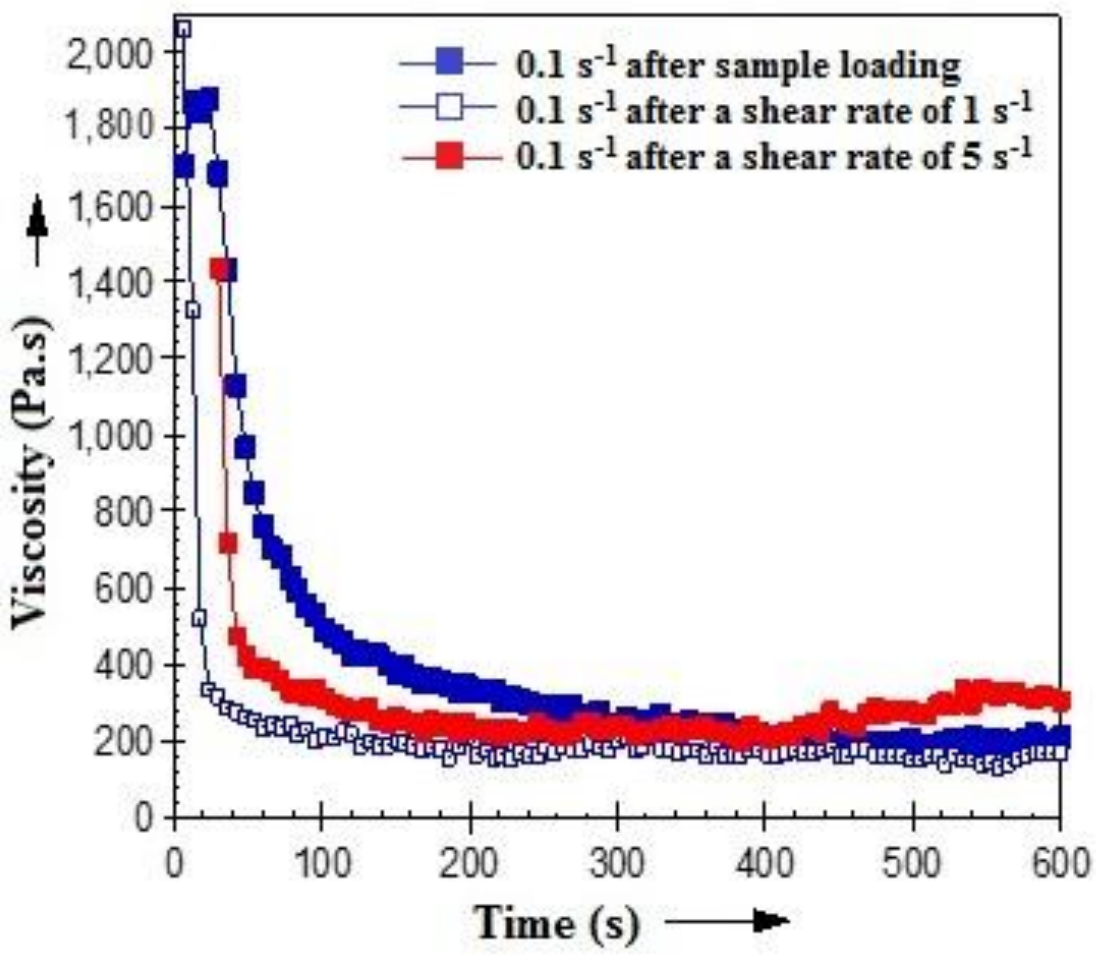

Figure 5.3: Reproducibility of viscosity for shearrates of 0.1, 1, and 5 s^{-1}

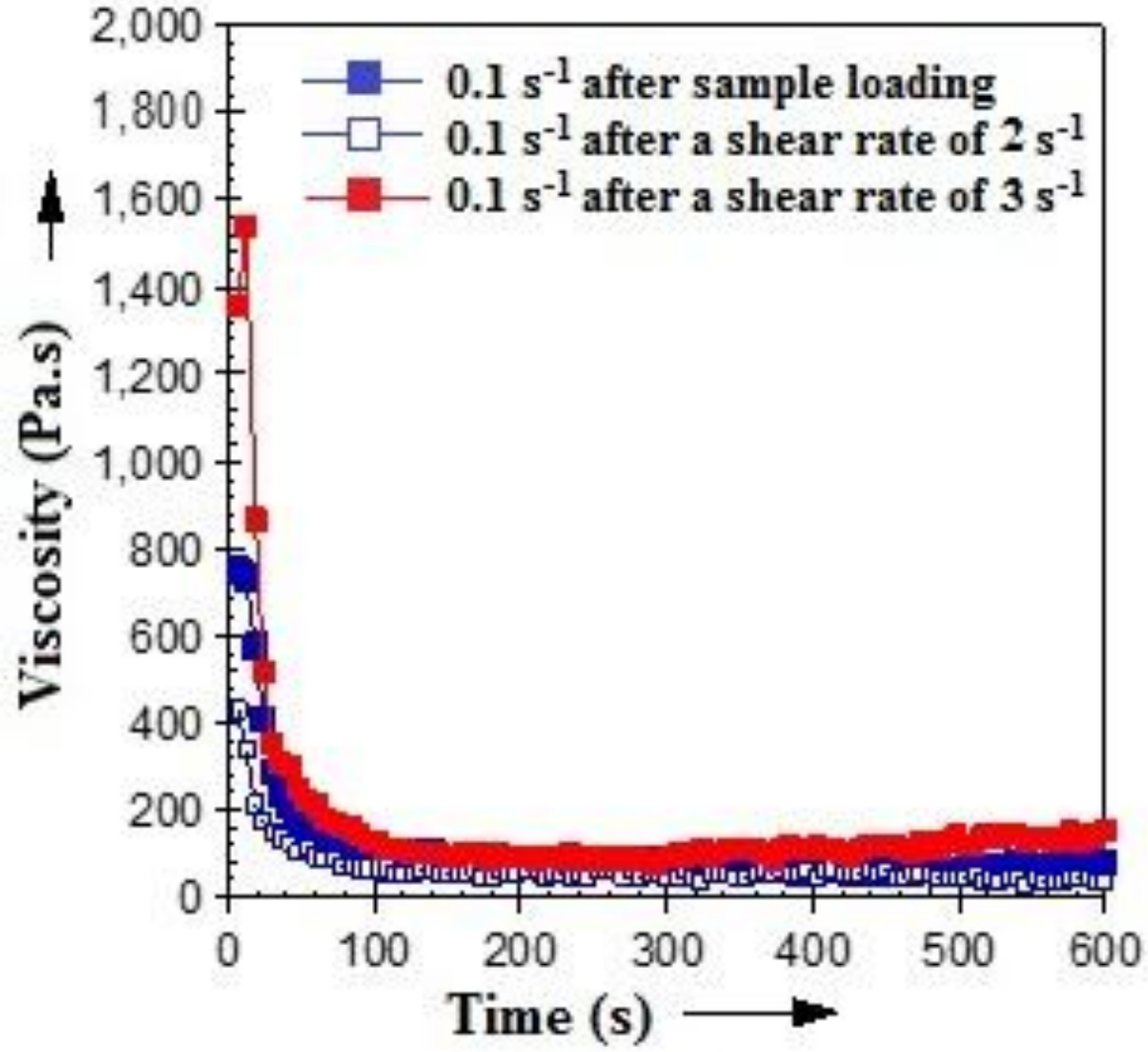

Figure 5.4: Reproducibility of viscosity forshear rates of 0.1, 2, and 3 s^{-1}

Here, all the three curves are plotted at the same shear rate of 0.1 s^{-1} for 600 s. This shows that once the sample is sheared at a particular shear rate, it gets denatured and if the shearing is applied again at a previous shear rate, reproducible results are not obtained. In Figure. 5.3, all the readings were taken at 0.1 s^{-1} shear rate, once immediately after loading and the other two after the sample was sheared at 1 s^{-1} and 5 s^{-1} respectively. Similarly, in Figure. 5.4, one reading was obtained after loading, and the other two after shear rates of 2 s^{-1} and 3 s^{-1} respectively.

Here we can observe that the readings taken after 1 s^{-1} and 2 s^{-1} shear rates lie in the range of approximately 80-85% of the initial 0.1 s^{-1} values. While the readings after 5 s^{-1} and

3 s^{-1} overlap the initial values and exceeds beyond those of 0.1 s^{-1}. Thus, 2 s^{-1} shear rate is considered as the higher limit of the shear rate range beyond which the sample structure is completely denatured. Hence, the pre-shear can be applied either in the range of 0.1 to 2 s^{-1} or for a constant value lower than 2 s^{-1}.

Another conclusion that can be drawn from these graphs is the minimum time limit for which this pre-shearing should be performed. This time will vary from sample to sample depending upon its nature and material constituents. This pre-shearing time is observed as the value beyond which the apparent viscosity values become nearly constant with time. Here, it can be detected that nearly constant viscosity starts to occur between 500 and 600 s. Henceforth, the pre-shearing time for all rheological experiments for this shear thickening fluid was taken as the maximum time limit, i.e.600 s.

3. The comparison of the shear stress with time for the mixture sample at different resting times:

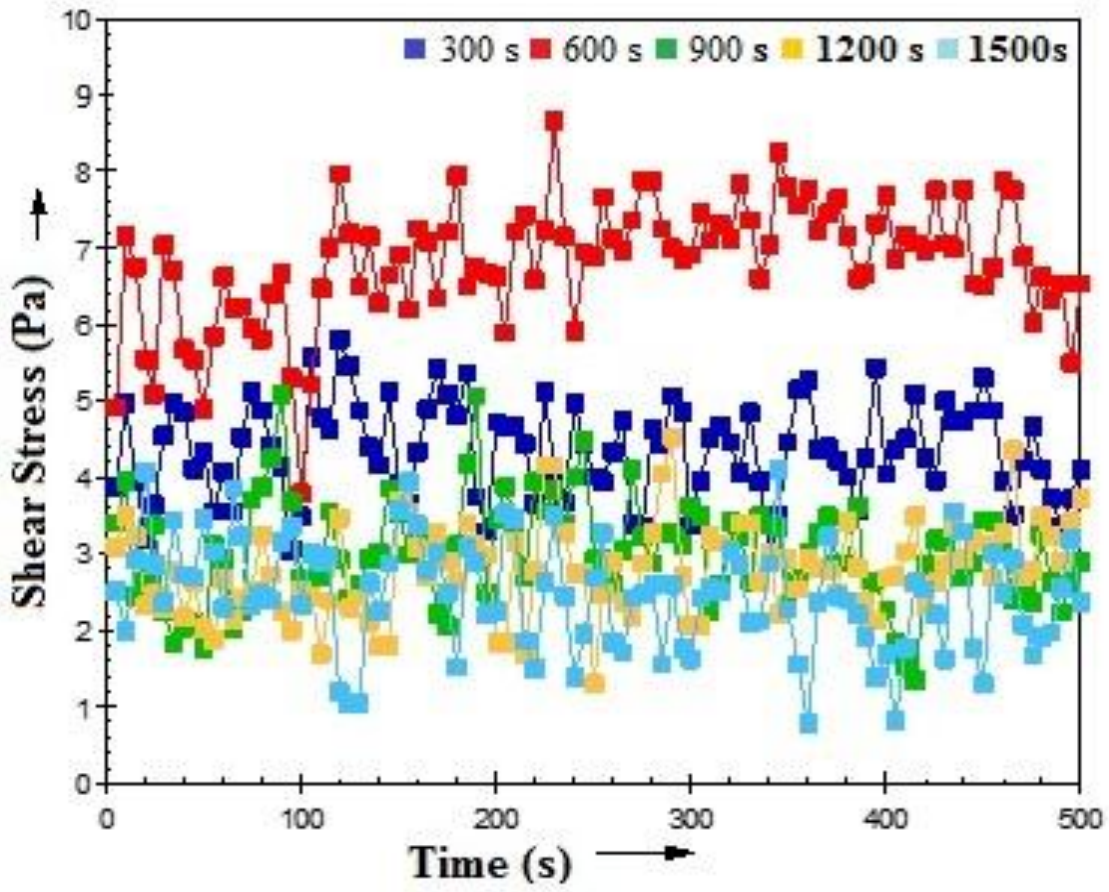

Figure 5.5: Shear rate variation after different resting times:
300 s (Dark Blue), 600 s (Red), 900 s (Green), 1200 s (Yellow), 1500 s (Light Blue)

No constant value for the shear stress is obtained, but it can be deduced from figure. 5.5, that the values of the shear stress under goes a large variation upto 900 s but beyond that, i.e. for the values of 1200 s and 1500 s, it nearly lies in the same range as that of the 900 s data. Hence, it can be established that the maximum time after which no significant changes occur in the shear stress measurement values, is the resting time of the sample. From literature, it is known that mostly the values of resting time exceeds the pre shear time, which is also true in the present case.

4. Comparison of shear stress for different values of shear rates:

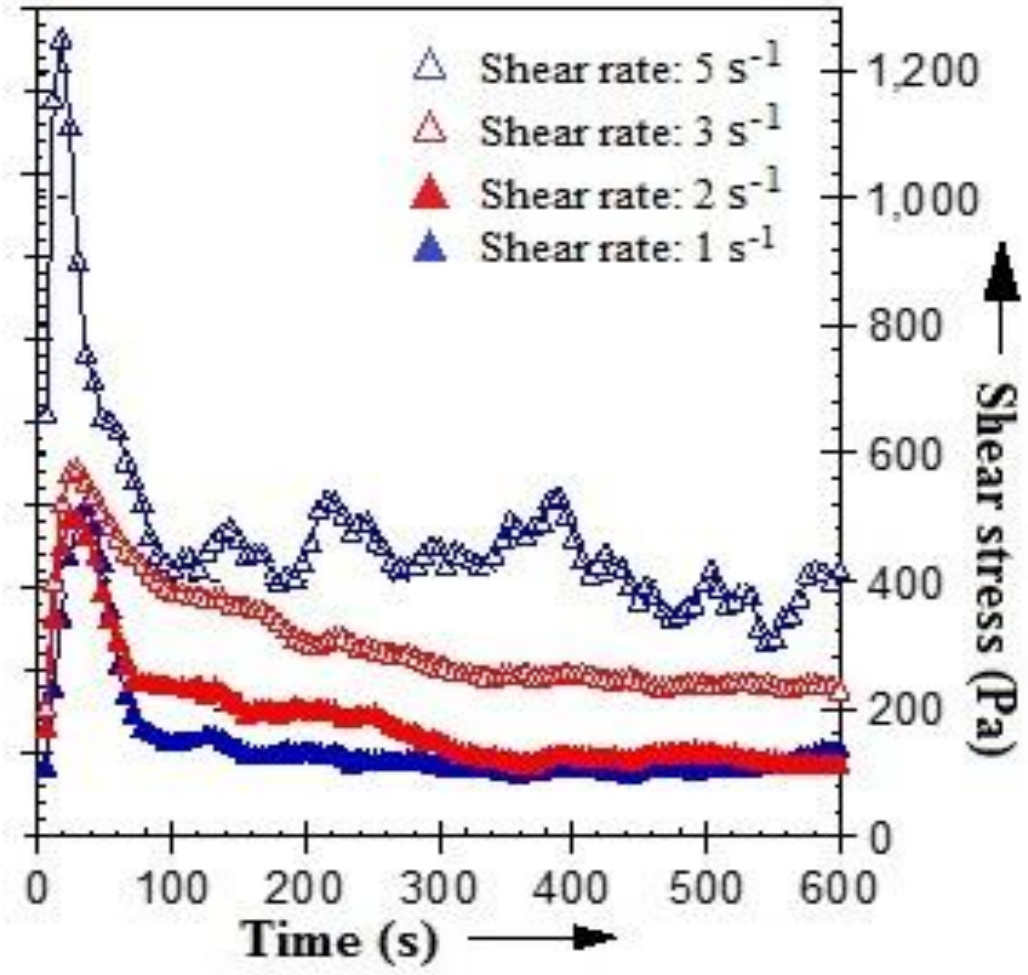

Figure 5.6: Shear stress variation for different values of shear rates (1, 2, 3, 5 s^{-1})

Figure. 5.6 compares how the shear stress changes with time for different values of shear rates. On increasing the shear rates form 1 s^{-1} to 5 s^{-1}, the shear stress along the time interval also increases, as well as becomes more modulating.

5. Steady shear rotational tests:

The main rotational rheological tests of the same sample mixture were performed both with (figure. 5.9 and figure. 5.10) and without (figure. 5.7 and figure. 5.8) pre-shearing conditions. Each test was repeated twice so as to ensure reproducibility of results. From their respective graphs it can be concluded that the rheological tests performed without pre-shearing leads to continuous shear thickening (gradual increase in viscosity), while those performed after the pre-shearing procedure showed discontinuous shear thickening (abrupt increase in viscosity) (Brown and Jaeger, 2013).

At low shear rates the particles are influenced only by Brownian motion. Beyond a critical shear rate, the hydrodynamic forces induce interactions between the particles (Khandavalli and Rothstein, 2014).

a. **Tests without pre-shear:**

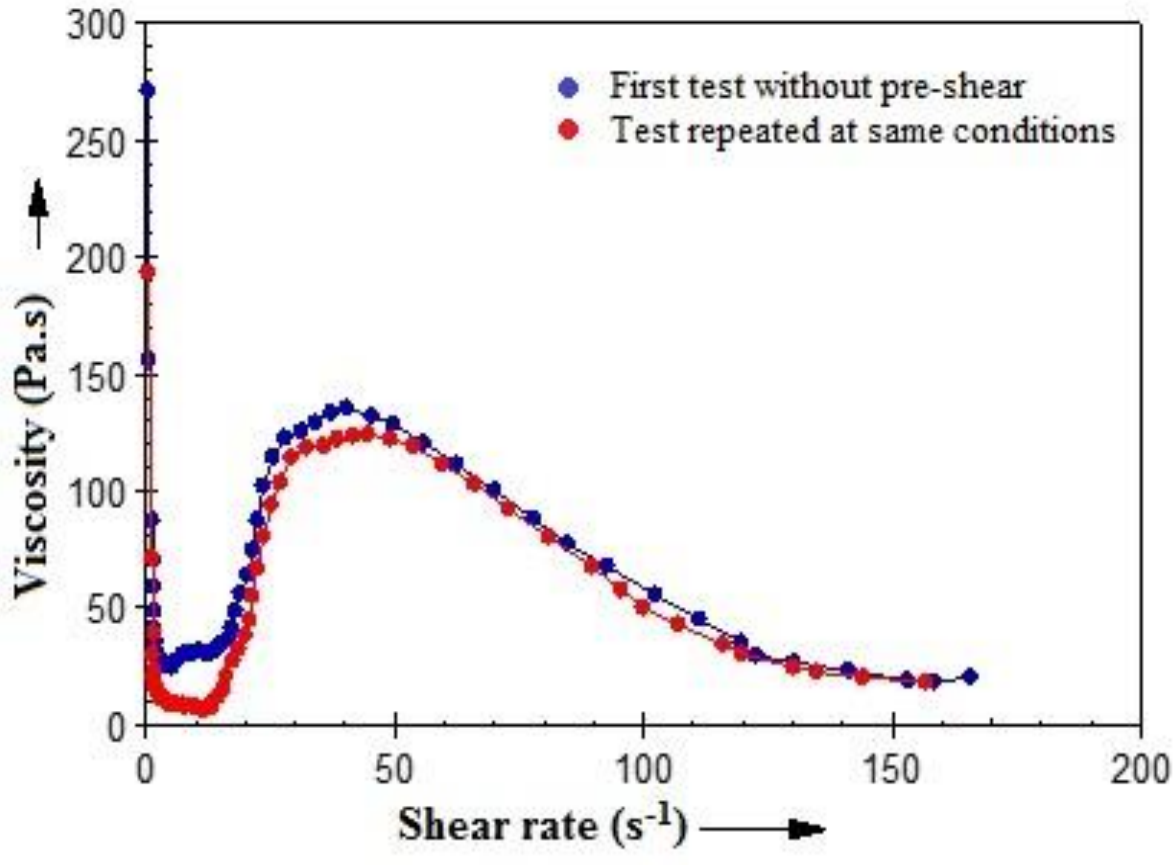

Figure 5.7: Shear rate vs. viscosity curves for rotational tests without pre-shear.

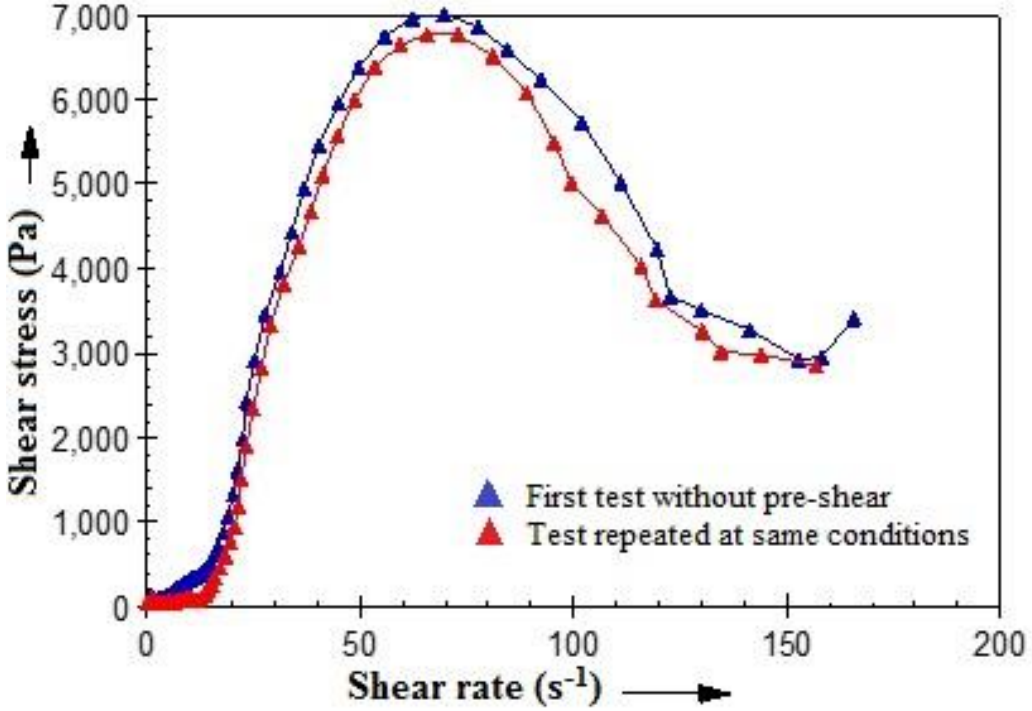

Figure 5.8: Shear rate vs. stress curves forrotational tests without pre-shear.

b. Tests with pre-shear:

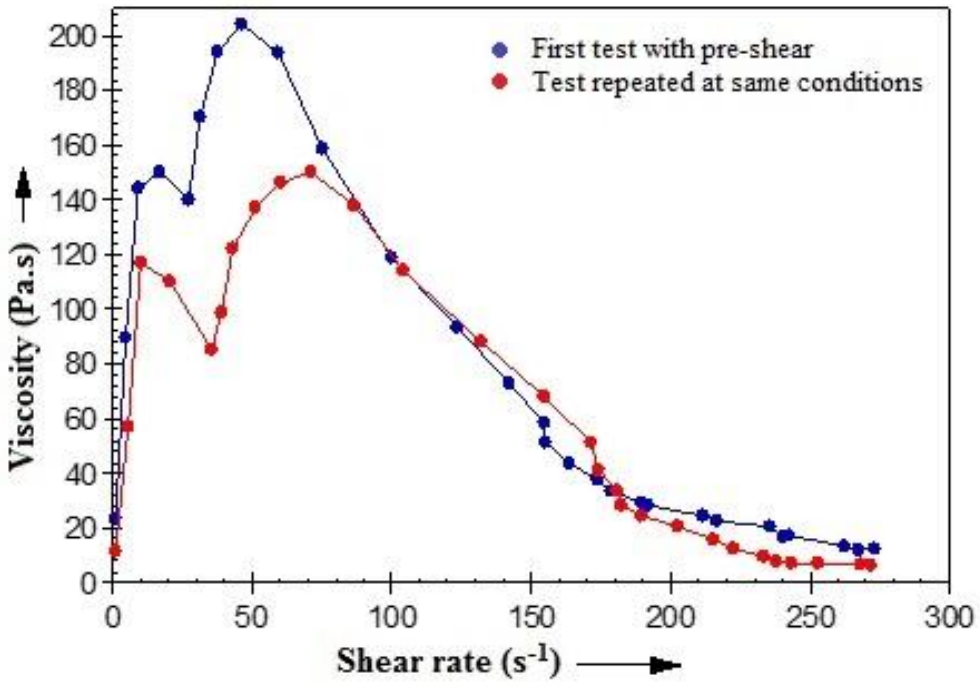

Figure 5.9: Shear rate vs. viscosity curves forrotational tests with pre-shear.

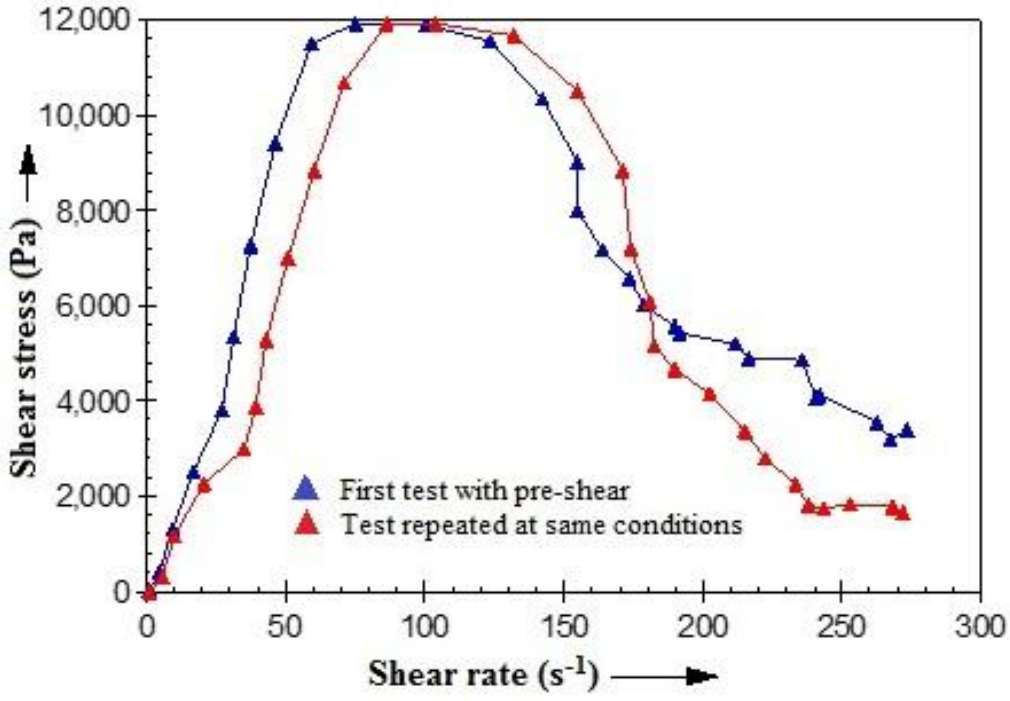

Figure 5.10: Shear rate vs. stress curves for rotational tests with pre-shear.

It was also observed that the values of the critical viscosity as well as the critical shear rate increases when pre-shearing was done on the sample (Table 5.1). This makes it a better rheological testing procedure especially for ballistic applications. On comparing the repeated experiments in both the cases, the new shear thickening curves are plotted below the previous ones. This shows that for every new loading of sample, due to the microstructural distortion the viscosity of the sample decreases but the nature of the curves remain the same.

Table 5.1: The critical and maximum viscosities and shear rates obtained during the rotational rheological tests, with and without pre-shearing the sample:

TYPE OF TEST	**CRITICAL VISCOSITY**	**CRITICAL SHEAR RATE**	**MAXIMUM VISCOSITY**	**MAXIMUM SHEAR RATE**
	Pa.s	s^{-1}	Pa.s	s^{-1}
Without Pre-shear	30.9	13.3	135.4	40.4
	8.1	12.9	124.5	44.8
With Pre-shear	140.1	27.2	204.1	46.1
	85.2	35.2	150.3	70.9

B. OSCILLATORY TESTS

The pre-shearing in case of oscillatory tests, gives an information regarding the structural breakdown of the sample. Here, the sample is sheared at low as well as high strain percentages and a comparison of the graphs deduce the minimum strain % at which the sample remains stable and the strain % at which its structure is distorted.

For oscillatory tests, pre-shearing gives the minimum strain percentage, at which the sample remains in equilibrium state for a fixed period of time. The storage modulus, G' is the parameter, which ensures this stability and thus is used for this test. This minimum strain percentage obtained is used in the main rheological tests, as the lower limit of the strain. This lower limit varies from sample to sample. The frequency was kept constant at 10 rad s^{-1} in all cases.

1. Comparison of sample behavior for different loadings:

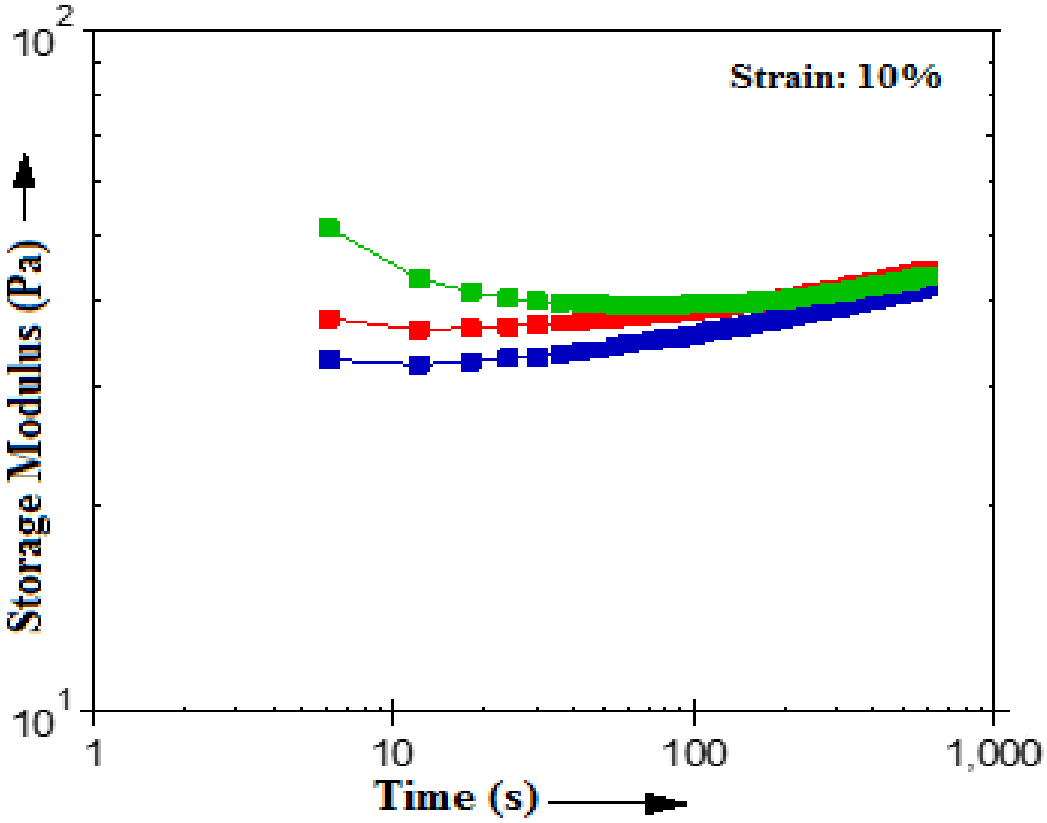

Figure 5.11: Sample behaviour at 10% strain for different loadings.

In these dynamic tests, the storage modulus is used as the parameter in the time sweep test to demonstrate how the nature of the sample changes with time. It can be observed from the figure. 5.11, that every time a new loading is done the readings at the same strain rate percent (here 10%), differs. The initial deformation is large as compared to further values. As the values of G' changes with time it becomes stable in nature.

2. Comparison of high strain rate percentages:

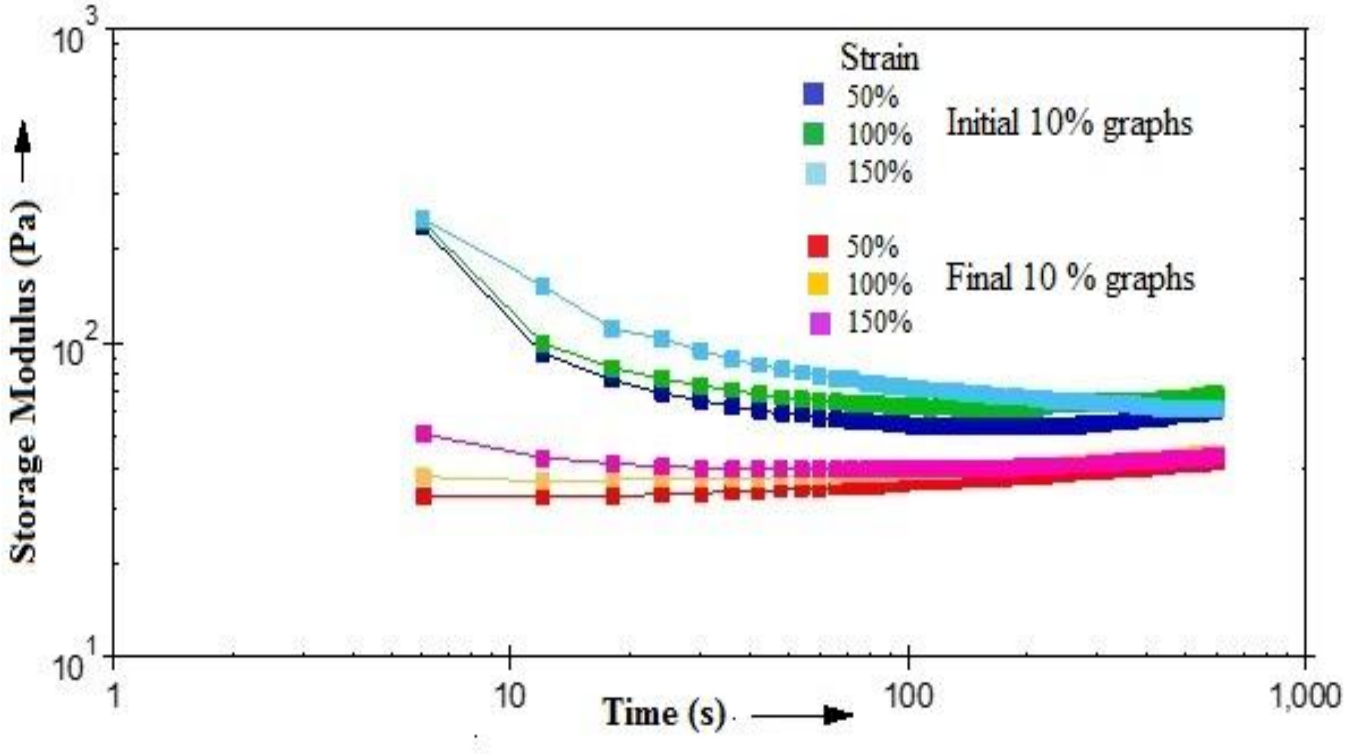

Figure 5.12: Storage modulus at strain rates of 10, 50, 100 and 150%.

The higher strain percent comparison in the oscillatory tests, was done as a 'time sweep' module. In figure. 5.12, all curves plotted are at 10% strain and 10 rad s^{-1} frequency. The readings of the upper three curves were taken at 10% as the initial readings, after sample loading. The three lower curves were also plotted at 10%, but after the increased strain percentage of 50, 100 and 150% respectively. This checks the reproducibility as well as the structural change of the sample after shearing at higher strain percentages.

3. Comparison of low strain rate percentages:

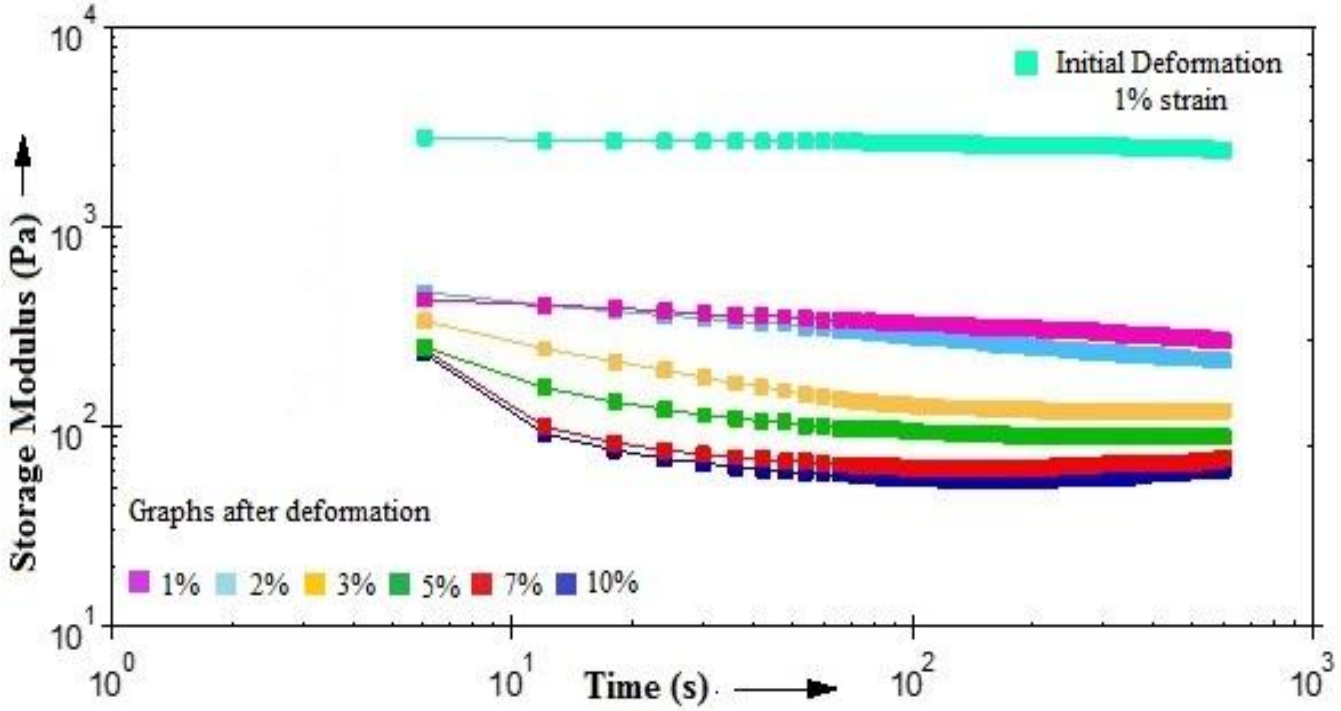

Figure 5.13: Storage modulus at strain rates of 1, 2, 3, 5, 7, 10%.

From figure. 5.13, it can be observed that the initial deformation of the sample increases as the strain % increases. The storage modulus shows a nearly straight line at a strain rate of 1% and on reaching till 10% strain, a large initial deformation is noticed. On comparing the readings with respect to time, the graph shows that at least a time interval of 100 s is needed for the G' values to become stable or nearly constant. But this cannot be applicable for extremely higher strain percentages as the structural deformation will be very large.

4. Resting time evaluation for oscillatory tests:
5.

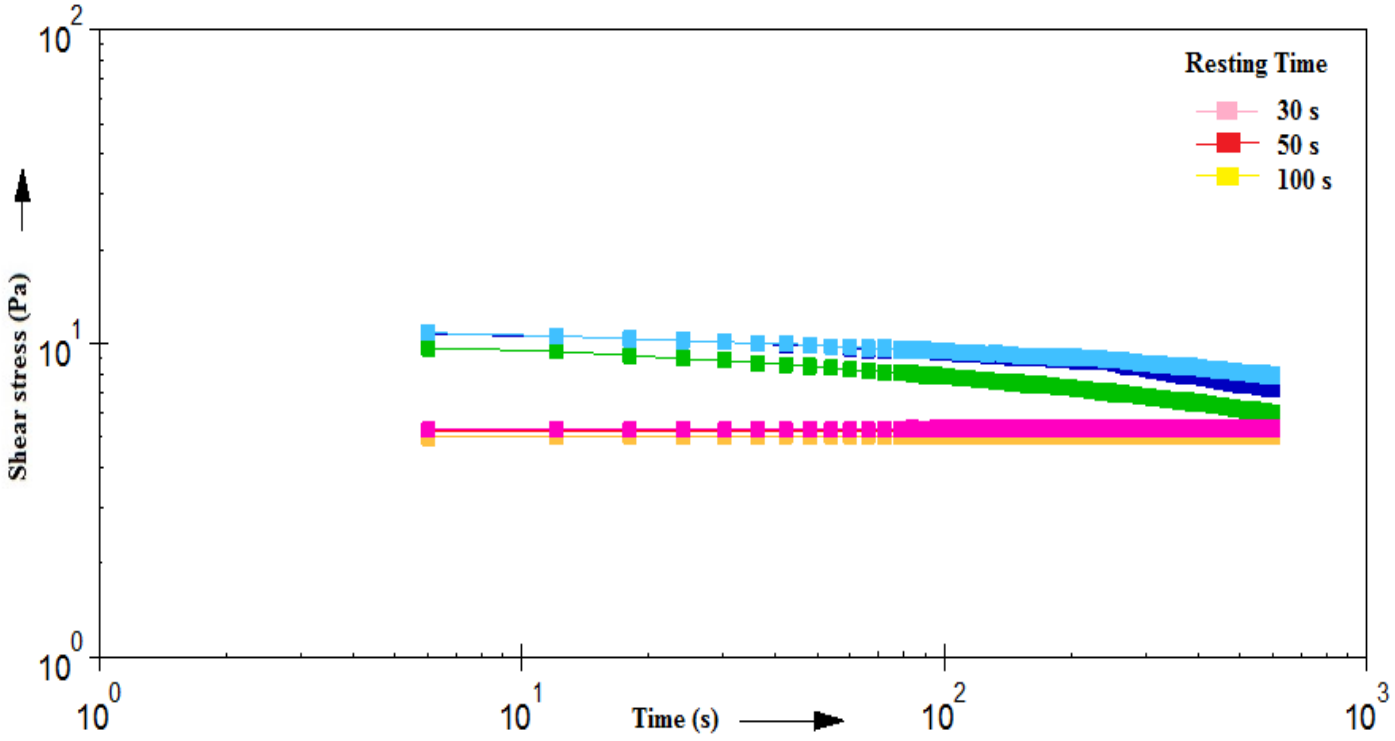

Figure 5.14: Shear stress variation with time for different values of resting time.
30 s (Pink), 50 s (Red), 100 s (Yellow)

In figure. 5.14, the upper three stress curves are those plotted at 1% strain provided just after loading. The lower three curves are those obtained at 1% strain, preceded by deformation rates of 10% each but with varying resting times. The curve plotted after 30 s rest shows a similar nature as its initial value, hence can be considered as the resting time for this sample.

6. Dynamic shear oscillatory tests:

The main rotational rheological tests of the same sample mixture were performed both with (figure. 5.17 and figure 5.18) and without pre-shearing (figure 5.15 and figure. 5.16) conditions. Each test was repeated twice so as to ensure reproducibility of results.

a. Tests without pre-shear:

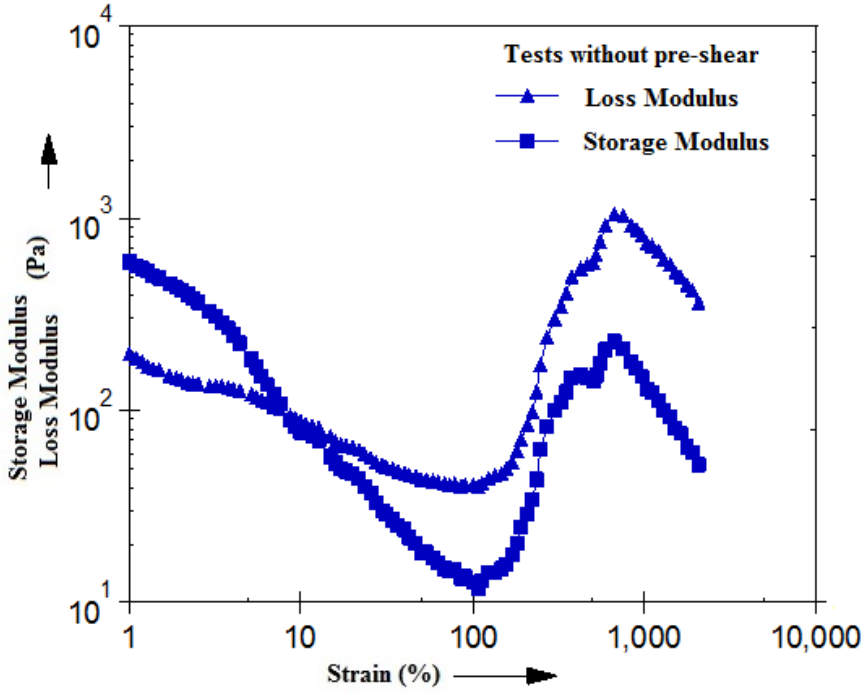

Figure 5.15: Evaluation of storage modulus and loss modulus at a strain percent range of 1% to 2000%, without applying pre-shearing and resting time.

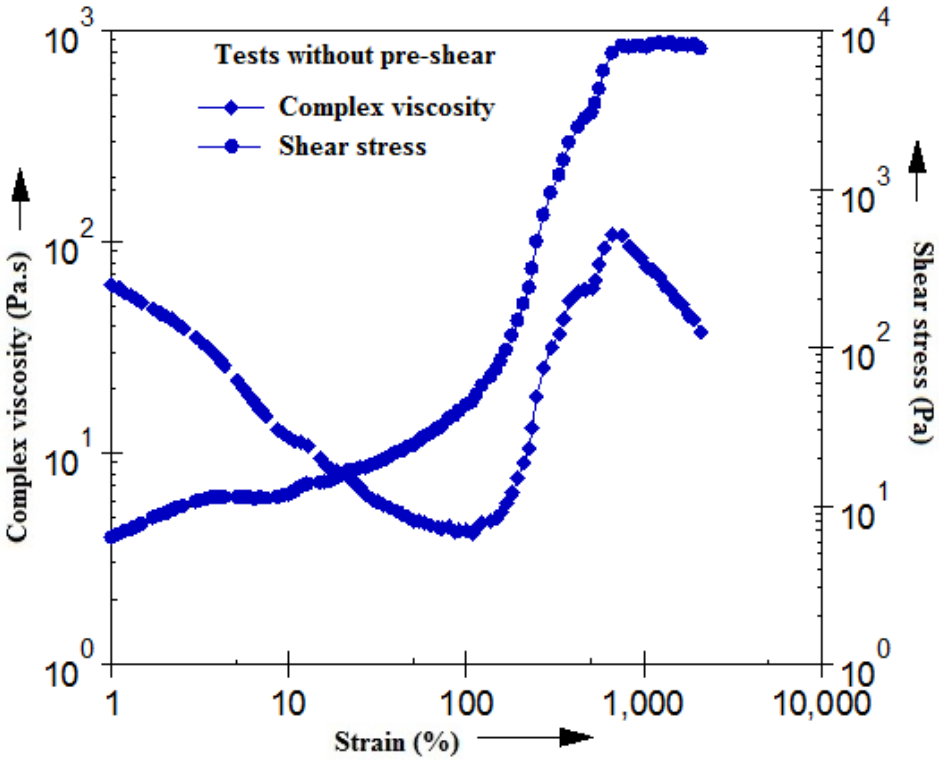

Figure 5.16: Evaluation of complex viscosity and shear stress at a strain percent range of 1% to 2000%, without applying pre-shearing and resting time.

b. Tests with pre-shear:

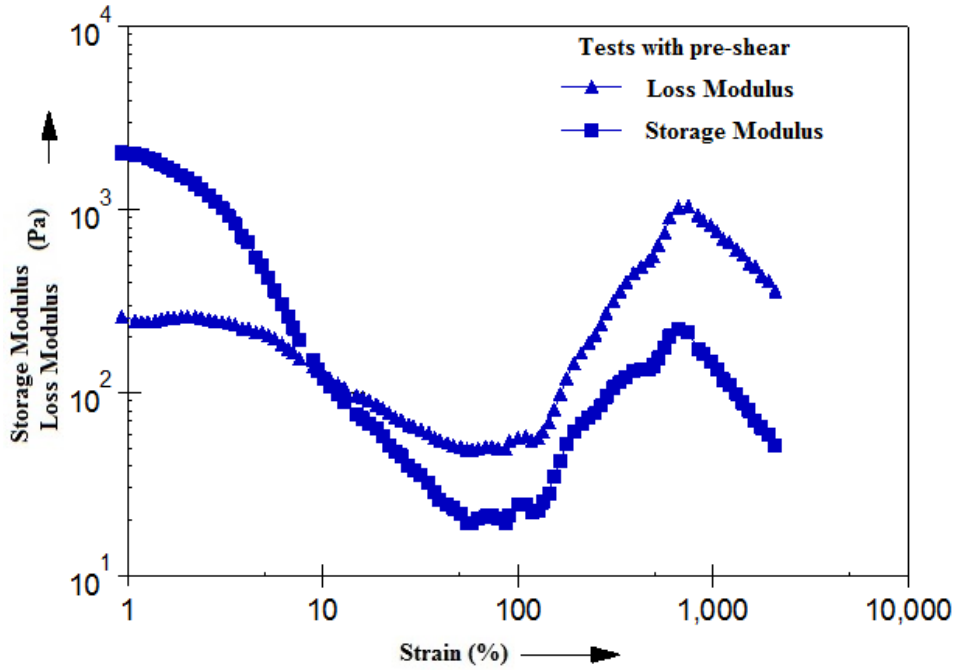

Figure 5.17: Evaluation of storage modulus and loss modulus, at a strain percent range of 1% to 2000%, after applying pre-shearing and resting time.

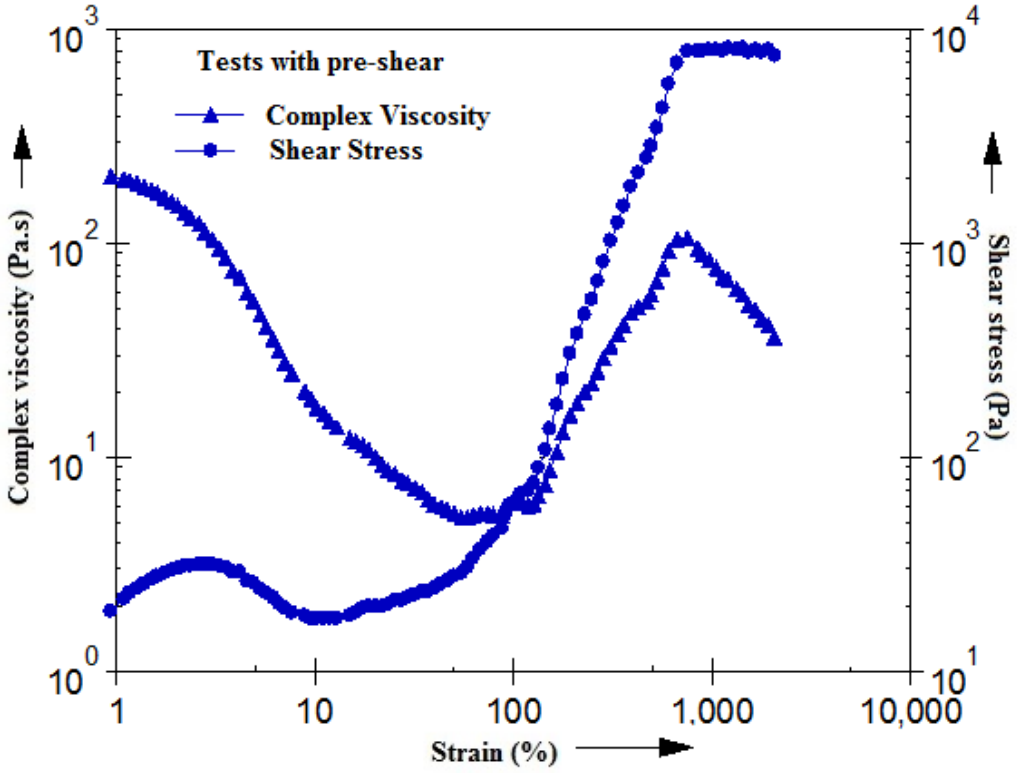

Figure 5.18: Evaluation of complex viscosity and shear stress at a strain percent range of 1% to 2000%, after applying pre-shearing and resting time.

In both these cases it is observed that initially, the values of storage modulus are greater than those of the loss modulus, up-till a cross over point is reached.

c. Comparison of the two cases:

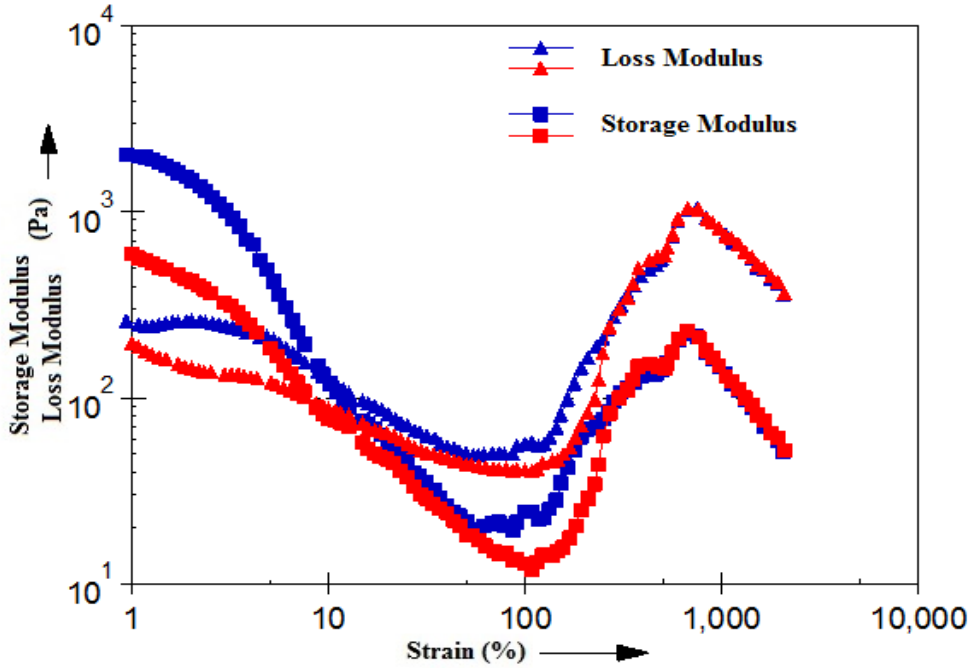

Figure 5.19: Comparison of storage and loss modulus for oscillatory tests with and without pre-shear.

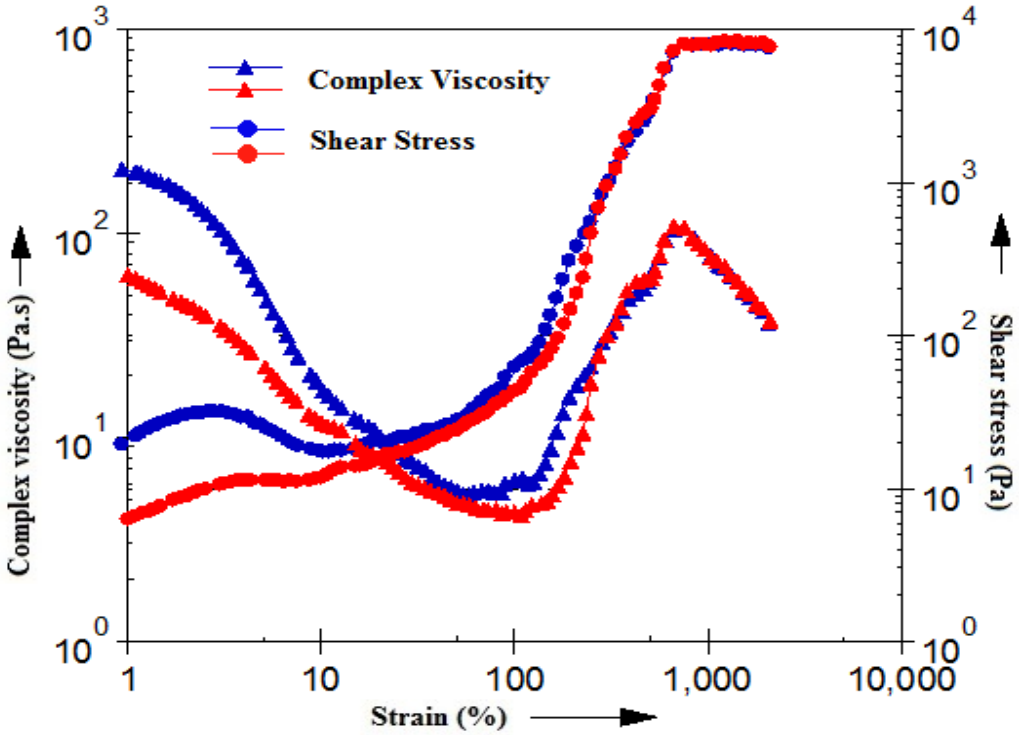

Figure 5.20: Comparison of complex viscosity and shear stress for oscillatory tests with and without pre-shear.

From the oscillatory tests results, it can be concluded that no significant changes in the values of the four main parameters, (i.e. storage modulus, loss modulus, complex viscosity and shear stress) were observed on application of pre-shear to the mixture STF sample. The nature of graphs in both these cases remain the same (figure. 5.19 and figure. 5.20).

6.2 HNT-FUMED SILICA NANO-COMPOSITE TEST RESULTS

A. Rotational tests (steady shear test)

The thickening effect of HNT-SiO_2 compounded shear thickening fluid system is improved as compared to that of the monodispersed system. Also if we compare this system with nano silica-fumed silica system, high viscosity is obtained at high shear rate even at a very low percentage of added HNT. Figure. 5.21 gives us the basic rheological test results of the 1% HNT-fumed silica compounded STF, in which viscosity vs. shear rates have been plotted for three different loadings of the composite sample. This also helps us in ensuring the reproducibility of the fluid sample. The parameters obtained from the three repeated tests (blue, green and red respectively) are presented in tabulated form below (Table 5.2).

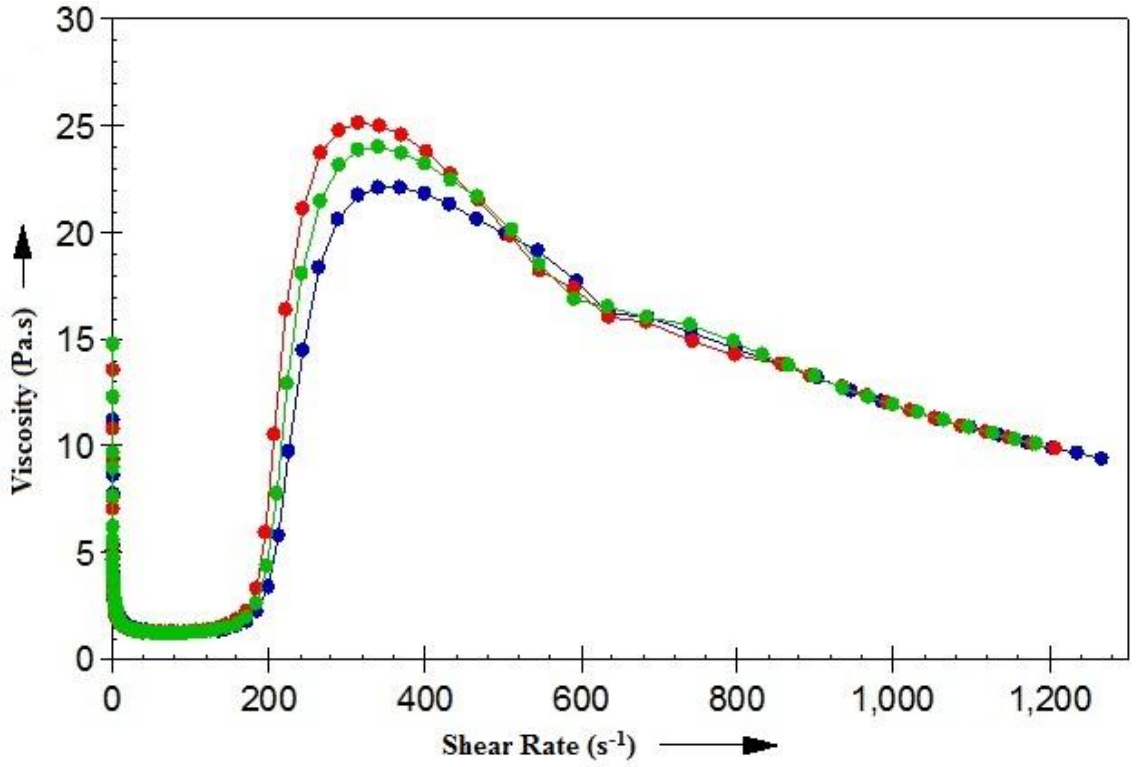

Figure 5.21: Viscosity vs shear rate for HNT-fumed silica composite STF. Reproducibility at different times (red, green and blue) are also shown for the same sample.

Table 5.2: Reproducibility of the rheological properties of 1% HNT-fumed silica composite shear thickening fluid

Tests	Critical shear rate ($\dot{\gamma}_c$) (s^{-1})	Critical viscosity (η_c) (Pa.s)	Maximum shear rate ($\dot{\gamma}_{max}$) (s^{-1})	Maximum viscosity (η_{max}) (Pa.s)
Test 1 (Blue)	171.9	1.8	341.7	22.1
Test 2 (Green)	172.2	1.9	342.0	24.0
Test 3 (Red)	172.2	2.3	316.2	25.1

The mechanism of the observed behaviour can be explained as follows:

Initially, when the sample is loaded on the geometry, it possess the zero shear viscosity (between 11 to 15 Pa.s in the present case). At this time the mixture of HNT and fumed silica is bonded together by strong hydrogen bonding, which helps in maintain a uniform dispersed phase. When the rheological tests starts the hydrogen bonding forces are unaffected by the weak inter particle forces, which can be in the form of Brownian forces or other stochastic particle-particle interactions. At very low shear rate the deformation is not permanent and the microstructure can restore itself, but eventually the viscosity of the sample continuously decreases on application of shear. As the shear rate increases, the hydrodynamic force starts to dominate and the nanotubes align themselves in same direction in layered fashion. In such a case the recovery of the system to its original state is not possible. On further increase in the shear rate, clusters of fumed silica on halloysite nanotubes are created in exfoliated pattern. As soon as a critical shear rate is reached the thickening starts and continues upto a maximum shear rate, beyond which again a decrease in viscosity is observed.

Comparison of rotation tests for different composition of HNT-FS composite STF:

A substantial outcome was observed relating to the rise in theshear thickening property, by increasing the weight fraction of the clay nano filler in the composite shear thickening fluid. A clear transition from discontinuous to continuous shear thickening was observed (figure. 5.22 and figure. 5.23) even with just 2% increase in the weight percentage, but at the cost of decrease in the maximum viscosity. This is in accordance with the fact that

particle volume fraction at which discontinuous shear thickening occurs decreases as the particle aspect ratio increases (Wetzel *et al.*, 2004).

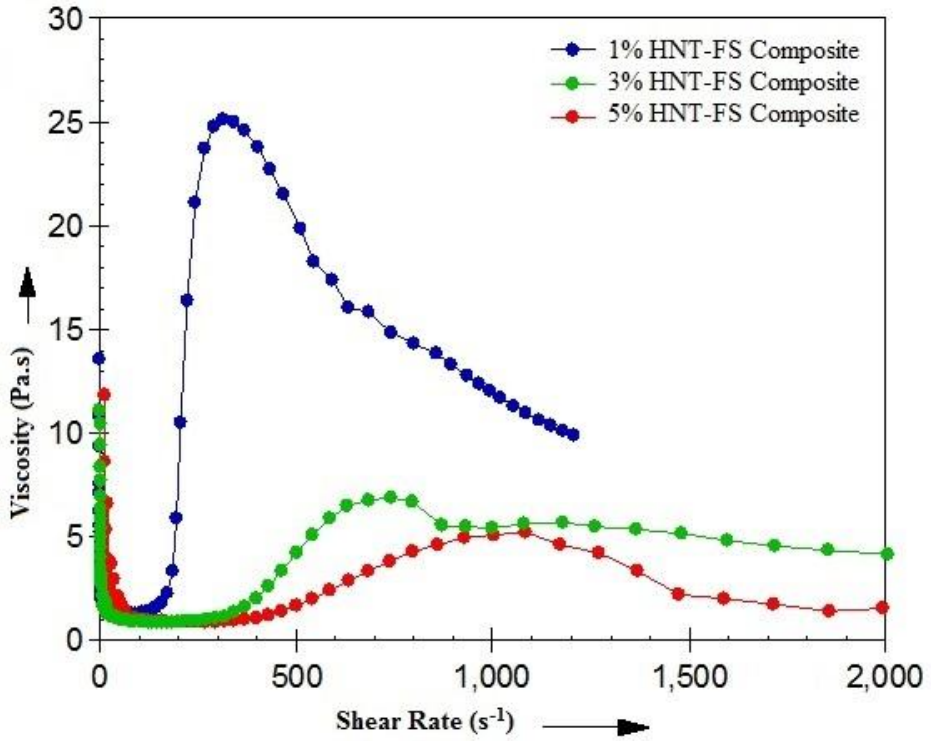

Figure 5.22: Comparison of the steady state viscosity of 1%, 3% and 5% HNT by weight in the HNT-fumed silica composite STF.

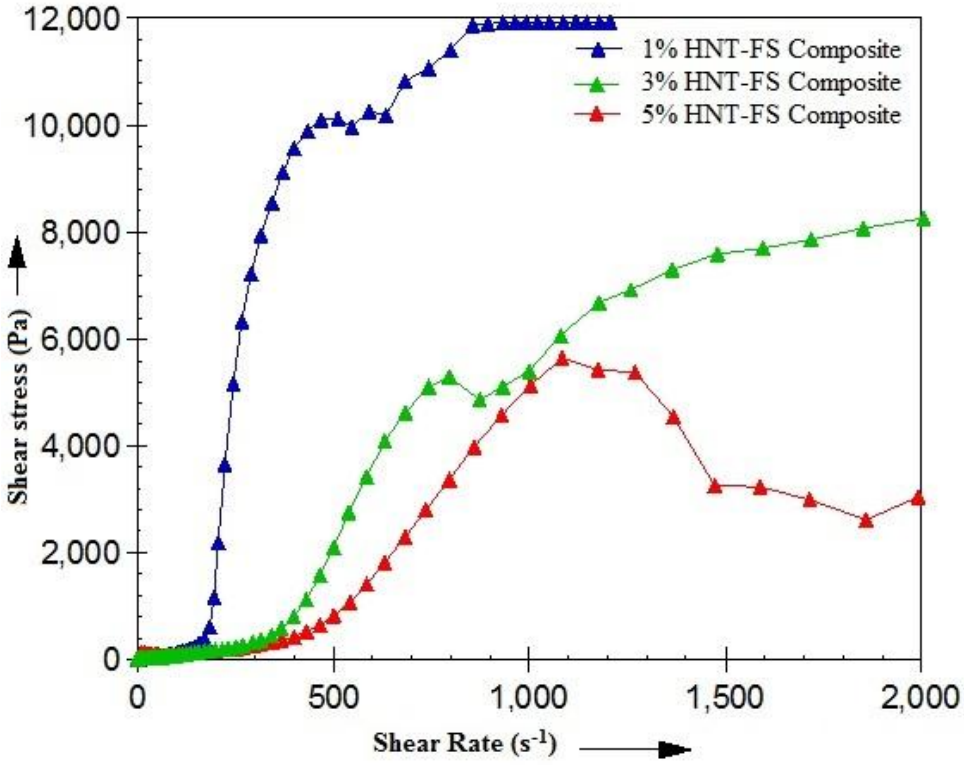

Figure 5.23: Comparison of the steady state shear stress of 1%, 3% and 5% HNT by weight in the HNT-fumed silica composite STF.

The higher critical shear rates obtained on increasing the weight percentage of HNT in the composite STF is believed to be due to greater and stronger interactions between the nano particles as well as with the polymer medium. Due to its cylindrical shape the large surface area provides relatively more lubrication forces between HNT-fumed silica hydroclusters and PEG as compared to that between only fumed silica hydroclusters and PEG medium. Another reason for the high critical shear rates of larger weight percentage HNT-fumed silica composite could be attributed to the enrichment effect that leads to the formation of larger clusters, as compared to lesser weight percentages of the HNT composite (Wang et al, 2014).

B. Temperature variation tests

The basic steady shear test conducted at 25^{o}C is considered as the basis for all temperature variation tests. The rheological properties were checked at different temperatures in the range 0^{o}C to 55^{o}C. For the lower temperatures, a steep rise in viscosity is observed in the graph, which gradually becomes gentler on increasing the temperature. An inverse relationship is observed between viscosity and shear rate with respect to temperature in figure. 5.24. That is, as the temperature goes on increasing from 25^{o}C, the value of critical shear rate achieved is very high whereas the maximum viscosity attained is even below its zero shear viscosity. For temperatures below 25^{o}C the maximum viscosity has a larger elevation but at the cost of very low shear rate, such that does not become satisfactory as a high impact resistant material. This has been shown in the tabulated form in table 5.3.

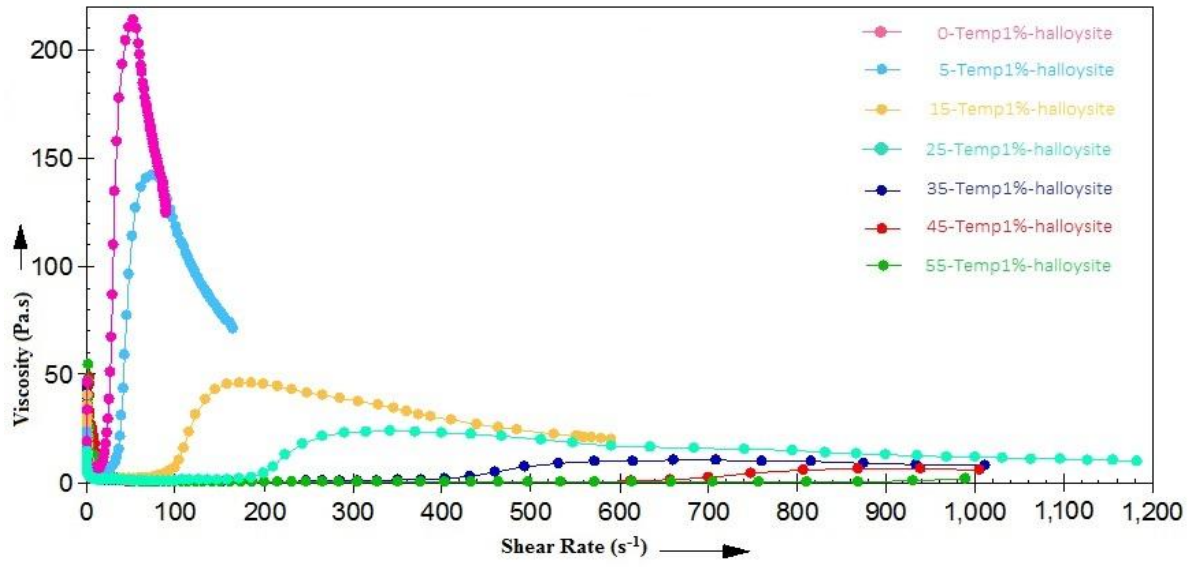

Figure 5.24: Temperature variation tests conducted for 1% HNT-fumed silica composite at different temperatures ranging from 0^{o}C to 55^{o}C.

Table 5.3: Critical shear rate and maximum viscosity at different temperatures

Temperature (℃)	0	5	15	25	35	45	55
Critical shear rate (s^{-1})	10.1	11.5	40.4	122	187	226	404
Maximum viscosity (Pa.s)	214	142	46.3	27.5	10.4	6.61	1.79

A similar investigation relating the temperature with shear rate was also done by Srivastava, showing a significant effect of temperature on the shear thickening behaviour (Srivastava et al., 2011). But higher critical shear rates were obtained in the present case using a composite shear thickening fluid constituting tubular shaped particles. Such temperature studies are necessary for designing the body armour such that it can be used in the varying temperature regions.

Similar temperature tests were conducted for higher concentration (weight %) of halloysite nano tubes in the HNT-FS composite STF:

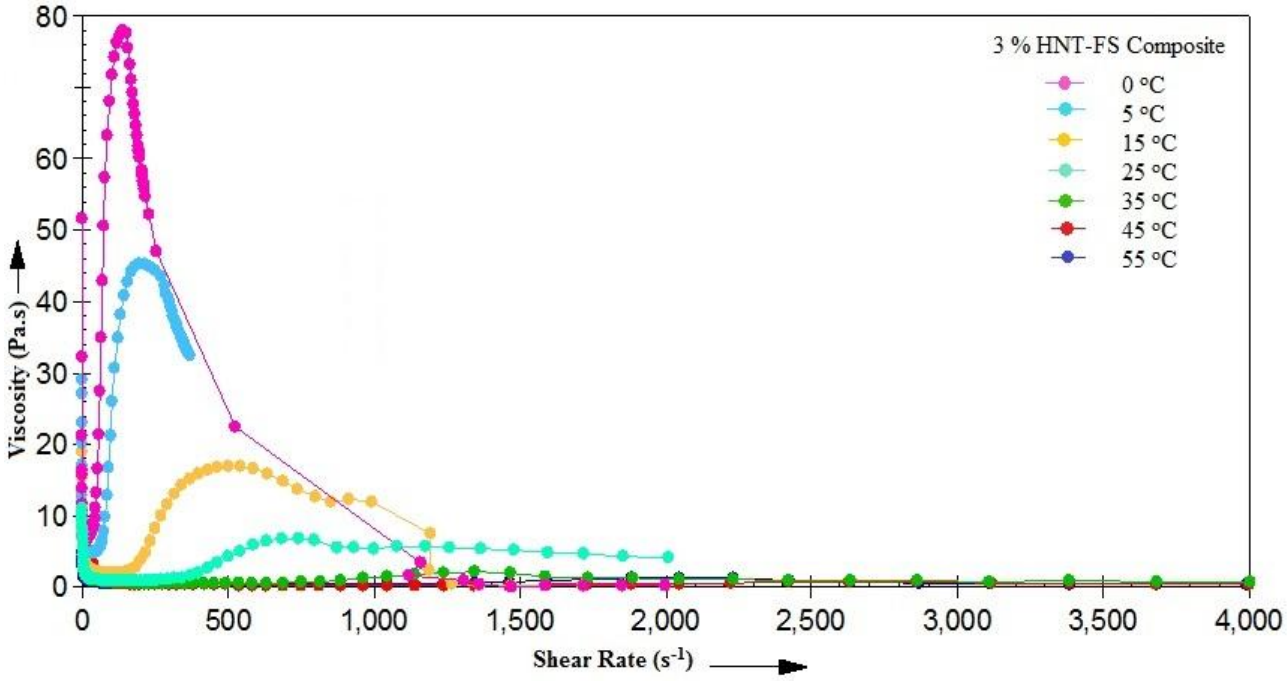

Figure 5.25: Temperature variation tests conducted for 3% HNT-FS composite at different temperatures ranging from 0°C to 55°C

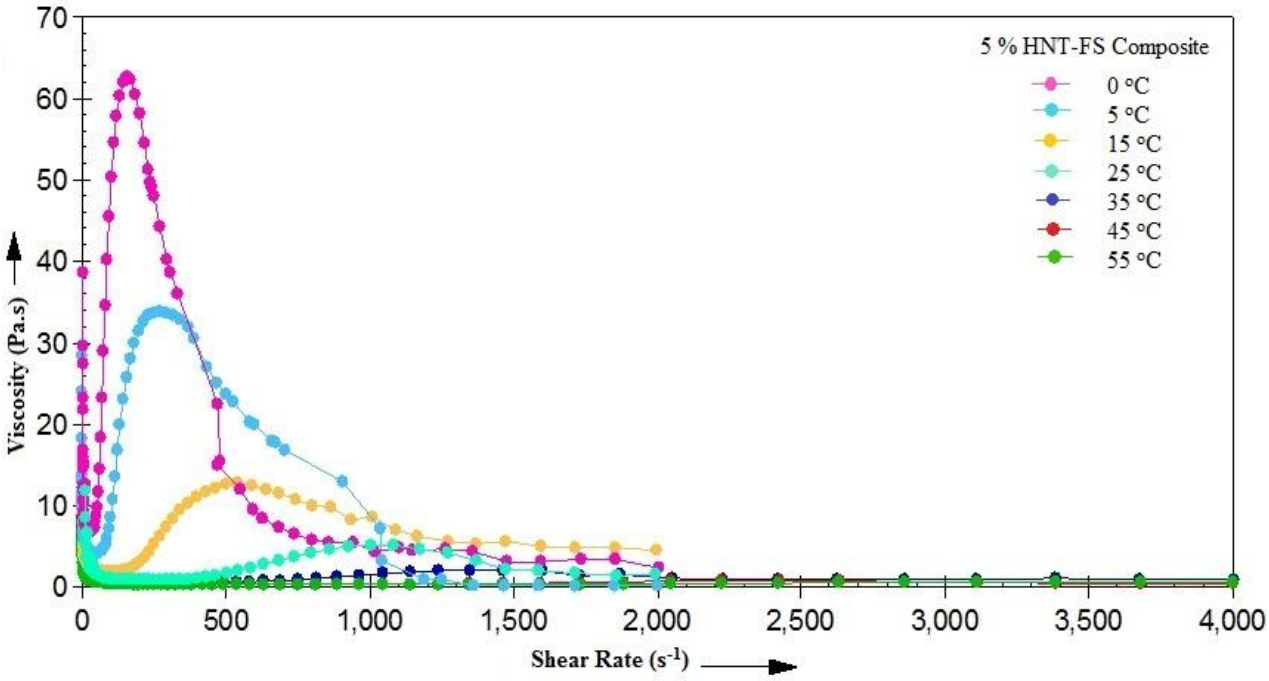

Figure 5.26: Temperature variation tests conducted for 5% HNT-FS composite at different temperatures ranging from 0°C to 55°C

Earlier researches showed that heat treatment of the solid raw materials for STF can lead to a drastic change in the thickening behaviour of the suspension formed (Chu *et al.*, 2014). The shear stress and shear rate may decrease and there can be an abrupt rise in the viscosity with shear rate. But, in our present case we see a change in the thickening behaviour of the formed shear thickening suspension at different temperature values. In contrast to the pre-treatment effect, a reverse nature of the fluid is observed, i.e., on increasing the temperature the maximum viscosity attained keeps on decreasing and the critical shear rate further shifts to a higher value. From the above two plots showing the temperature variation in the higher concentration samples (figure. 5.25 - 3% by weight and figure. 5.26 - 5% by weight) of HNT-fumed silica composite, the sudden shoot up of the viscosity is at 0^{o}C, which occurs at very low critical shear rate. Alternately, at the higher temperature values the viscosity rise is minuscule and with highly unclear critical shear rate.

Another notable factor from the above figures is the decrease in the higher viscosity value obtained at different temperatures. Generally, with the addition of more solid phase materials in the suspension the concentration of the suspension increases. But, on comparing the rheological property at a particular temperature, it turns out that the maximum viscosity is continuously decreasing on increasing the concentration of the HNT in the STF. This might be because of two reasons:

1. With the increase in weight percentage of the solid phase it becomes more and more difficult to disperse it properly in the dispersion medium. Thus, much more sonication time is needed so that there is an equal spreading or distribution of particles in the fluid. But the disadvantage of a greater sonication time is that it reduces the viscosity of the synthesized fluid sample to a great extent.
2. The second reason could be the shape and size of the solid filler material, the halloysite nano tubes. Due to its elongated tubular shape the hydrocluster formation of the fumed silica and HNT may not be as big as those which can lead to a greater solidification of the fluid on any impact and thus result in a lower maximum viscosity after shear thickening.

A comparison of different compositions of HNT-FS composite at the extreme temperatures are shown as follows:

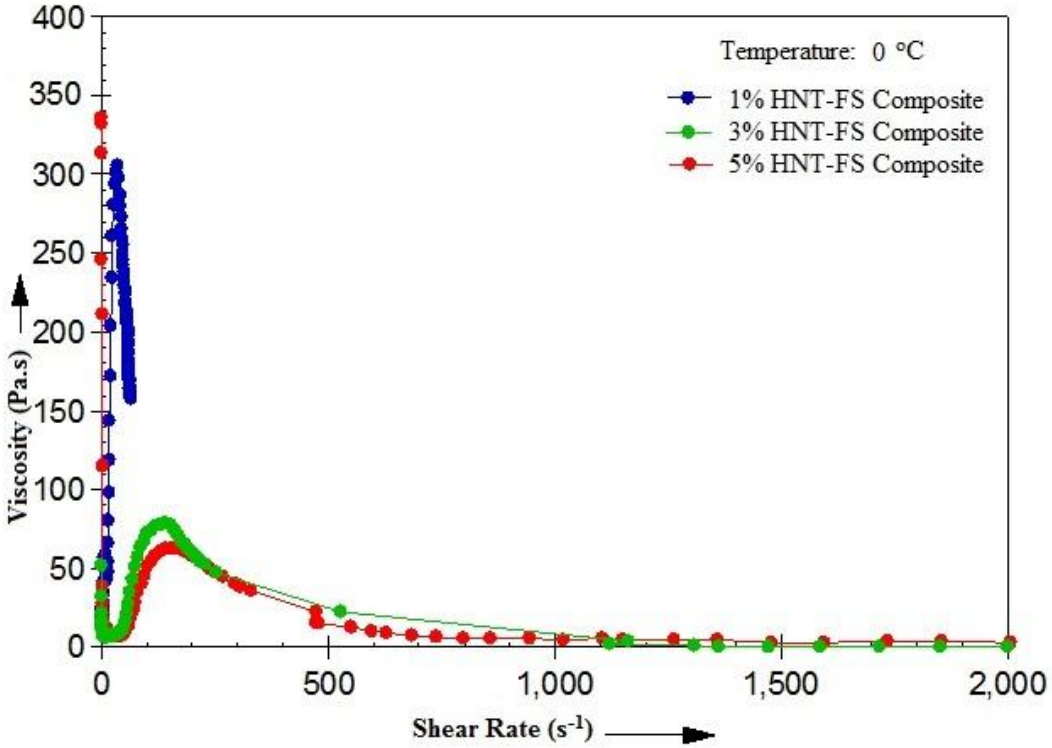

Figure 5.27: Comparison of 1%, 3% and 5% HNT-fumed silica composition STF at 0^{o}C

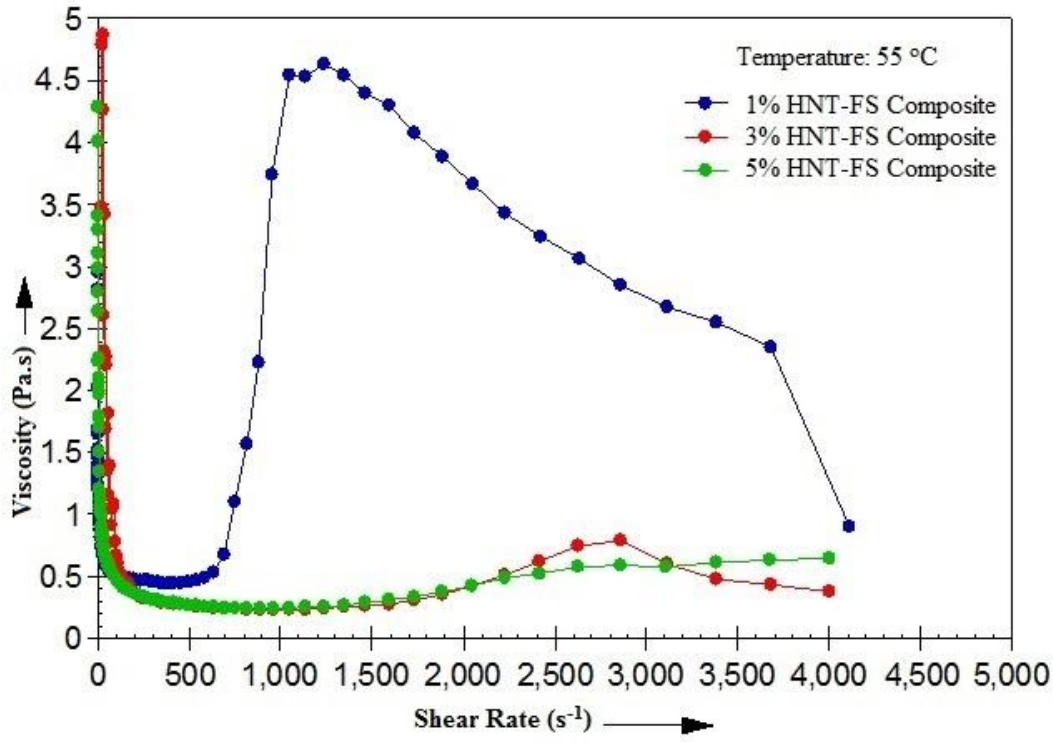

Figure 5.28: Comparison of 1%, 3% and 5% HNT-fumed silica composition STF at 55^{o}C

C. Oscillatory Tests

The non-linear oscillatory shear experiments are useful for characterising the onset of shear thickening as well as for determining the time scale required to generate the shear thickening response. The elastic modulus, G', and the loss modulus, G'', is strictly defined in the linear viscoelastic regime. Thus, their values at large strain amplitudes may have ambiguous physical meaning. However, the measurement of G' and G'' at a fixed frequency can provide meaning information.

In order to optimize and predict the behaviour of the complex dispersed system, it is important to elucidate the parameters influencing the rheological characters of the system. Here the oscillatory tests plays a vital role in checking the viscoelastic response of the system. The changes in the dynamic modulus parameters with oscillation frequency provides the microstructure details existing in the system (Russel *et al.,* 1989). The utility of dynamic rheological studies lies in the fact that materials can be probed in their resting state without causing disruption of their undefined structure (Macosko, 1994). Their dynamic rheology often gives a direct correlation with microstructure than steady state rheology (Raghavan *et al.*, 2000).

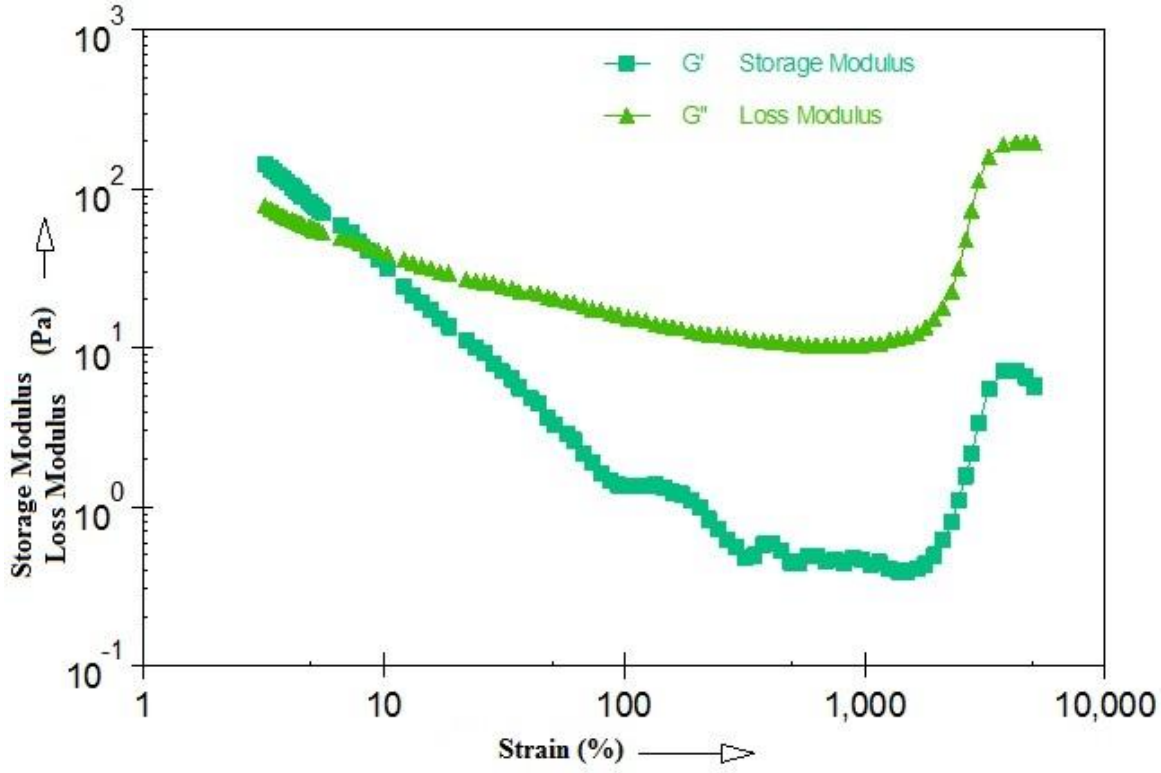

Figure 5.29: The dynamic shear tests where storage (elastic) modulus and loss (viscous) modulus is generated at both high and low strain percentages.

The dynamic shear tests shown in figure. 5.29 and figure. 5.30, were performed at a fixed frequency of 10 rad s^{-1} and shear strain range of 1% to 2000%. It is clearly seen that both the elastic modulus G' as well as the viscous modulus G'' show an abrupt jump to a higher level at a particular strain %. This indicates that the composite suspension exhibits strain thickening at high stain amplitudes. The LVE (linear viscoelastic) range obtained was 1.64% which was further used for the frequency sweep tests. The viscoelastic response under non-oscillatory conditions, indicates that the suspension remains non-flocculated up till the crossover point is reached, with a microstructure composed of discrete units.Figure. 5.30 shows a distinct rise in the complex viscosity with the increase in the strain percentages, and attaining a maximum value of nearly 20 Pa.s.

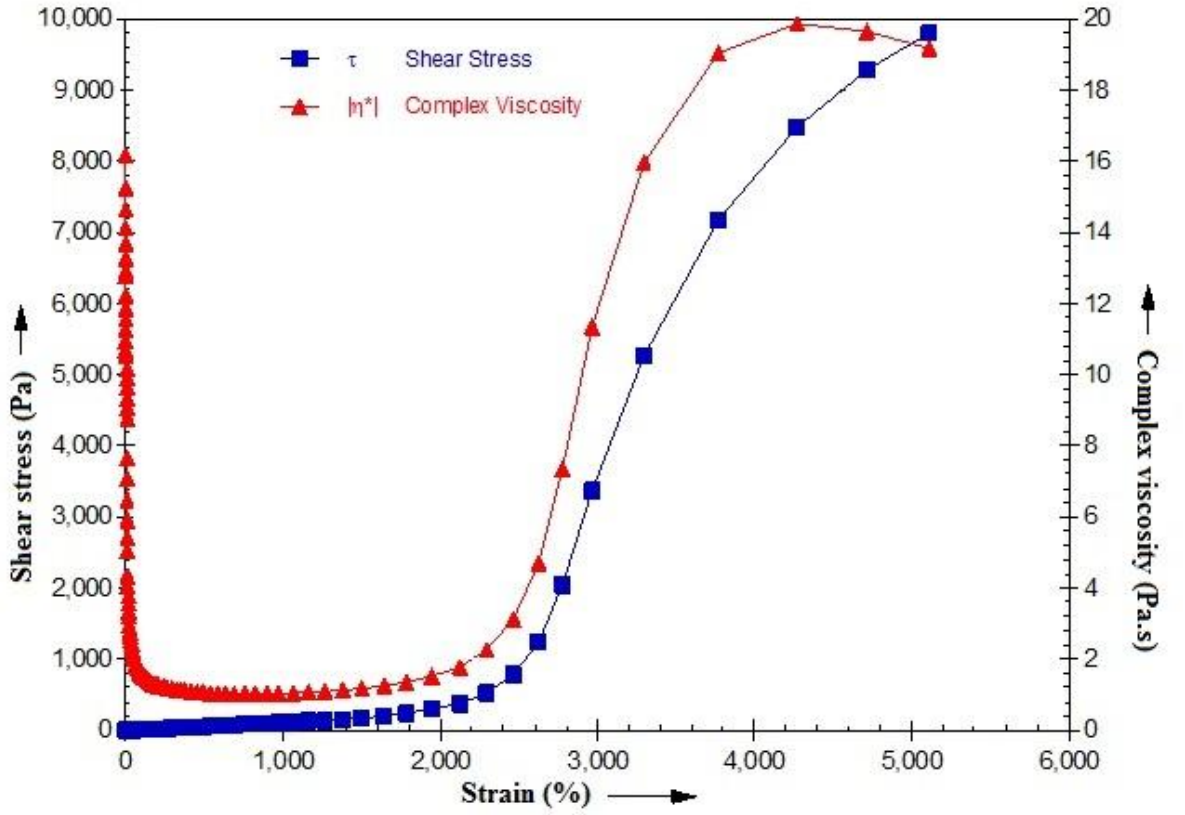

Figure 5.30: Change in complex viscosity and shear stress with the increase in strain percentage.

Similarly, for higher concentration of halloysite nano tubes in the STF composite (3% and 5% by weight), the dynamic behaviour varies as shown in figures. 5.31 and 5.32 respectively. For higher filler weight percent samples too, the tests were conducted at a constant frequency of 10 rad s^{-1}.

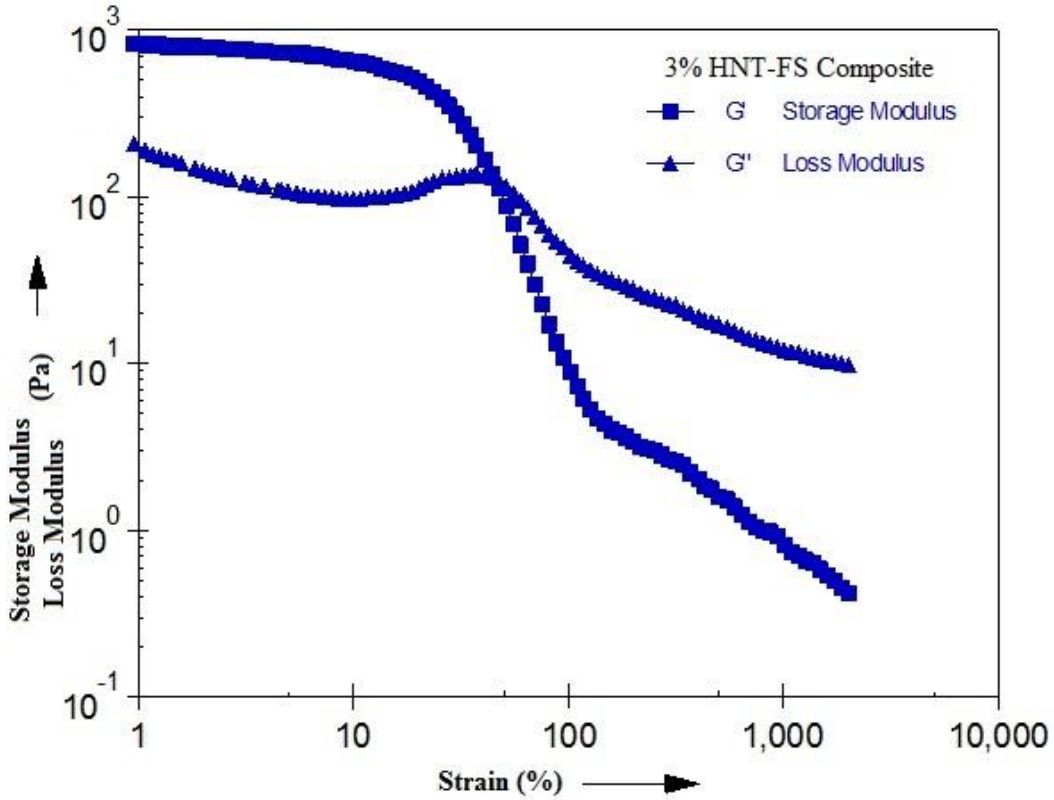

Figure 5.31: The dynamic shear test for 3% HNT-fumed silica composite, where storage modulus and loss modulus is generated at both high and low strain percentages.

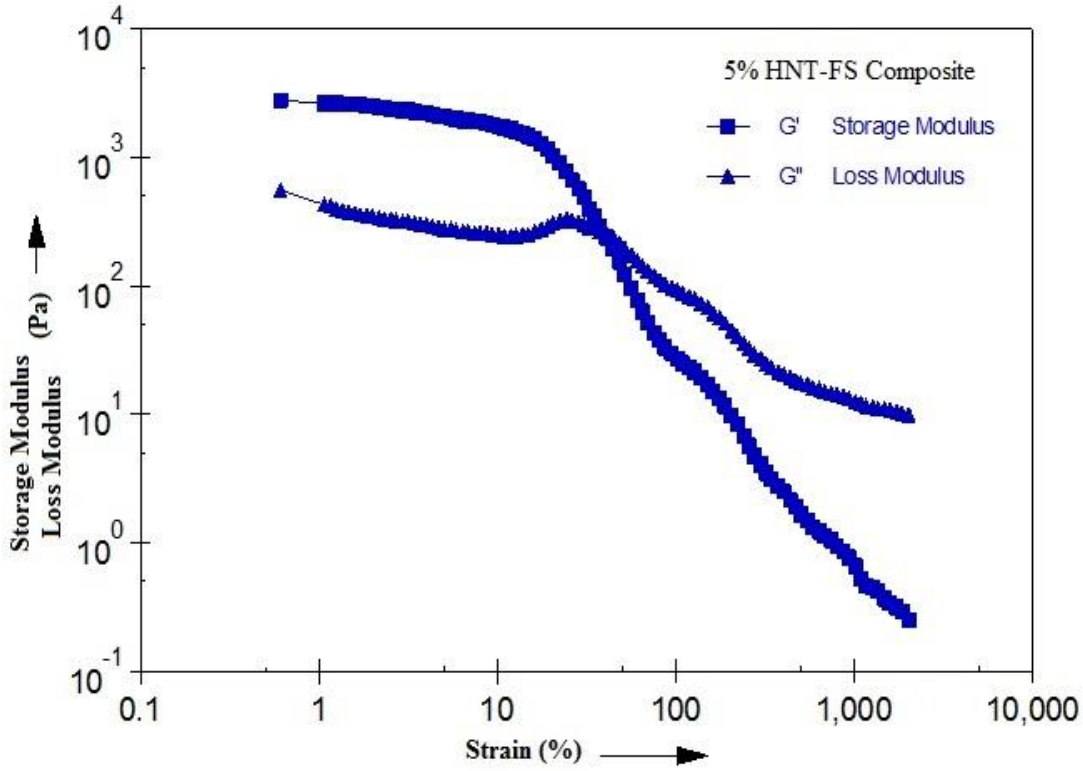

Figure 5.32: The dynamic shear tests for 5% HNT-fumed silica composite, where storage modulus and loss modulus is generated at both high and low strain percentages.

For higher concentration composites a clear crossover is visible showing the transformation of the fluids from soft solids to fluid like behaviour at high values of strain percentages. This also shows that no gel formation occurs in both the high concentration samples, till the storage modulus dominates the viscous modulus.

a. Amplitude Sweep test

The strain sweeps obtained at different frequencies were depicted as a function of the complex shear modulus$|G^*|$ (figure. 5.35).Complex modulus is a function of both storage and loss modulus and is depicted as:

$$G^* = G' + iG''$$

It is a measure of the material's overall resistance to deformation. An increase in the complex modulus thus corresponds to a larger torque response exerted by the sample. The transition to strain thickening behaviour occurs at smaller strains as the frequency of deformation is increased this transition can be seen in figure. 5.33 and figure 5.34.

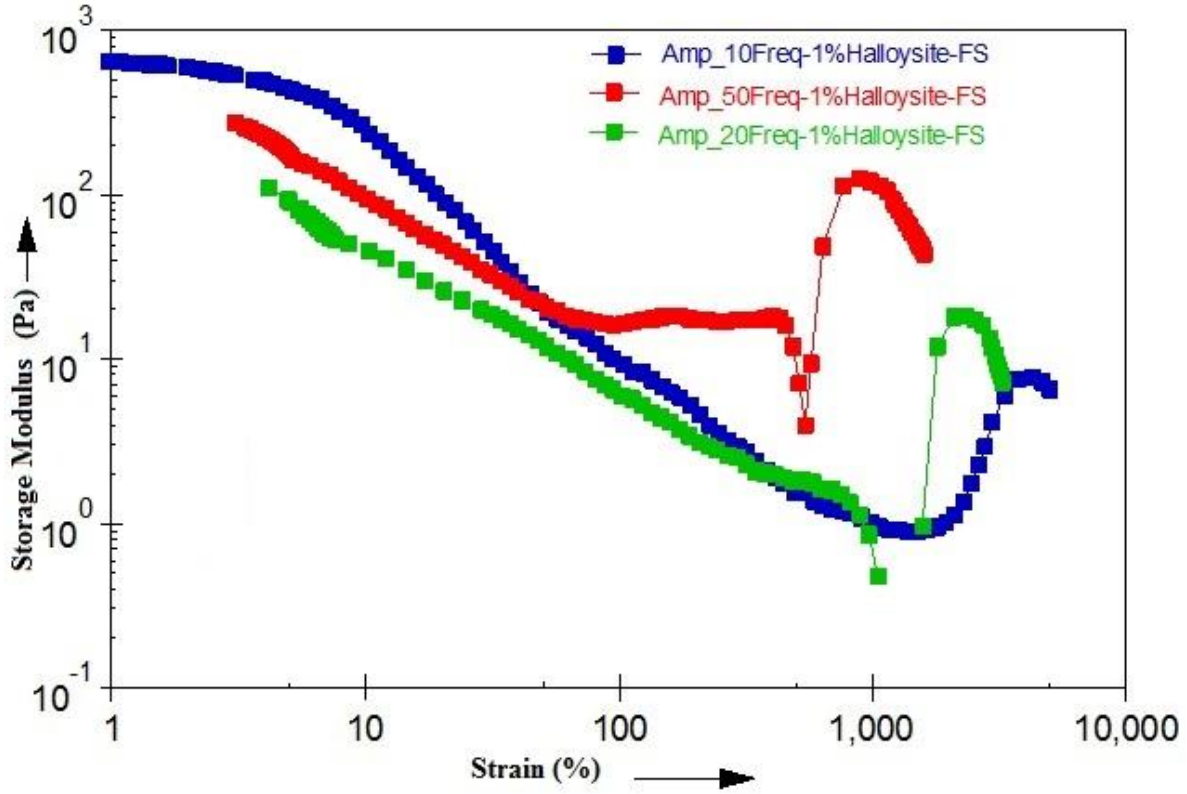

Figure 5.33: Change in the storage modulus at frequencies of 10, 20 and 50 rad s^{-1} in a wide strain percentage range.

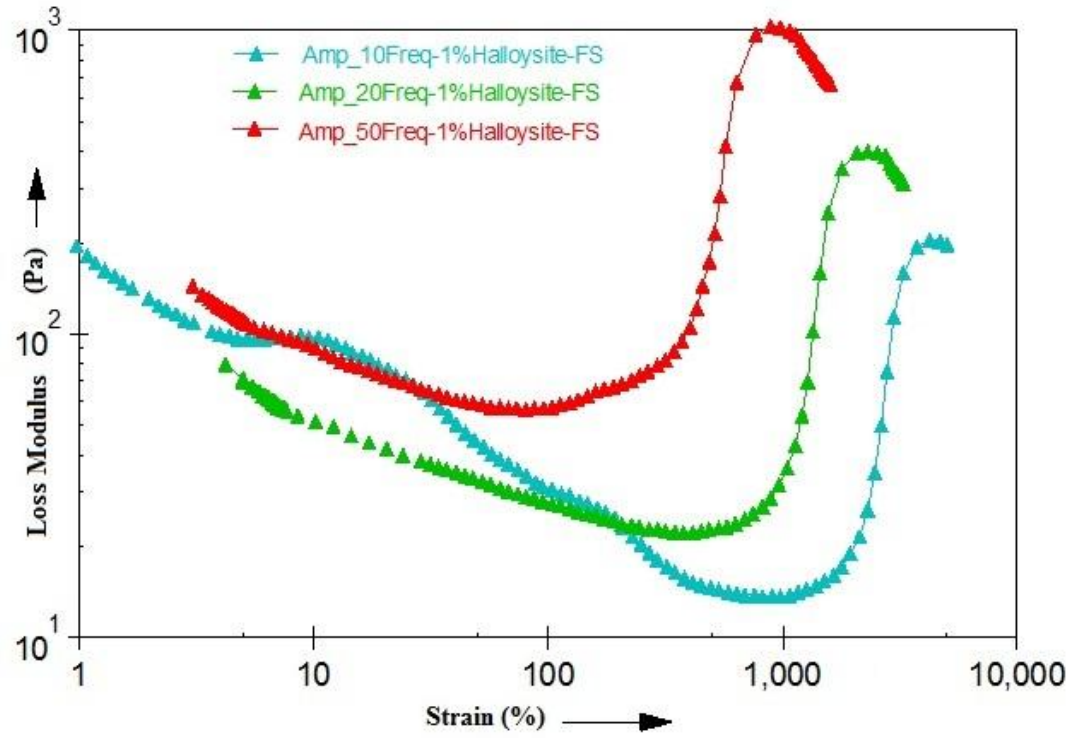

Figure 5.34: Change in the loss modulus at frequencies of 10, 20 and 50 rad s^{-1} in a wide strain percentage range.

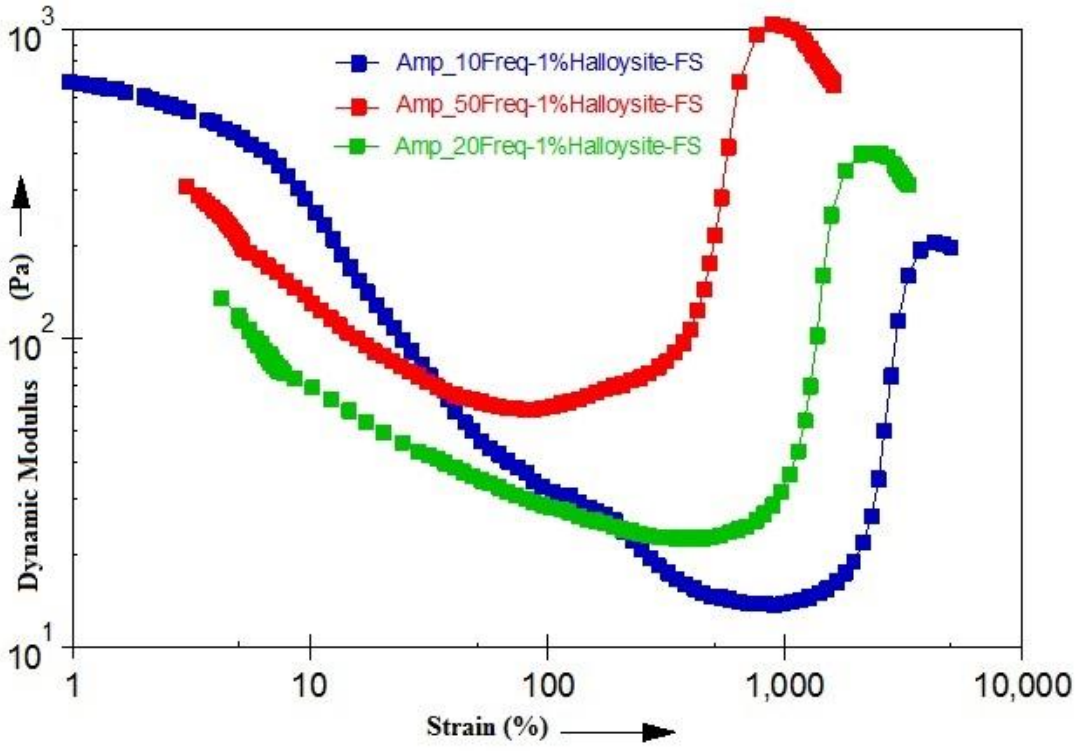

Figure 5.35: Amplitude sweep tests conducted at three different frequencies of 10 rad s^{-1}, 20 rad s^{-1} and 50 rad s^{-1} (Blue, green and red respectively)

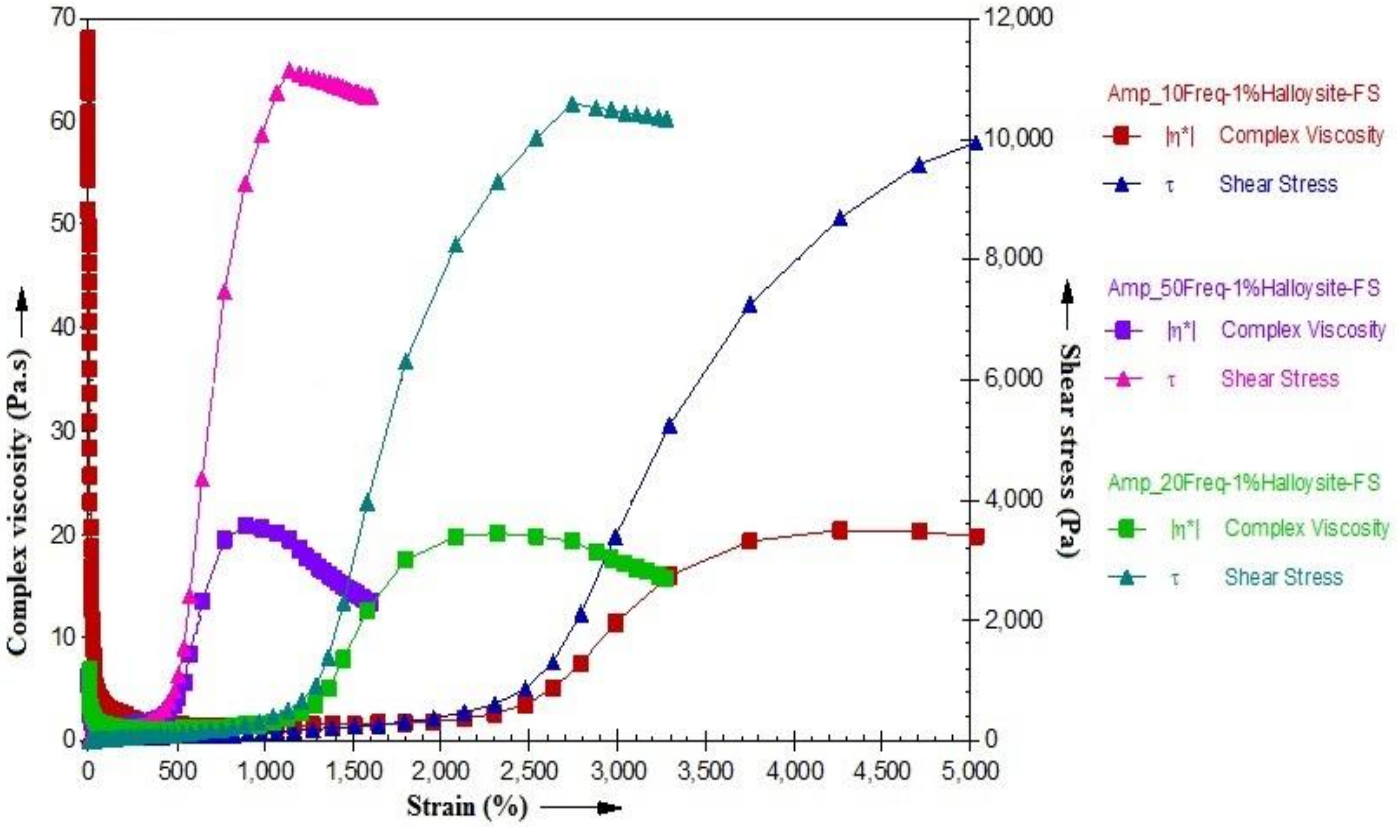

Figure 5.36: Complex viscosity and shear stress plots for three different frequencies of 10 rad s^{-1}, 20 rad s^{-1}, and 50 rad s^{-1}

The complexviscosity is the ratio of the dynamic modulus to the frequency of deformation, represented as:

$$\eta^* = \frac{G^*}{\omega}$$

Lee and Wagner demonstrated that the critical strain required for thickening to occur is inversely proportional with the frequency of oscillations (Lee and Wagner, 2003). A study by Laun et al., also showed that, a critical shear rate was required for the thickening behaviour at low frequency for rotational tests, whereas a minimum shear strain was necessary at high frequency for the oscillatory tests (Laun *et al.*, 1991).From the above figure. 5.36, it is clearly shown that the fall in the complex viscosity occurs as the frequency of oscillations increases but at a lower strain percentage. For lower frequency (10 rad s^{-1}) the complex viscosity is nearly stable, but is obtained at higher strain percentages.

It can also be seen that the sharp rise in the complex viscosity can be obtained at a higher value of angular frequency of oscillation of the sample fluid. The fall in the complex

viscosity starts to occur as the strain percentage increases. For lower frequency (10 rad s^{-1}) the complex viscosity does not fall much and is nearly stable, even if the strain percentage is increased by a large amount. For the defence application, when a projectile impacts on the armour, the viscosity of the shear thickening fluid inside it surges instantly. In order to maintain the fluid's viscosity at a higher value, even with extremely large values of strain, the frequency of oscillations should be kept at the lowest. This slight stable nature will help to lessen the impact of the bullet to a large extent, before a complete fall in the viscosity occurs causing the fluid to thin, thereby showing its reversible nature. Similar, amplitude sweep graphs plotted for different frequencies for different STF compositions are:

For the 3% HNT-fumed silica composites too (figures. 5.37 and 5.38) the amplitude sweep tests were conducted but the rise in the complex viscosity was found to be continuous and much less than that observed for 1% composite. Even the torque responses at different frequencies did not show as effective results as those for 1% composite. This showed that the nano fillers should only be present in a limited amount without exceeding a fixed percentage so as to give the most effective results.

Similar deductions could be made for the 5% HNT-fumed silica composite as well, with even lower values of complex viscosity (figures. 5.39 and 5.40).

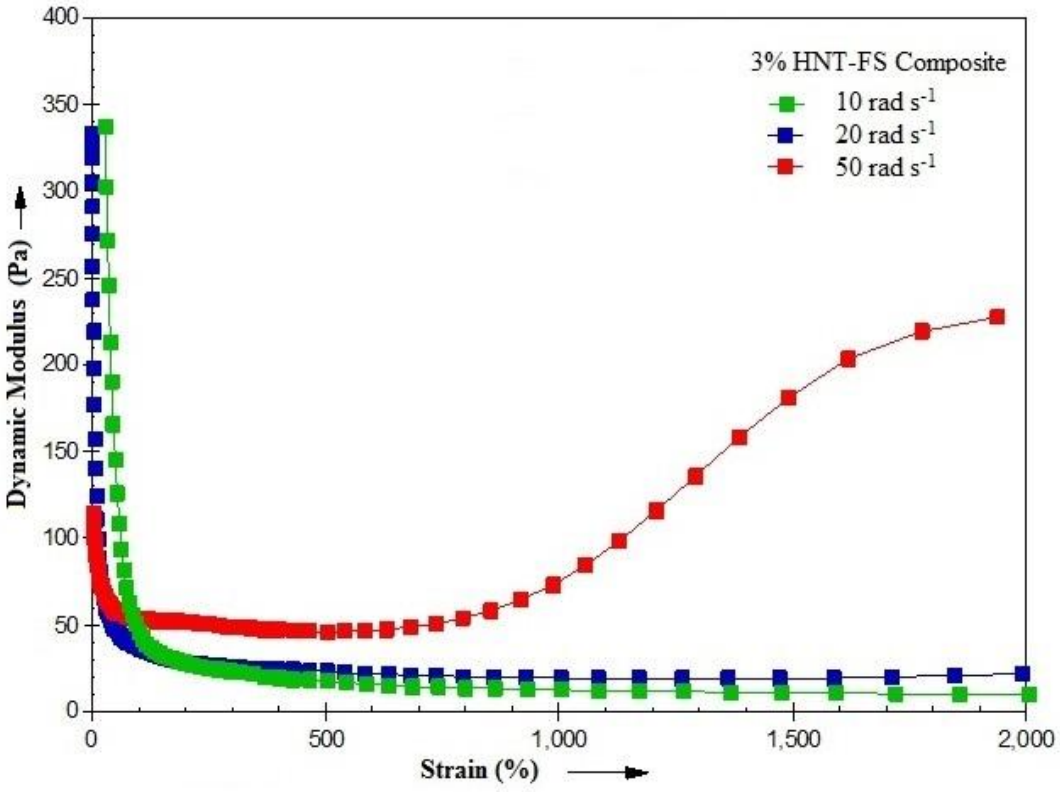

Figure 5.37: Dynamic modulus at three different frequencies of 10 rad s^{-1}, 20 rad s^{-1} and 50 rad s^{-1} (Green, blue and red respectively) for 3% HNT-FS composite

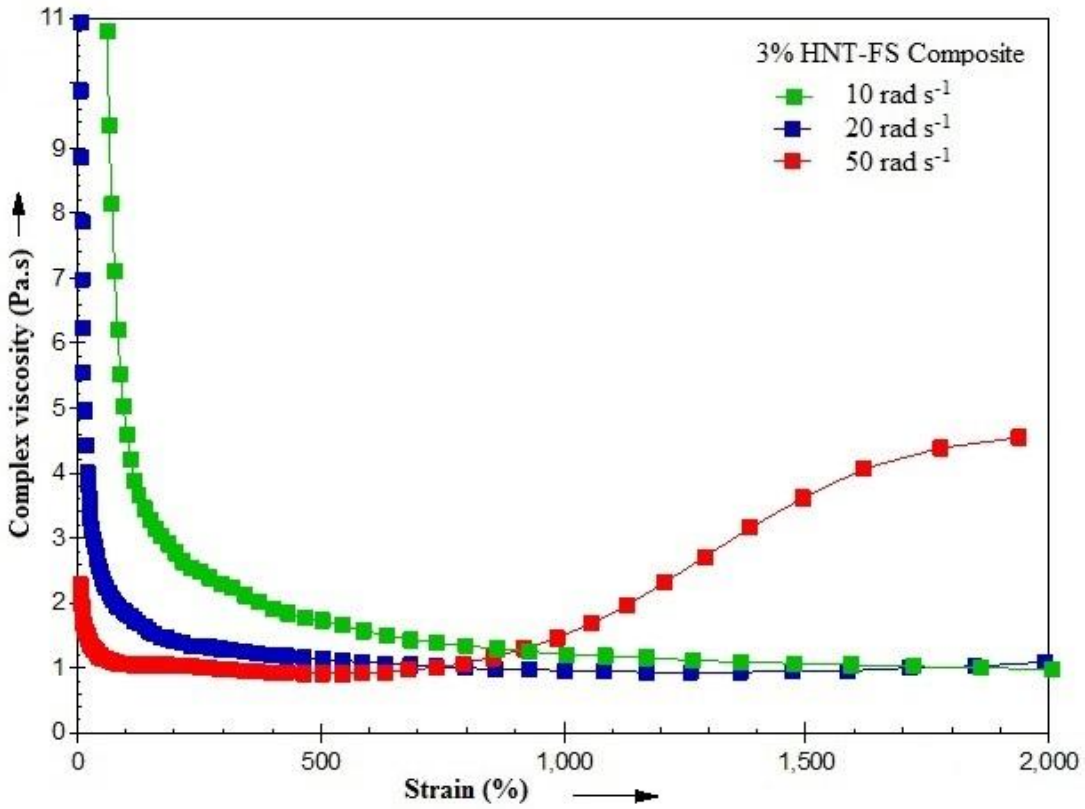

Figure 5.38: Complex viscosity at three different frequencies of 10 rad s^{-1}, 20 rad s^{-1} and 50 rad s^{-1} (Green, blue and red respectively) for 3% HNT-FS composite

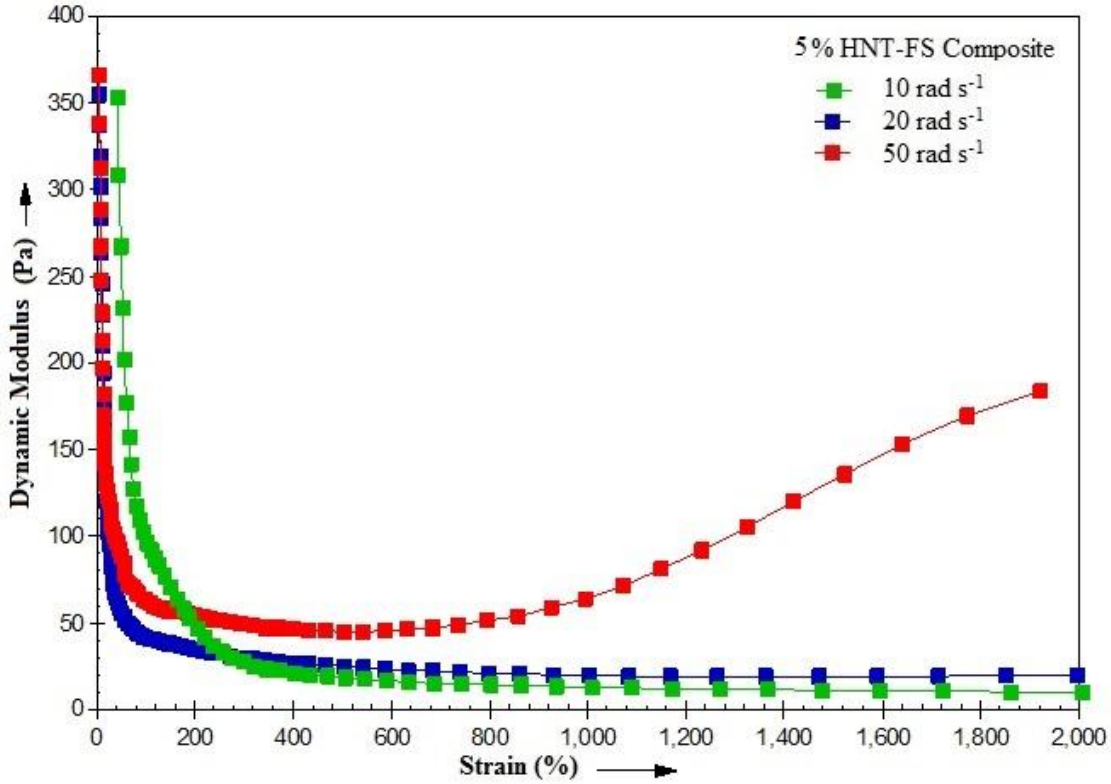

Figure 5.39: Dynamic modulus at three different frequencies of 10 rad s^{-1}, 20 rad s^{-1} and 50 rad s^{-1} (Green, blue and red respectively) for 5% HNT-FS composite

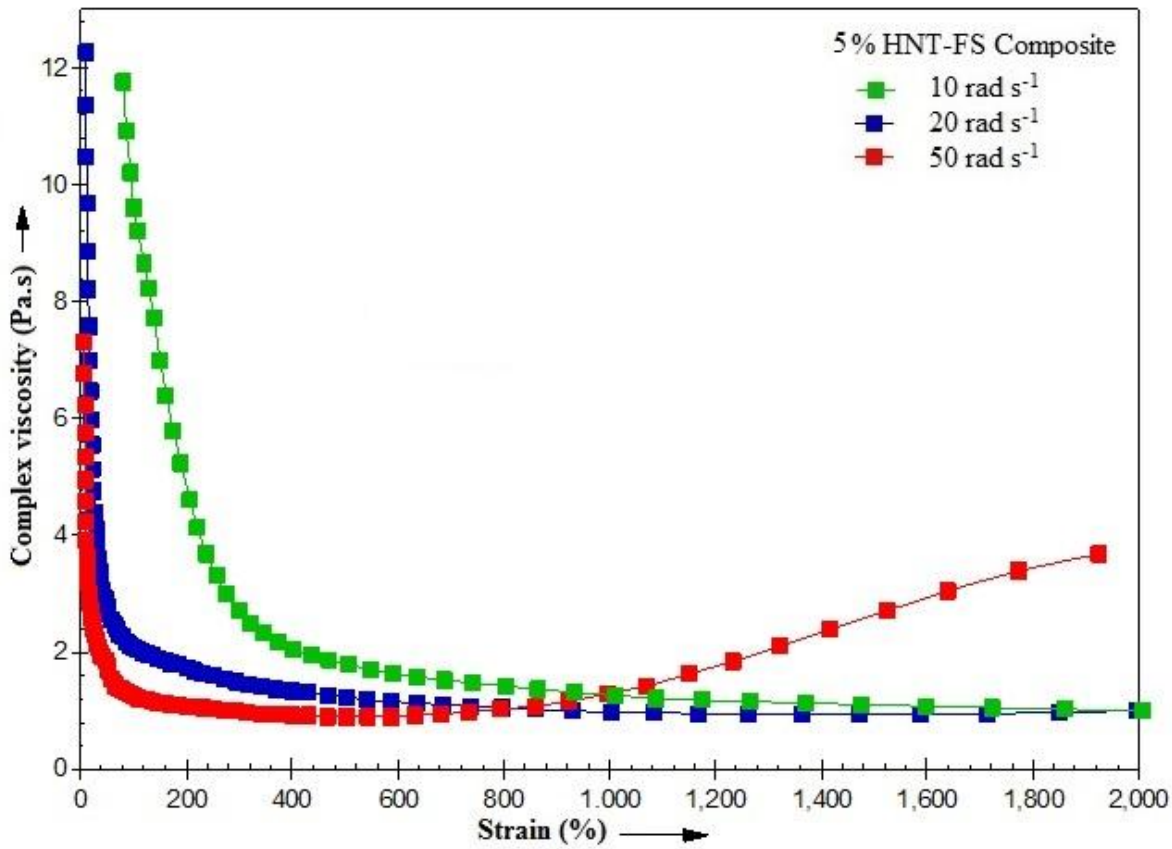

Figure 5.40: Complex viscosity at three different frequencies of 10 rad s^{-1}, 20 rad s^{-1} and 50 rad s^{-1} (Green, blue and red respectively) for 5% HNT-FS composite

b. Frequency sweep test

The frequency sweep test conducted on the sample at a wide frequency range and a constant strain amplitude (1%) also demonstrates the strain thickening phenomenon. Here the linear thickening can be observes at lower frequencies and nonlinear at higher frequencies. A rapid decrease in complex viscosity occurs upto 40 rad s^{-1} and beyond this the complex viscosity increases continuously.

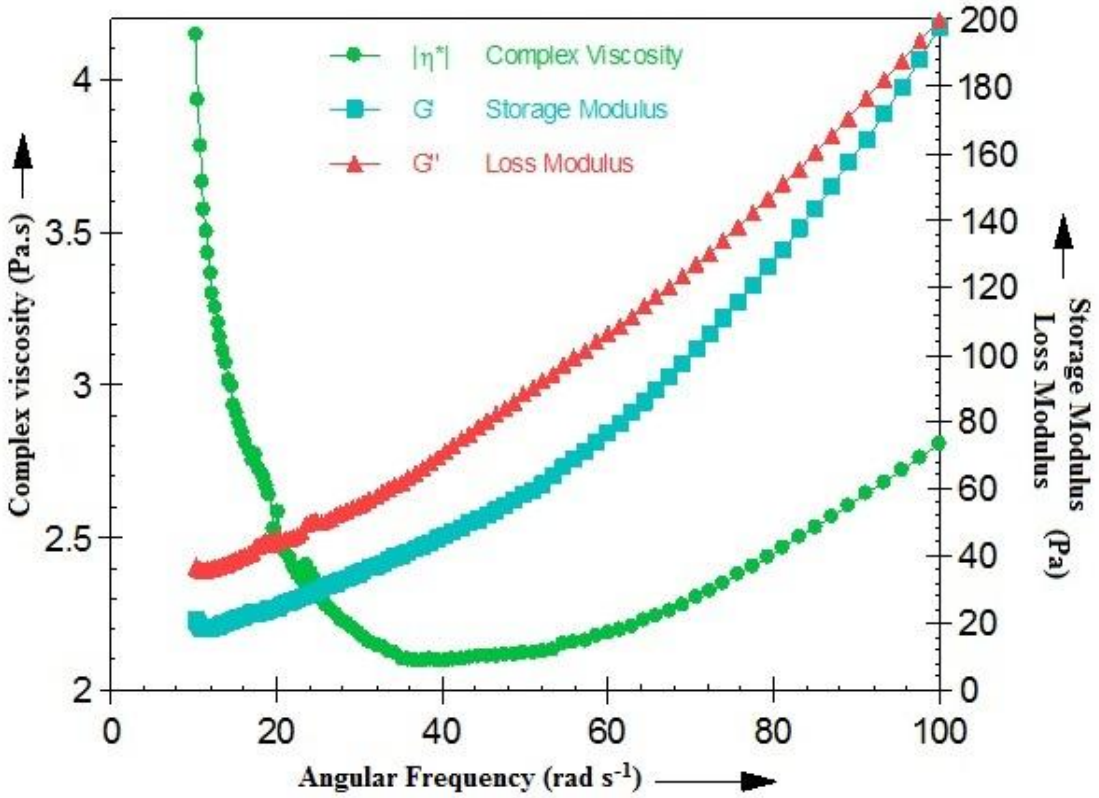

Figure 5.41: Frequency sweep tests where the variation of the storage and loss modulus with the change in frequency, shows the linear and the nonlinear viscoelastic behaviour of the composite. A sharp fall and gradual rise in complex viscosity is also seen.

From figure 5.41, it is clear that the viscous modulus exceeds the elastic modulus, over the entire frequency range. Such dynamic response shows that this system of colloidal dispersion depicts a sol-like behaviour consisting of distinct non-flocculated units. Throughout the frequency range the plot of loss modulus is nearly linear while that of the storage modulus curves at high frequency. This shows that at higher frequencies the ability of the material to dissipate energy decreases while its storage capacity increases. The above experiment can also be performed with higher strain percentage to compare the moduli behaviour with change in frequency.

Frequency sweep comparison tests for different weight percentages of HNT-fumed silica composite STF:

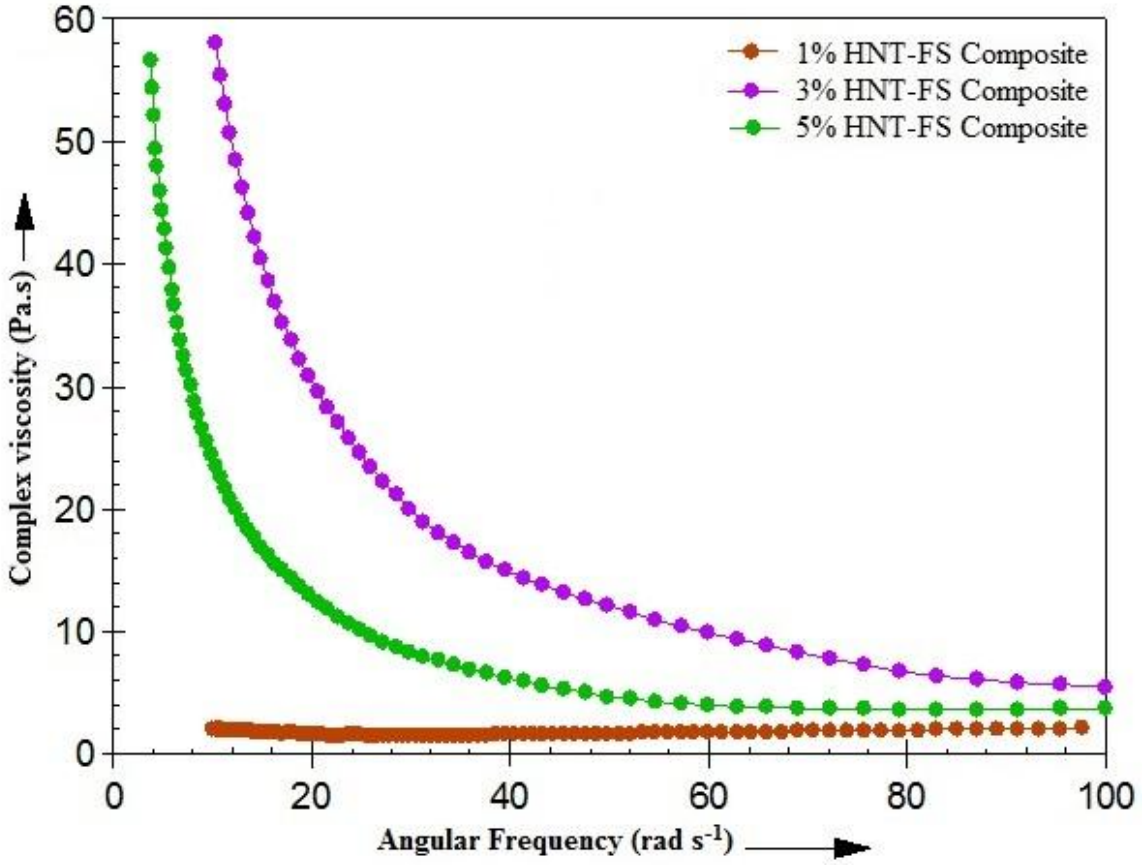

Figure 5.42: Frequency sweep tests where the variation of complex viscosity is shown with the change in frequency for 1%, 3%, and 5% (weight %) HNT-FS Composite

Figure 5.42 shows that no thickening behaviour or the rise in the complex viscosity was observed for 3% and 5% HNT-fumed silica composite samples at low strain amplitude (1%) and at lower frequency range. Even though a clear and significant rise in the complex viscosity was observed for the 1% sample from 40 to about 100 rad s^{-1} frequency range, the comparison for all three samples could not be made.

Dynamic modulus comparison for different composition HNT-Fumed Silica STF at higher strain percentages:

The oscillatory tests were even conducted at high strain amplitudes (100 % strain) to obtain the behaviour of elastic modulus and loss modulus with the increasing stress and the change of the overall dynamic modulus with the change in frequency.

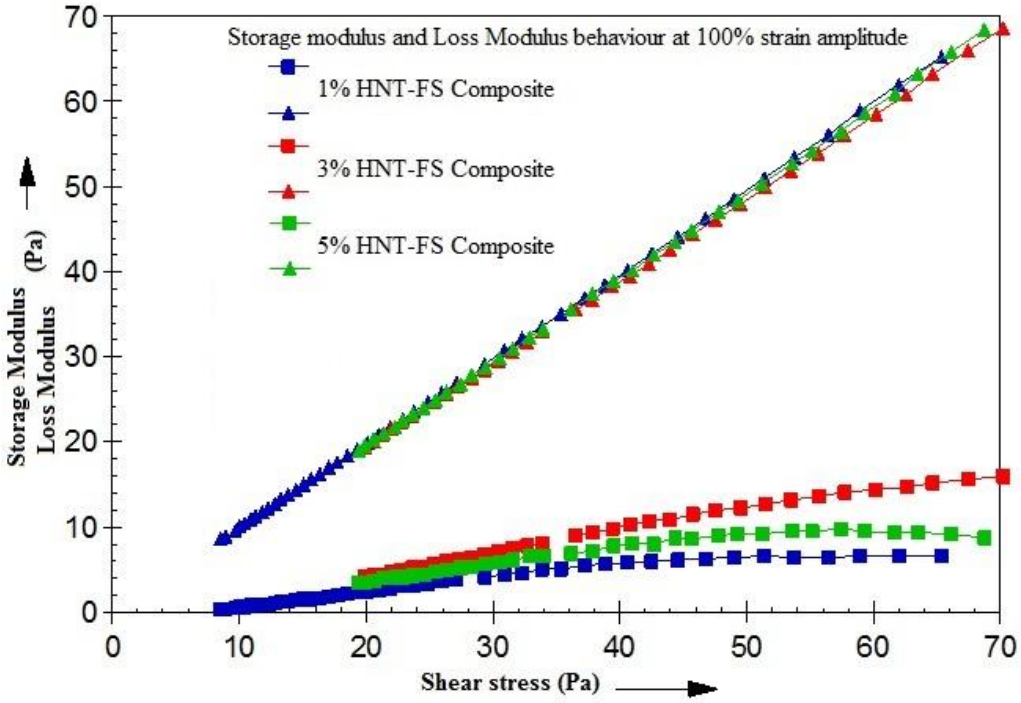

Figure 5.43: The effect on increasing HNT concentration in the composite on storage and loss modulus for 1%, 3% and 5% HNT-Fumed silica composite STF

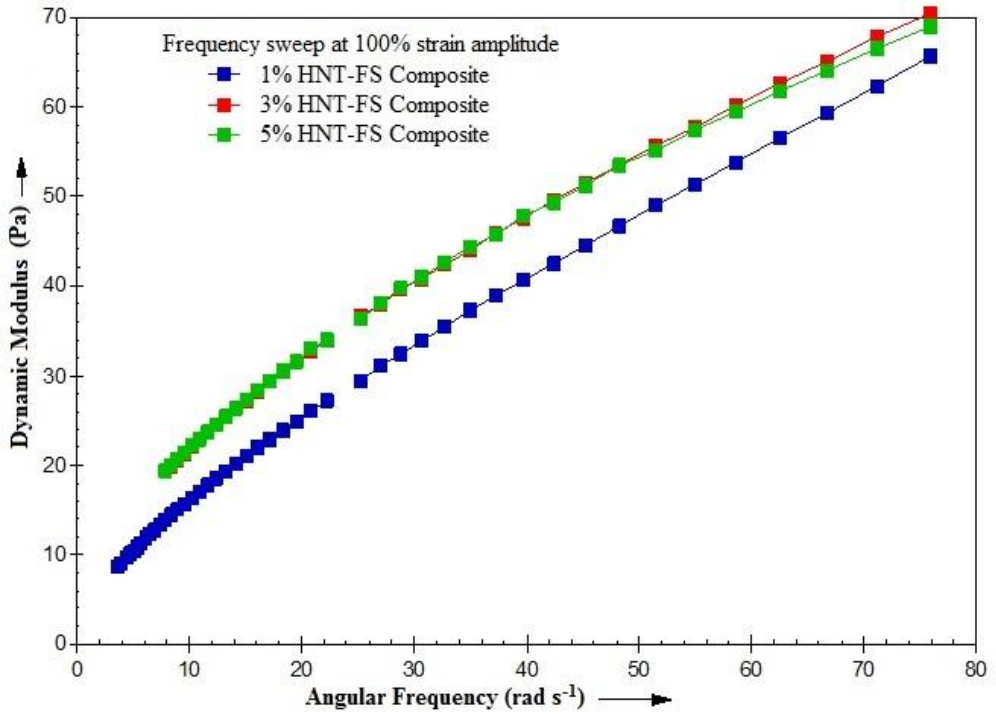

Figure 5.44: The effect on increasing HNT concentration in the composite on the overall comparison of the dynamic modulus for 1%, 3% and 5% HNT-Fumed silica composite STF

From the dynamic rheology at high strain amplitude (figure. 5.43 and figure. 5.44), it is clear that the loss modulus exceeds the storage modulus for the entire range of the frequency and is nearly linear. This shows the absence of flocs in the fluid sample.

CONCLUSION

In the present study, initially a basic understanding of the shear thickening property of Non-Newtonian fluids was reported. Then a bi-dispersed shear thickening suspension was prepared constituting nano silica, fumed silica and poly ethylene glycol. This shear thickening fluid, being a polymeric liquid mixture is considered to be viscoelastic in nature i.e. on deformation neither does it loses its original shape permanently nor does it completely attain its original properties. Some previous history always remains inside this fluid, which has to be removed to obtain accurate results for the rheological tests. A set protocol was developed for the entire process of rheological testing. The technique studied here was 'pre-shearing', which involves two main parameters as the:

i. Limit of reversibility, and
ii. Equilibrium (resting) time.

Another composite shear thickening suspension was prepared using halloysite nanotubes (HNT) with an aspect ratio of 40, fumed silica and polyethylene glycol. The effect of rod shaped particles blended with spherical particles was studied at different weight percentages of HNT. This STF mixture, being composed of a polymeric liquid is also considered to be viscoelastic. To examine the behaviour of this composite fluid, various steady shear as well as oscillatory tests were conducted.

The major conclusion that can be drawn from the rheological tests of the above two mixtures are:

- The initial properties of the sample change for every new loading before conducting any tests.
- It is better to keep a lower pre-shear value than a large one so as to cause minimum structural changes in the sample. In case of rotational tests, the shear rate was found to be in range of 0.1 s^{-1} to 2 s^{-1}. An optimum value of 1 s^{-1} is kept for all rotational tests. In case of oscillatory tests, a strain of 1% is generated as the pre-shear condition.
- The duration for which this shear or strain is applied is also important. This is kept as 600 s for rotational tests and 100 s for oscillatory tests.
- The resting time given to the sample to stabilize or achieve an equilibrium state can be both more or less than the pre shearing time. For rotational tests this duration is of 900 s and for oscillatory tests it is just 50 s.

- This protocol can lead to a significant increase in the critical viscosity as well as the critical shear rate, for spherical particle shear thickening fluid.
- For the HNT-SiO_2 compounded shear thickening fluid, the clusters formed are elongated, non-spherical structures, which gives rise to a higher increase in viscosity as compared to that obtained from the spherical particles.
- Critical shear rate is directly proportional to the temperature and maximum viscosity of the sample is inversely proportional to temperature.
- The transition to strain-thickening behavior occur at smaller strains as the frequency of the deformation is increased. Critical viscosity (η^*) does not fall much with the increase in the strain %.
- The stable nature of 1% HNT-fumed silica composite at low frequency and high strain % lowers the effect of the projectile to a large extent.
- Non-flocculated suspensions show a better thickening behaviour at high amplitude as well as high frequency.

Such findings can open up the possibility of creating new designs for smart suspensions and thus produce specific shear thickening fluids for a wide variety of applications.

FUTURE RESEARCH PROSPECTS

More and more experimental as well as theoretical work is being continuously done in the field of shear thickening fluid, and it has given rise to potential applications in different fields on one hand, but at the same time it has intensified the surge to find out its greater prospects. There still remain a lot of unanswered questions which will become the base of future research in shear thickening fluids, especially in defence research. Some of the future research prospects are enlisted below:

1. To check the field responsiveness of shear thickening fluids.
2. Improvement of thermal stability and moisture resisting property of shear thickening fluids.
3. Enhancement in the energy absorptive capacity of the shear thickening fluids.
4. Study of the effect of wall slip and the time dependent behaviour of the HNT-FS composite.
5. Synthesis and studies of STF composites with higher molecular weight silica (400 nm or more) and HNT.
6. The study of polymer-polymer interactions and the polymer particle interactions on the composite STF, leading to their extensional rheological studies.
7. Reduction in the sedimentation rate of the dispersed phase using analytical techniques. If the Brownian movement of nano particle is larger than itself in weight then the probability of settlement is rare. This can lead to a study of the stability of STF thereby providing a consistent nature in its properties throughout its life.
8. Maximum work done on STFs is focused on the solid spherical shaped particles. Studies involving the experimental, theoretical or numerical implementations have already been done on large scale for spherical particles. For non-spherical particles (rod/tubular shaped, platelets, disc shaped etc.), such intensive studies have to be performed.
9. Morphological characterization of the STF composites has to be done.
10. The gap size and geometry effect on the shear history variation of the STFs.
11. Modelling approaches of the HNT-FS composite STF.
12. Dynamic simulation studies involving Stokesian Dynamics method of the composite STF suspensions.
13. Calculation of the rate at which the phase transition of STF occurs from liquid to solid and back, when subjected to high impact, using dimensionless numbers.

14. The continuous and discontinuous behaviour of composite colloidal suspensions.
15. Study of lubrication forces between the solid phase particles and the dispersion medium in composite STFs.
16. Further investigation is needed on the shear thickening behavior of the dense suspensions. It is a challenge as to why all dense suspensions do not observe shear thickening behavior.
17. The comparative study of soft particles and hard particles exhibiting shear thickening behavior.
18. To obtain a simple and systematic way of presenting the effect of simultaneous factors affecting STF.
19. Halloysite nanotubes (HNTs) in their raw form have weak affinity for polymers. Thus the surface treatment or surface modification of HNTs being highly desirable to improve its performance.
20. Study of spherical (silica) as well as non-spherical (TiO_2, HNTs, CNTs) in plastic epoxy matrix offering improved antiballistic resistance and improved flexibility.
21. Study of decomposition of shear thickening fluids, thus making it biodegradable and environment friendly.

REFERNCES

Ayadi A. J., Soro J., Kamoun A., Baklouti S., Study of clay's mineralogy effect on rheological behaviour of ceramic suspensions using an experimental design, IJRRAS, 14 (2) (2013).

Banchio A. J., Brady J. F., Accelarated stokesian dynamics: Brownian motion, J. Chem. Phys. 118, 10323 (2003).

Barnes H. A., Shear-thickening ("Dilatancy") in suspensions of non-aggregating solid particles dispersed in Newtonian liquids, Journal of Rheology, 33(2), 329-366 (1989).

Barnes H. A., The yield stress-a review or $'\pi\alpha\nu\tau\alpha\ \rho\varepsilon\iota'$-everything flows?, J. Non-Newtonian Fluid Mech., 81, 133-178 (1999).

Bender J., Wagner N. J., Reversible shear thickening in monodisperse and bidisperse colloidal dispersions, J.Rheol, 40 (5), 899 (1996).

Boersma W.H., Baets J.M., Laven J., Stein H.N., Time-dependent behaviour and wall slip in concentrated shear thickening dispersions, J. Rheol 35(6), 1093-1120, (1991).

Bossis G., and Brady J. F., The rheology of Brownian suspensions, J Chem Phys, 91, 3, 1866-1874 (1989).

Brady J.F., Bossis G., The rheology of concentrated suspensions of spheres in simple shear flow by numerical simulation, J. Fluid Mech., 155, 105 (1985).

Brady J.F., Bossis G., Stokesian Dynamics, Ann. Rev. Fluid Mech. 20 (1988) 111-157.

Brady J.F., Phillips R.J., Lester J.C., Bossis G., Dynamic simulation of hydrodynamically interacting suspensions, J. Fluid Mech., 195, 257-280 (1988).

Brown E., Jaeger H. M., Dynamic jamming point for shear thickening suspensions, PRL, 103 (8), 086001 (2009).

Brown E., Jaeger H.M., Shear thickening in concentrated suspensions: phenomenology, mechanisms, and relations to jamming, Reports on Progress in Physics, 77, 046602 (2013).

Chang K.C., Yeh F. Y., Chen T. W., 18th International Conference on Composite Materials, Jeju Island, Korea, 2011.

Chen J., Spear S.K., Huddleston J.G., Rogers R.D., Polyethylene glycol and solutions of polyethylene glycol as green reaction, Green Chemistry, 7 (2), 64-82 (2005).

Chen Y., Xu W., Zeng G., Liu W., Shear thickening behaviour of precipitated calcium carbonate particles suspensions in glycerin, Applied Rheology, ApplRheo-25-12466 (2015).

Chen Q., Zhu W., Ye F., Gong X., Jiang W., Xuan S., pH effects on shear thickening behaviours of polystyrene-ethylacrylate colloidal dispersions, Material Research Express 1 015303 (2014).

Christie T., Thompson B., Brathwaite B., Mineral Commodity Report 20-Clays, Institute of Geological and Nuclear Sciences, 2011.

Cherizol R., Sain M., Tjong J., Review of Non-Newtonian mathematical models for rheological characteristics of viscoelastic composites, Green and Sustainable Chemistry 5, 6-14 (2015).

Chow M.K., Zukoski C.F., Gap size and shear history dependencies in shear thickening of a suspension ordered at rest, J. Rheol., 39(1) (1995).

Chu B., Brandy A. T., Mannhalter B. D., Salem D. R., Effect of silica particle surface chemistry on the shear thickening behaviour of concentrated suspensions, J. Phys D: Appl. Phys. 47-335302 (2014).

Chu C. E., Groman J. A., Sieber H. L., Miller J. G., Okamoto R. J., Katz J. I., Hysteresis and lubrication in shear thickening of cornstarch suspensions, Soft Condensed Matter, arXiv:1405.7233v1 (2014).

Cohen D., Shear thickening fluid reinforced fabrics for use with an expendable spacecraft, US0296435 (2008).

Cosgrove T., Colloid Science: Principles, methods and Applications, Blackwell Publishing (2005).

Crawford N. C., Williams K. R., Boldridge D., Liberatore M. W., Shear-induced structures and thickening in fumed silica slurries, Langmuir 29, 12915-12923 (2013).

Dawson C. R., Li N.N., O'Brien D. E., Method of using a well treating fluid, US4397354 (1983).

De los Reyes J. C., Stadler G., A non-smooth model for discontinuous shear thickening fluids: analysis and numerical solution, Interfaces and Free Boundaries, 16(4), 575-602 (2014).

Decker M. J., Halbach C. J., Nam C. H., Wagner N. J., Wetzel E. D., Stab resistance of shear thickening fluid (STF) –treated fabrics, 67(3-4), 565-578 (2007).

Desai R., Upadhyay R.V., Anomalous increase in the magnetorheological properties of magnetic fluid induced by silica nanoparticles, Materials Research Express, 1, 046116 (2014).

Ding J., Tracey P., Li W., Peng G., Whitten P.G., Wallace G.G., Review on shear thickening fluids and applications, Textiles and Light Industrial Science and Technology (TLIST), 2(4), 161-173 (2013).

Drake E.N., Calcavecchio P., Shear thickening composition, US4442241 (1984).

Dullaert K., Constitutive equations for thixotropic dispersions, Ph.D thesis, Katholieke Universiteit Leuven, Belgium (2005).

Durlofsky L., Brady J.F., Bossis G., Dynamic simulation of hydrodynamically interacting particles, J. Fluid Mech., 180, 21-49 (1987).

Frank A., Understanding Rheology of Structured Fluids, TA Instruments, AAN016.

Galindo-Rosales F.J., Rubio-Hernandez F.J., Velazquez-Navarro Jose F., Shear-thickening behaviour of Aerosil R816 nanoparticles suspension in polar organic liquids, Rheol Acta 48, 699-708 (2009).

Galindo-Rosales F.J., Rubio-Hernandez F.J., Static and dynamic yield stresses of Aerosil 200 suspension in polypropylene glycol, Applied Rheology, ApplRheol-20-22787 (2010).

Galindo-Rosales F.J., Rubio-Hernandez F.J., Sevilla A., An apparent viscosity function for shear thickening fluids, J. Non-Newtonian Fluid mech. 166, 321-325 (2011).

Harvey C. C., Murray H. H., Clays-An Overview, Industrial Minerals and Rocks, 335-342.

Hasanzadeh M., Mottaghitalab V., The role of shear-thickening fluids (STFs) in ballistic and stab-resistance improvement of flexible armour, JMEPEG, 23, 1182-1196 (2014).

Harrera J., Anik M., Elzawawy A., Budhoo Y., Application of shear thickening Non Newtonian fluid to minimize head and neck injury, Eleventh LACCEI Latin American and Caribbean Conference for Engineering and Technology (LACCEI'2013) International Competition of Student Posters and Paper, Cancun, Mexico, August 14 - 16, 2013.

Hebraud P., Lootens D., Concentrated suspensions under flow: shear thickening and jamming, Mod. Phys. Lett. B 19, 613 (2005).

Hoffman R.L., Discontinuous and dilatant viscosity behaviour in concentrated suspensions I. Observation of flow instability, J. Rheol, 16, 1, 155-173 (1972).

Hoffman R.L., Discontinuous and dilatant viscosity behaviour in concentrated suspensions II. Theory and experimental tests, J. Colloid Interface Science, 46, 491 (1974).

Hoffman R.L., A study of the advancing interface. I. Interface shape in liquid-gas systems, Journal of Colloid and Interface Science, 50(2), 228-241 (1975).

Hoffman R.L., Discontinuous and dilatant viscosity behaviour in concentrated suspensions III. Necessary conditions for their occurrence in viscometric flows, Advances in Colloid and Interface Science, 17(1), 161-184 (1982).

Hoffman R.L., Explanations for the cause of shear thickening in concentrated colloidal suspensions, Journal of Rheology, 42, 111 (1998).

Hong C. H., Liu Y. D., Choi H. J., Carbonyl iron suspension with halloysite additive and its magnetorheology, Applied Clay Science, 80-81, 366-371 (2013).

Idzkowska A., Szafran M., The effect of nano-SiO2 particle size distribution on rheological behaviour of shear thickening fluids, Archives of Metallurgy and Materials, 58(4), 0167 (2013).

Joanna A., Elsa R., Oleksander S., Brijesh V., Multi layered apparatus for stopping projectiles, US20070178374A1 (2007).

Khan S.A., Baker G.L., Colson S., Composite polymer electrolytes using fumed silica fillers: rheology and ionic conductivity, Chem. Mater. 6, 2359-2363 (1994).

Khandavalli S.K., Rothstein Jonathan P., Extensional rheology of shear thickening fumed silica nanoparticles dispersed in an aqueous polyethylene oxide solution, J. Rheol., 58(2), 411-431 (2014).

Kirkwood J. E., Kirkwood K.M., Lee Y.S., Egres R.G., Wetzel E. D., Wagner N.J., Yarn pull-out as a mechanism for dissipating ballistic impact energy in Kevlar® KM-2 fabric Part II: Predicting ballistic performance, Textile Research Journal, 74 (11), 939 (2004).

Kurahatti A. V., Surendranathan A. O., Kori S. A., Singh N., Kumar A. V. R., Srivastava S., Defence applications of polymer nanocomposites, Defence Science Journal, 60(5), 551-563 (2010).

Kushan M.C., Gurgen S., Unalir T., Cevik S., Novel approach for armour applications of shear thickening fluids in aviation and defence industry, International Conference of Scientific Paper, AFASES, Brasov, May 22-24 (2014).

Larsen D. H., Use of clay in drilling fluids, in Clays and Clay Technology, Bull. 169.

Laun H. M., Bung R., Schmidt F., Rheology of extremely shear thickening polymer dispersions (passively viscosity switching fluids), J. Rheol, 35, 999 (1991).

Lee Y. S., Wagner N. J., Dynamic properties of shear thickening colloidal suspensions, Rheol Acta 42, 199-208 (2003).

Lee Y.S., Wetzel E.D., Wagner N.J., The ballistic impact characteristics of Kevlar® woven fabrics impregnated with a colloidal shear thickening fluid, J. Mater. Sci., 38, 2825-2833 (2003).

Lee Y.S., Wetzel E.D., Egres Jr. R.G., Wagner N.J., Advanced body armour utilizing shear thickening fluids. In Proceedings of the 23rd Army Science Conference 2002, Orlando, Florida, December 2-5, 2002.

Lootens D., Hebraud P., Lecolier E., Damme H. V., Gelation, shear thinning and shear thickening in cement slurries, Oil & Gas Science and Technology - Rev. IFP, 59(1), 31-40 (2004).

Macosko C. W., Rheology: Principles, Measurements and Applications, VCH Publishers, New York, 1994.

Maranzano B.J., Wagner N.J., The effect of interparticle interactions and particle size on reversible shear thickening: Hard-sphere colloidal dispersions, J.Rheol., 45(5), 1205-1222 (2001).

Mintz D., Irani C.A., Shear thickening well control fluid, US4391925 (1983).

Montgomery S. T., MacKnight W. J., Introduction to polymer viscoelasticity, 3rd Edition, Wiley-Interscience (2005).

Parfitt R. L., Greenland D. J., The adsorption of poly(ethylene glycol) on clay minerals, Clay Minerals, 8, 305 (1970).

Raghavan S. R., Walls H.J., Khan S. A., Rheology of silica dispersions in organic liquids: New evidence for solvation forces dictated by hydrogen bonding, Langmuir, 16, 7920-7930 (2000).

Raghavan S. R., Khan S. A., Shear-induced microstructural changes in flocculated suspensions of fumed silica, J. Rheol., 39(6), 1311-1325, (1995).

Raghavan S. R., Khan S. A., Shear-thickening response of fumed silica suspensions under steady and oscillatory shear, Journal of Colloid and Interface Science, 185, 57-67 (1997).

Raghavan S.R., Hou J., Baker G.L., Khan S.A., Colloidal interactions between particles with tethered non polar chains dispersed in polar media: direct correlation between dynamic rheology and interaction parameters, Langmuir 16, 1066-1077 (2000).

Rosen B. A., Laufer C. H. N., Kalman D. P., Wetzel E. D., Wagner N. J., Multi-threat performance of kaolin-based shear thickening fluid (STF)-treated fabrics, proceedings of SAMPE 2007, Baltimore, Maryland, June 3-7, 2007.

Russel W. B., Saville D. A., Schowalter W. R., Colloidal Dispersions, Cambridge University Press, Cambridge, 1989.

Sha X., Yu K., Cao H., Qian K., Shear thickening behaviour of nanoparticles suspensions with carbon nanofillers, J. Nanopart Res, 15:1816 (2013).

Sun Y., Bao H. D., Guo Z. X., Yu J., Modeling of the electrical percolation of mixed carbon fillers in polymer-based composites. Macromolecules, 42,459-463 (2009).

Tabassum M., Ye L., Chang L., Friedrich K., Mode-I Fracture behaviour of a shear thickening fluid as adhesive layer under different loading rates, 13th International Conference on Fracture, Beijing, China, June 16–21, 2013.

Tian T., Li W., Ding J., Alici G., Du H., Study of the temperature effect of shear thickening fluid, IEEE/ASME International Conference on Advanced Intelligent Mechatronics (AIM), Wollongong, Australia, 833-837, July 9-12, 2013.

Uddin F., Clays, nanoclays and Montmorillonite minerals, Metallurgical and materials transactions, 39A (2008).

Wagner N. J., Brady J.F., Shear thickening in colloidal dispersions, Physics Today, 27-32 (2009).

Wahyudi S., Koseki J., Sato T., Miyashita Y., Effects of pre-shearing history on repeated liquefaction behaviour of sand using stacked-ring shear apparatus, Bulletin of ERS, 46 (2013).

Wang Y., Zhu Y., Fu Y., Preparation of HNT-SiO2 compounded shear thickening fluid, NANO: Brief Reports and Reviews, 9(8), 1450100 (2014).

Warren J., Offenberger S., Toghiani H., Pittman Jr. C.U., Lacy T.E., Kundu S., Effect of temperature on the shear –thickening behaviour of fumed silica suspensions, ACS Appl. Mater. Interfaces, 7, 18650-18661 (2015).

Wetzel E. D., Lee Y.S., Egres R.G., Kirkwood K.M., Kirkwood J.E., Wagner N.J., The effect of rheological parameters on the ballistic properties of shear thickening fluid (STF)-Kevlar composites, NUMIFORM (2004).

Wu X. J., Wang Y., Yang W., Xie B. H., Yang M. B., Dan W., A rheological study of temperature dependent microstructural changes of fumed silica gels in dodecane, Soft matter, 8, 10457 (2012).

Wyss H.M, Larson R.J., Prof. Weitz D.A., Oscillatory Rheology: Measuring the Viscoelastic behaviour of Soft Materials, G.I.T Laboratory Journal, 3-4, 68-70 (2007).

Xu Y.L., Gong X.L., Peng C., Sun Y.Q., Jiang W.Q., Zhang Z., Shear thickening fluids based on additives with different concentrations and molecular chain lengths, Chinese Journal of Chemical Physics, 23(3), 342-346 (2010).

Yeh F. Y., Chang K. C., Chen T. W., Smart viscous dampers utilizing shear thickening fluids with silica nanoparticles, 15 WCEE, Lisboa (2012).

Yu K., Cao H., Qian K., Jiang L., Li.H., Synthesis and stab resistance of shear thickening fluid (STF) impregnated glass fabric composites, FIBRES & TEXTILES in Eastern Europe, 20, 6A(95), 126-128 (2012).

Zhang X. Z., Li W. H., Gong X. L., The rheology of shear thickening fluid (STF) and the dynamic performance of an STF-filled damper, Smart Mater. Struct., 17, 035027 (2008).

Zhu W. K., Numerical analysis of shear thickening fluids for blast mitigation applications, Master's Thesis, Naval Postgraduate School, Singapore (2011).